uOttawa

L'Université canadienne
Canada's university

FACULTÉ DES ÉTUDES SUPÉRIEURES ET POSTOCTORALES

uOttawa

L'Université canadienne
Canada's university

FACULTY OF GRADUATE AND POSDOCTORAL STUDIES

Maciek Kepka

AUTEUR DE LA THÈSE / AUTHOR OF THESIS

M.A.Sc. (Mechanical Engineering)

GRADE / DEGREE

Department of Mechanical Engineering

FACULTÉ, ÉCOLE, DÉPARTEMENT / FACULTY, SCHOOL, DEPARTMENT

Analysis of Formation Control Schemes for Vehicles Subject to Kinematic Constraints

TITRE DE LA THÈSE / TITLE OF THESIS

Dan Necsulescu

DIRECTEUR (DIRECTRICE) DE LA THÈSE / THESIS SUPERVISOR

CO-DIRECTEUR (CO-DIRECTRICE) DE LA THÈSE / THESIS CO-SUPERVISOR

EXAMINATEURS (EXAMINATRICES) DE LA THÈSE / THESIS EXAMINERS

M. Liang

D. Redekop

J. Sasiadek

Gary W. Slater

LE DOYEN DE LA FACULTÉ DES ÉTUDES SUPÉRIEURES ET POSTDOCTORALES /
DEAN OF THE FACULTY OF GRADUATE AND POSTDOCORAL STUDIES

Analysis of Formation Control Schemes for Vehicles Subject to Kinematic Constraints

Thesis submitted to the University of Ottawa
in partial fulfillment of the requirements for the degree of

Master of Applied Science
in Mechanical Engineering

by Maciek Kepka

Ottawa-Carleton Institute for Mechanical and Aerospace Engineering
University of Ottawa
Ottawa, Ontario, Canada

Your file Votre référence
ISBN: 0-494-11313-8
Our file Notre référence
ISBN: 0-494-11313-8

Abstract

This thesis focuses on control schemes for vehicle platoons. The study uses transfer function and Lyapunov function analysis, as well as computer simulations carried out to evaluate the performance of existing control schemes and to test the new control schemes proposed in this thesis. One of the results is a control algorithm that allows an indefinite number of followers to stay in formation behind a leader that follows a planar trajectory. In the design of this control scheme, the amount of information used by followers was minimized. Since the focus of the study is on the dynamics of a large formation of vehicles, individual vehicles were modeled in the simplest way possible: as point masses with a controlled acceleration vector applied to the point mass and subject to kinematic constraints.

This thesis also presents further development of the string stability approach, extended from 1D (curvilinear) motion to 2D (planar) motion.

Table of Contents

Acknowledgement

This thesis research was conducted under the guidance of Professor Dan Necsulescu from the University of Ottawa. Professor Necsulescu has many years of experience in the area of control systems and mechatronics. He also possesses a laboratory equipped with advanced mechatronic devices and high-speed digital controllers. He has been instrumental in my study of this area of mechanical engineering. I would like to thank him for guiding me through this process and for making sure that my work satisfied the appropriate academic requirements. I am very grateful for his patience and understanding.

I would also like to thank fellow graduate students Giurgea, Basic, Xinming, Cheng, Kang, Jiang, Khatri and Gilbank who have shared with me their knowledge and experience.

Lastly, I would like to express my sincere appreciation to my family and friends for their constant support in this undertaking, in particular to Maria, Michal, Helen and Hanna.

List of symbols

Note that vector quantities are generally in bold font.

a_i acceleration of i-th vehicle

$\mathbf{a}_i$ acceleration vector of i-th vehicle

a_x, a_y x and y-components of acceleration vector

a-lag time delay on acceleration feedback (acceleration is the control variable)

A amplitude (y-direction) of the sinusoidal path of the leader in planar motion

b constant component of the x-direction velocity of the leader in planar motion

c derivative feedback gain

d amplitude of the sinusoid added to the constant b of the x-direction velocity

D period (x-direction) of the sinusoidal path of the leader in planar motion

e_i spacing error distance of i-th vehicle

e_i^s path-wise spacing error of i-th vehicle

$\mathbf{e}_i$ spacing error vector of i-th vehicle

$g(t)$ time-domain spacing error transfer function (impulse response)

$G_i(s)$ s-domain spacing error transfer function, i.e.: Laplace transform of $g(t)$

i vehicle index, leader has index 1, first follower index 2, and so on

k proportional feedback gain

l_i achieved inter-vehicle spacing distance

l_i^s achieved spacing distance in front of i-th vehicle, path-wise

$\mathbf{l}_i$ achieved spacing vector in front of i-th vehicle

L desired inter-vehicle spacing distance, linear or path-wise

L_i desired inter-vehicle spacing distance in front of i-th vehicle

$\mathbf{L}_i$ desired inter-vehicle spacing vector in front of i-th vehicle

m_i mass of i-th vehicle, usually assumed to equal $1kg$ to simplify calculations

n_i normal distance from i-th vehicle to leader's path, i.e.: normal spacing error of i-th vehicle

N Number of vehicles in a platoon

r path curvature at a given point on the planar trajectory

$\mathbf{r}_i$ position vector of i-th vehicle

R roadway half-width in planar motion

s_i path-wise position of i-th vehicle

u_i control input of i-th vehicle (usually equal to acceleration)

v_i speed (velocity magnitude) of i-th vehicle

$\mathbf{v}_i$ velocity vector of i-th vehicle

x_i absolute position of i-th vehicle in 1D motion

Definitions

Autonomous system: system that is not subjected to external excitation.

DOF: vehicle degrees of freedom, 1 for linear motion, 3 for planar motion.

Down the platoon: towards the end of the platoon (increasing vehicle index i).

Equilibrium point: a state of the system that will be maintained indefinitely (as $t \to \infty$), given that no external perturbations are present.

Heuristic: a guideline or common-sense (not scientifically proven) decision-making method used in problem-solving processes.

Jerk or jerkiness: abrupt changes or discontinuities in a vehicle's acceleration.

Lyapunov's direct method: energy-like function (usually called V) of the system's parameters and generalized coordinates. The nature of the function and of its time-derivative give information on the stability of the system around an equilibrium point.

Lyapunov's indirect method: analysis of a linearized system that also applies to a certain operating region of the non-linear system.

l_2*-string stability*: the property of a string of vehicles moving in single-file to attenuate spacing errors down the platoon to signals with bounded mean energy, but not necessarily with bounded magnitude.

Path: the locus of positions of a vehicle over a time interval.

Platoon: usually single-file formation of vehicles with one leader and any number of followers.

Spacing error: the difference between the desired inter-vehicle spacing L_i and the actual inter-vehicle spacing.

Spacing policy: the method of determining the desired inter-vehicle spacing L_i.

String stability: the property of a string of vehicles moving in single-file to attenuate spacing errors down the platoon.

Trajectory: the set of time-related positions of a vehicle.

Up the platoon: towards the leader of the platoon (decreasing vehicle index i).

List of Figures

List of Tables

1. Introduction

This thesis work concentrated on the area of control systems for vehicle formations. A formation could be a linear platoon, such as a string of vehicles on a highway, a two-dimensional formation of vehicles moving in a plane or, perhaps, a formation of aircrafts where each vehicle has from three to all six degrees of freedom if modeled as a rigid body moving in 3D space. In this thesis, control schemes for platoons of vehicles moving in a single-file formation were investigated. The investigation started with the study of the behavior of a platoon in 1D (linear) motion and then continued with the analysis of the changes that occur in the properties of the platoon when it is composed of 3-DOF vehicles in 2D (planar) motion.

Real-time implementations of the above control schemes would be subject to technological constraints regarding information sensing and transmission of the relative speed and position between vehicles as well as constraints on the realization of control commands. These effects are represented by time-delays introduced into the computer simulations and by saturation limits imposed on accelerations.

2. Literature Review

Up to this point, considerable insight has been gained in the control of individual vehicles subject to holonomic [1, 2] and nonholonomic [3] constraints. Many studies have also been performed in the guidance and control of linked vehicles such as trains or wheeled tractor-trailer assemblies. Attention has also been given to target tracking which can be

thought of as a formation with a leader and only one follower. Increasing attention has been given to the control of groups of vehicles moving together in a specific formation, with a leader and several followers and "cooperative control has recently emerged as a framework for establishing teams of autonomous vehicles whose task it is to perform a mission with a common goal" [4].

2.1 Platoon Stability

Two dimensions must be considered when analyzing the stability of a platoon of vehicles: time t and vehicle index i. Considering time t, perturbations must not amplify with time which is the more traditional notion of stability. Considering vehicle index i, perturbations must not amplify down the platoon (as i increases) which refers to *string stability*. For complex or nonlinear systems, stability with respect to time is often assessed using Lyapunov theory [5, 6]. A form of Lyapunov analysis has also been applied to strings of interconnected systems [7, 8].

The notion of string stability has been defined for long vehicle platoons (possibly with an infinite number of followers) undergoing linear motion. The necessary conditions of string stability were studied in substantial detail by Canudas de Wit, Brogliato, Swaroop, Hedrick and others [1, 2, 9]. Applications exist in automated highway systems as well as in other systems that make use of formations with large numbers of followers. String stability has usually been discussed with regard to 1D (linear) motion.

An important element present in all platoon stability or formation stability studies is the unpredictability of the leader's trajectory [10]. In some control schemes, followers have a real leader. In other schemes, the trajectory to be followed is a "virtual" trajectory in that no

actual vehicle is following it. In such a setup, all real vehicles are followers and the target trajectory can be thought of as the trajectory of a "virtual leader". One example of such an approach for 1D motion can be found in [11] where the target trajectory was the desired position of the center of mass of a group of vehicles. The authors developed a stable control scheme using dynamic inversion and Lyapunov stability theory.

A "Vector Lyapunov Function Approach" was developed in [7] where the authors used a special Lyapunov function method to find an enlarged parameter domain of stability for a string of an infinite interconnected system. It should be noted that Lyapunov stability theory is difficult to apply to systems of infinite dimension because of the difficulty in finding an appropriate Lyapunov function. Its advantage is that stability with respect to time can be evaluated, and, with more advanced Lyapunov techniques, also stability with respect to vehicle index i (string stability).

Other important factors affecting string stability are processing delays and synchronization of controllers. These can be due to the controller itself or to inter-vehicle communications. Analytical studies of the effects of such delays can be found in [12] and [13]. The simulations presented in this thesis use a fixed-step solver which updates all signal loops simultaneously. This is equivalent to a physical system where all controllers are triggered together by a global trigger signal or by well-synchronized internal clocks. The undesirable effects of unsynchronized controllers are thus not modeled in the simulations presented in this thesis.

2.2 Planar (2D) Formation Control

The notion of formation hold error propagation (which is related to the problem of string stability) is increasingly being extended to motion in more than one dimension.

The most basic method for lateral motion control or "lane-keeping" is the use of lane markers and sensors. Stability issues resulting from this configuration are discussed in [14]. This thesis will study control schemes that rely solely on information about the motion of platoon members (no external reference markers are used).

Canudas de Wit and Ndoudi-Likoho have formulated a single-file control scheme that imitates the motion of rigidly connected vehicles (train-like vehicle or TLV [15]). The authors stated that string stability problems could be avoided altogether as long as enough information was available to each follower regarding the motion of other vehicles in the formation. This was confirmed by Papadimitriu and Tomizuka [13] who showed that, under certain circumstances, inter-vehicle communications can eliminate the interconnection among the vehicles.

The simplest vehicle model that can be used to study string stability is a point mass. Such a vehicle model specifies the mass of each vehicle but assumes that the moment of inertia of each vehicle with regard to its centre of mass is zero. Two examples of coordinate frames that can be used to describe the motions of point masses are inertial coordinates and body-frame coordinates [10]. It is important to note that stability attained with respect to one set of coordinates does not imply stability with respect to other sets of coordinates.

A group of researchers [16] have proposed a design method for the control scheme of a platoon of unmanned autonomous ground vehicles moving in the same plane. Their method is based on a rigid body model of the vehicles, each vehicle having a mass and a moment of

inertia, and a state vector defined by position, orientation and their derivatives. The authors offered a mathematical analysis of a controller for an arbitrary number of vehicles using an internal model and a stabilizer approach. Their control scheme was then simulated in a small platoon with a leader and two followers. In addition to tracking the leader's trajectory, the followers were required to change their targeted position and orientation relative to the leader during the motion. The simulation gave satisfactory results.

Another 2D problem is the control of formations other than single-file. Mobile robots could maintain a formation of any shape, each shape having different control challenges [17]. The task is especially difficult when only local sensor information is available to individual robots [18].

One interesting approach to planar formation hold is using a heading-averaging method to coordinate the motions of autonomous agents. The aim of this method is to achieve a stable steady state where all agents move in the same direction, following a leader, without the use of centralized control [19]. The authors offered a simplified model that exhibited similar behaviour to bird flocking or fish schooling, without attempting to follow the leader's trajectory, but reaching a uniform final velocity after a period of time.

2.3 Related Motion Control Examples

A special 2D formation is discussed in [20] where a control scheme was developed for a fast-moving UAV following a slow-moving ground vehicle. Some geometric formulations proposed by the authors are used in the leader trajectory definition presented in this thesis.

Limitations applicable to trajectory planning are one major aspect of controlling the motions of a formation of vehicles. A straight-forward and yet comprehensive derivation of

some of these limitations was presented in [21] for an autonomous ground vehicle with fairly complex steering geometry. Although the present study does not focus on the kinematics of individual vehicles, the limitations placed on speed and turning radius in order to limit acceleration are still applicable.

An interesting approach to keeping track of the positions and motions of large numbers of bodies is the 'State-Time Space' approach proposed in [22]. The author used it to describe a situation with vehicles navigating among moving obstacles. Since tracking moving obstacles presents some similarities with tracking other vehicles, this approach could be used to describe the motion of formations of vehicles.

A large body of research also exists in the area of automated highway systems. The aim in this case is to develop automatic control algorithms for typical driving situations such as lane changes, separation from a platoon, joining a platoon, following a better actuated vehicle, etc, while maintaining formation stability [23-25].

2.4 3D Formation Control

More complex examples of formation motion control can be found in 3D motions of spacecraft, aircraft or submarines. Recently, intensive research has been conducted on coordinating motions of earth satellites [26-28]. Research has also been conducted on close formations of unmanned aircraft in order to use energy-saving aerodynamic effects [29]. Such formation flying techniques are modeled after various species of birds that use a type of V-formation to possibly save energy over long-distance flights and are concerned with maintaining a prescribed inter-vehicle spacing in the presence of vortices produced by the preceding aircraft.

2.5 Special Challenges of Formation Control

Formation motion often involves large numbers of vehicles that interact. This means that the formation may be dependent on the proper functioning of all its members. Considerable research has been done to develop control schemes that can deal with malfunctioning or disabled formation members so that adverse effects on the formation as a whole can be alleviated [30]. This thesis does not deal with such considerations.

3. Applications

Numerous applications of formations of automated vehicles have been identified in the literature: aerial imaging, ocean surveys, patrol or reconnaissance missions, automated highway systems, movement of agricultural machinery, mine-sweeping [31] and others.

Most vehicle control requiring independent vehicles to follow each other has been modeled based on human or animal formations. In 1974, the flight of Canada geese was studied in an attempt to identify the geometry of their formation flight and possible benefits that the birds may have from it [32]. In 1992, Huth and Wissel modeled the schooling behavior of fish, assuming there was no real leader present [33]. It is possible that adequate control schemes can be developed to allow for more reliable and closer-spaced formation hold than what has been possible up to now following the operation of these formations.

Closely spaced formations of vehicles have applications in enabling more vehicles to move through a given channel. Vehicle movement in close formation can also result in considerable fuel savings for the follower vehicles. The above applications can become part

of modern transportation infrastructure that already makes extensive use of sensing and control technology to improve traffic efficiency.

It should be noted that the 2D motion analysis presented in this thesis uses a holonomic vehicle model that represents holonomic vehicles such as airplanes, ships, submarines or omnidirectional ground vehicles. The results of this thesis do not apply to nonholonomic vehicles such as regular ground vehicles that are subject to the constraint of zero lateral velocity.

4. Platoon Stability in Linear Motion

4.1 Vehicle and Platoon Model

In this study, vehicles are modeled as point masses m_i, $i = 1,2,\ldots N$, in 1D motion. A platoon of N vehicles is shown in figure 1.

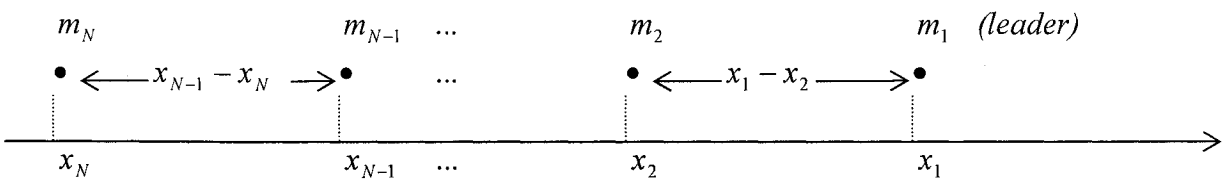

Figure 1 : Platoon with N vehicles moving in positive x-direction.

The following variables characterize the motion of the platoon:

u_1 is the system input (equal to acceleration profile of leader)

e_i is the state variable (spacing error of i-th vehicle)

The spacing error dynamics for each follower are expressed by the following equations:

$$e_i = x_{i-1} - x_i - L_i, \quad \dot{e}_i = \dot{x}_{i-1} - \dot{x}_i - \dot{L}_i, \quad \ddot{e}_i = \ddot{x}_{i-1} - \ddot{x}_i - \ddot{L}_i, \quad for\ i = 2,3,\ldots N \qquad (4.1.1)$$

where L_i is the desired spacing in front of *i*-th vehicle.

4.2 Spacing Policy

A *constant spacing policy* requires each vehicle to hold the same spacing $L_i = L$ to its predecessor no matter what the vehicle's speed is.

A *variable spacing policy* requires the *i*-th vehicle to hold a speed-dependent spacing $L_i = hv_i$ to its predecessor, where *h* is a constant.

4.3 String Stability

In linear motion, the predecessor-to-follower transfer function of spacing error is defined as follows:

$$G_i(s) = \frac{e_{i+1}(s)}{e_i(s)} \qquad (4.3.1)$$

where $|G_i(j\omega)|$ is the corresponding norm magnitude, and the time-domain form of $G_i(s)$, i.e. impulse response, is:

$$g_i(t) = L^{-1}G_i(s) \qquad (4.3.2)$$

String stability refers to spacing errors which are attenuated as they progress down the platoon. It was shown that the conditions for string stability are [1]:

$$|G_i(j\omega)| \leq 1, \forall \omega \geq 0 \quad and \quad g_i(t) \geq 0 \tag{4.3.3}$$

l_2 *-string stability* provides signals with bounded mean energy, but not necessarily with bounded magnitude. l_2 -string stability is less suitable for platooning applications. It was shown that the conditions for l_2 -string stability are [1]:

$$|G_i(j\omega)| \leq 1, \forall \omega \geq 0 \quad and \quad g_i(t) < 0 \tag{4.3.4}$$

String instability exists when spacing errors are amplified as they progress down the platoon. It was shown that the condition for string instability is [1]:

$$|G_i(j\omega)| > 1, \forall \omega \geq 0 \tag{4.3.5}$$

4.4 Linear Motion Control with Constant Spacing Policy

This control scheme is characterized by:

- constant inter-vehicle spacing L
- forward-looking (local) information only, sensed by the i-th vehicle: e_i *and* $\dot{e}_i$
- PD control law with acceleration u as the control variable and gains k and c:

$$u_i = k_i e_i + c_i \dot{e}_i \tag{4.4.1}$$

- actual accelerations $\ddot{x}_i$ identical at any time to acceleration commands u_i:

$$\ddot{x}_i = u_i \tag{4.4.2}$$

i.e.: transfer function of each vehicle is:

$$\frac{x_i(s)}{u_i(s)} = \frac{1}{s^2} \tag{4.4.3}$$

4.4.1 Analysis Using Transfer Function of Spacing Error

The vehicle model and the PD controller give the closed-loop vehicle system shown in figure 2.

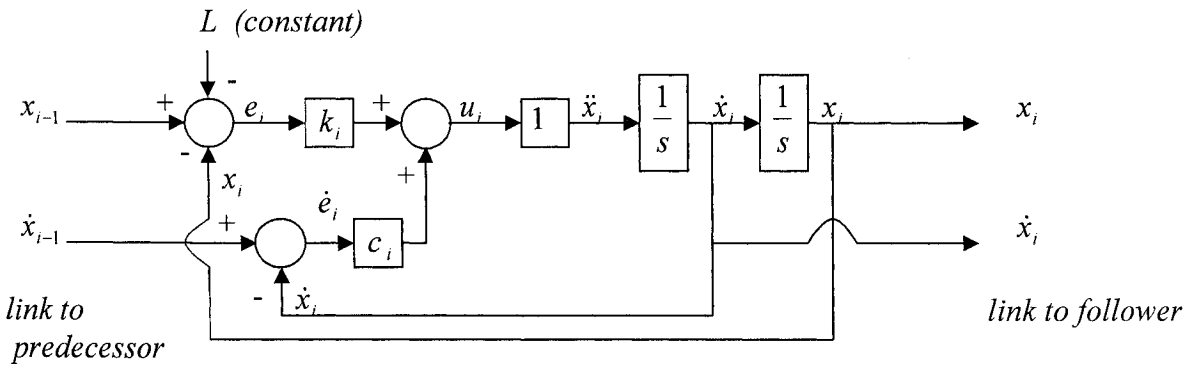

Figure 2 : Block diagram of PD control of *i*-th vehicle following a constant spacing policy. The vehicle is modeled as a double integrator.

The spacing error transfer function derivation obtained in [1] is shown below. From equations 4.1.1, 4.4.1 and 4.4.2, we have:

$$\begin{aligned}\ddot{e}_{i+1} &= u_i - u_{i+1} \\ &= k_i e_i + c_i \dot{e}_i - (k_{i+1} e_{i+1} + c_{i+1} \dot{e}_{i+1})\end{aligned} \tag{4.4.4}$$

Take Laplace transform assuming zero initial conditions:

$$s^2 e_{i+1}(s) = k_i e_i(s) + c_i s e_i(s) - k_{i+1} e_{i+1}(s) - c_{i+1} s e_{i+1}(s)$$
$$(s^2 + k_{i+1} + c_{i+1} s) e_{i+1}(s) = (k_i + c_i s) e_i(s)$$

$$G_i(s) = \frac{e_{i+1}(s)}{e_i(s)} = \frac{c_i s + k_i}{s^2 + c_{i+1} s + k_{i+1}} \tag{4.4.5}$$

If all vehicles have identical control gains, $c_i = c$ and $k_i = k$, $\forall i = 2,3,...N$, then

$$G_i(s) = G(s) = \frac{cs + k}{s^2 + cs + k} \quad \text{and}$$

$$|G(j\omega)| = \frac{|c(j\omega) + k|}{|(j\omega)^2 + c(j\omega) + k|} = \frac{|k + c\omega j|}{|k - \omega^2 + c\omega j|} \tag{4.4.6}$$

For $k > 0$ and with $0 < \omega < \sqrt{2k}$

$$|k + c\omega j| > |k - \omega^2 + c\omega j| \quad \Rightarrow \quad |G(j\omega)| > 1$$

Therefore, with all vehicles having identical control gains, this control scheme will, for $0 < \omega < \sqrt{2k}$, lead to the amplification of spacing errors as we progress down the platoon (as the vehicle index increases), which results in string instability.

If control gains can vary from vehicle to vehicle, then, for a four-vehicle platoon, we obtain two associated transfer functions:

$$G_1(s) = \frac{e_3(s)}{e_2(s)} = \frac{c_2 s + k_2}{s^2 + c_3 s + k_3}$$
$$G_2(s) = \frac{e_4(s)}{e_3(s)} = \frac{c_3 s + k_3}{s^2 + c_4 s + k_4} \tag{4.4.7}$$

It was shown [1] that the stability condition of $|G_i(j\omega)| \le 1, \forall \omega \ge 0$ requires:

$$k_4 > k_3 > k_2 \quad \textit{and} \quad c_4^2 > c_3^2 + 2k_3 > c_2^2 + 2k_4 + 2k_3 \tag{4.4.8}$$

This suggests that the control gains should generally increase as vehicle index increases. If $g_i(t) \ge 0$, string stability will be achieved. If $g_i(t) < 0$, l_2-string stability will be achieved.

For both equal and variable control gains, collision-free motions depend on: the spacing L, the platoon initial conditions and the acceleration profile of the leading vehicle.

4.4.2 Analysis Using Lyapunov Function of Spacing Error

This analysis is based on [5]. In the case of platoons, the state vector $\mathbf{x}$ that should be considered is:

1D constant spacing: $\mathbf{x} = (e_i, \dot{e}_i)$ (4.4.9)

1D variable spacing: $\mathbf{x} = (e_i, v_{i-1} - v_i)$ (4.4.10)

2D local information

2D constant spacing: $\mathbf{x} = (\mathbf{e}_i, \mathbf{v}_{i-1} - \mathbf{v}_i)$ (4.4.11)

2D variable spacing: $\mathbf{x} = (\mathbf{e}_i, \mathbf{v}_{i-1} - \mathbf{v}_i)$

2D global information, constant spacing: $\mathbf{x} = (\mathbf{e}_i, \dot{\mathbf{e}}_i)$ (4.4.12)

The equilibrium point for all of the above systems is: $\mathbf{x} = (0,0)$ (4.4.13)

To apply Lyapunov's direct method to 1D motion with a constant spacing policy, consider the control law:

$u = ke + c\dot{e}, \quad k, c > 0$

Assuming the predecessor has zero acceleration (no sustained perturbation, autonomous system):

$u = -\ddot{e} = ke + c\dot{e}$ (4.4.14)

Consider the "energy-like" Lyapunov function:

$$V(\mathbf{x}) = \frac{1}{2}ke^2 + \frac{1}{2}\dot{e}^2, \quad \mathbf{x} = (e, \dot{e}) \tag{4.4.15}$$

This function is *positive-definite* because $V(\mathbf{0}) = 0$ and $V(\mathbf{x} \neq \mathbf{0}) > 0$

$$\begin{aligned} \dot{V} &= ke\dot{e} + \dot{e}\ddot{e} \\ &= \dot{e}(ke + \ddot{e}) \\ &= \dot{e}(ke - ke - c\dot{e}) \\ &= -c(\dot{e})^2 \leq 0, \quad \text{if } c > 0 \end{aligned} \tag{4.4.16}$$

Since $\dot{V}$ is *negative semi-definite*, the system is *stable* around the equilibrium point $\mathbf{x} = \mathbf{0}$. Because the invariant set is $M = (e = 0, \dot{e} = 0)$, the system is *asymptotically stable* by the Invariant Set Theorem [5].

Because the unperturbed system is linear, this also implies *total stability*, which means that the system can withstand *small sustained* perturbations [5]. In the case of the platoon of vehicles, the sustained perturbation is the sinusoidal acceleration profile of the leader ($u_1 = \sin t$).

Perhaps the Lyapunov analysis presented above can also be applied to the 2D constant spacing system with global information where the control law is $\mathbf{u}_i = k\mathbf{e}_i + c\dot{\mathbf{e}}_i$ and state vector is $\mathbf{x} = (\mathbf{e}_i, \dot{\mathbf{e}}_i)$.

4.4.3 Simulation Using Simulink Model

The Simulink model used in this control scheme as well as solver settings and description are shown in Appendix A. The study has the purpose of verifying that the results of the simulation agree with the mathematical analysis presented above. Figure 3 shows that vehicle spacing errors are *amplified* down the platoon. This agrees with the transfer function mathematical analysis. Also, signals do not seem to amplify over time which would agree with the Lyapunov function analysis.

The settings of the solver used for the simulation have a significant influence on the results. A fixed-step solver was used with a relatively small step size. This solver also suited the other more complex 2D simulations (performed in the latter part of this study) that incorporated time delays.

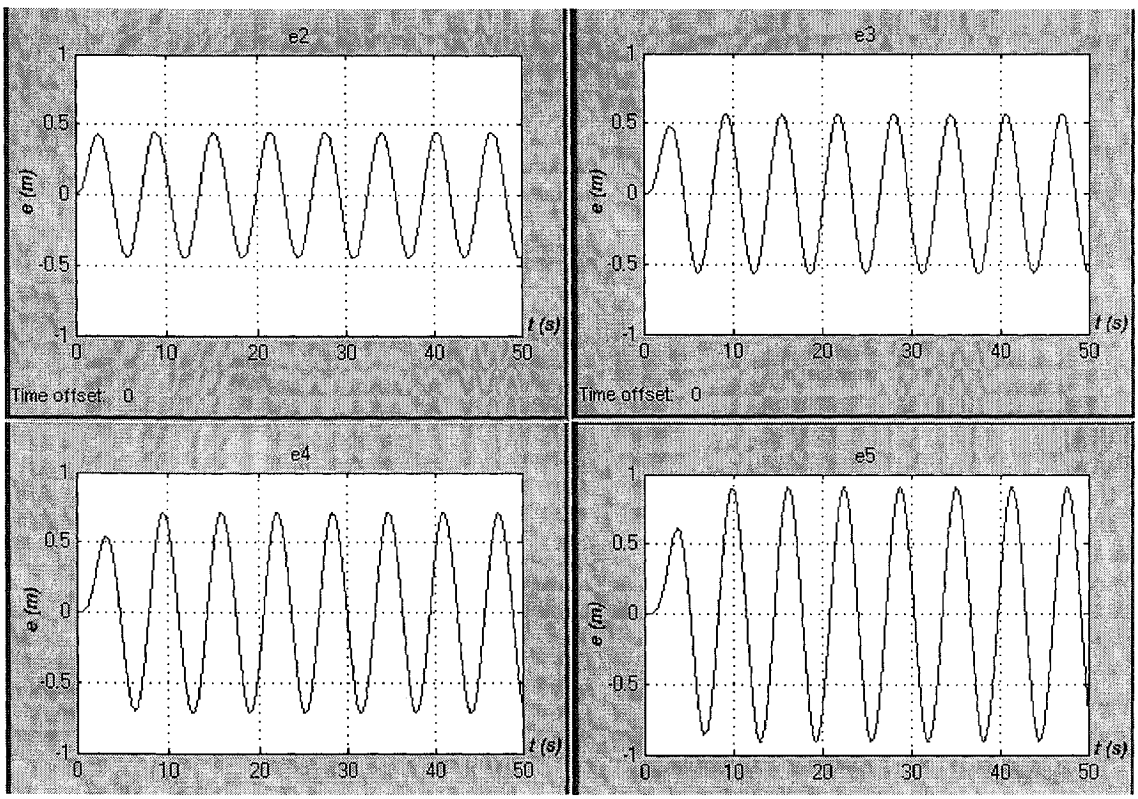

Figure 3 : Follower spacing errors for linear motion with a constant spacing policy and $u = \sin(t)$, $L = 2$ *m*, $c = k = 2$.

A result of the amplified spacing errors is an amplification of accelerations used by the followers down the platoon: they have amplitudes greater than the leader's acceleration amplitude of 1 ($u_1 = \sin t$, see figure 4). The physical interpretation of this result is that the control law is forcing each follower to use greater control effort than its predecessor, which is undesirable.

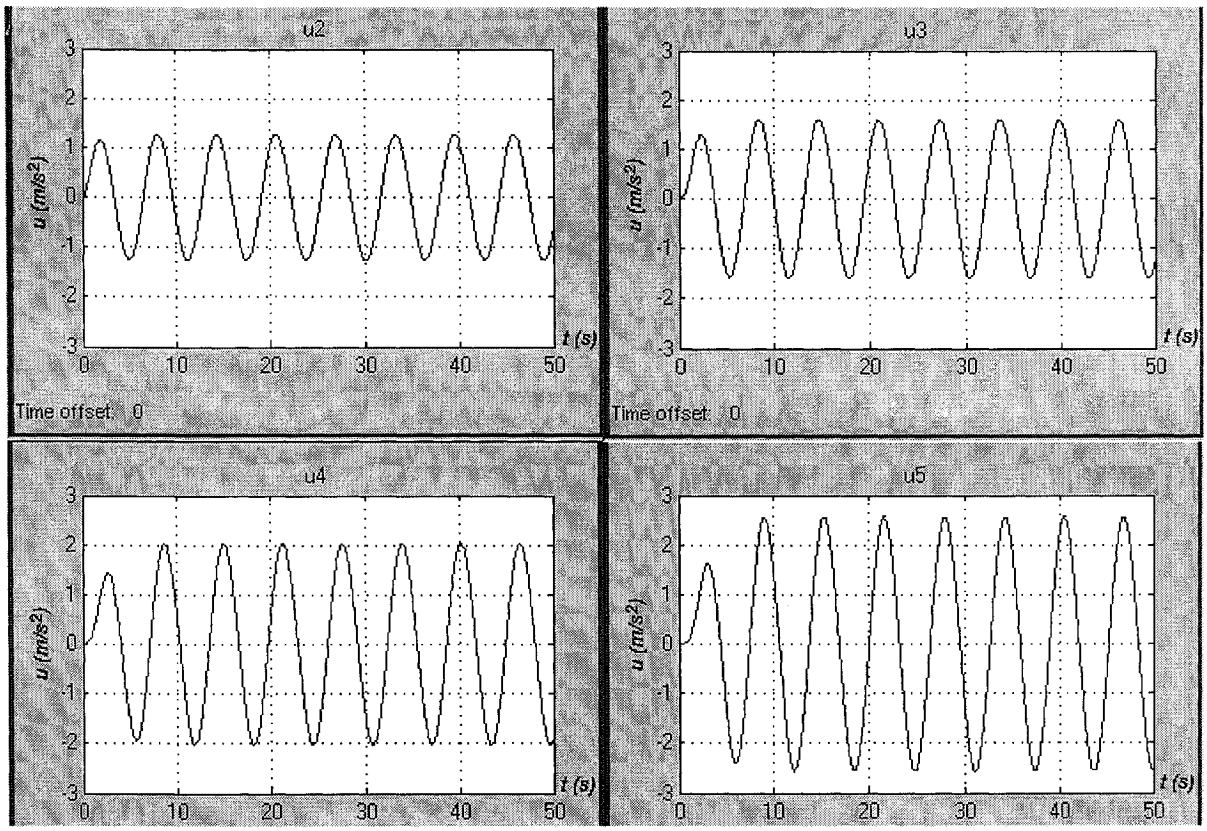

Figure 4 : Follower accelerations for linear motion with a constant spacing policy and $u_1 = \sin(t)$, $L = 2$, $c = k = 2$.

The velocities and trajectories that result from this control scheme become increasingly disturbed as the position of the follower is further down the platoon. From figure 5, we can

see that while the leader's velocity is positive ($v1 \geq 0$), the followers move increasingly forward and backward behind the leader with both positive and negative velocities.

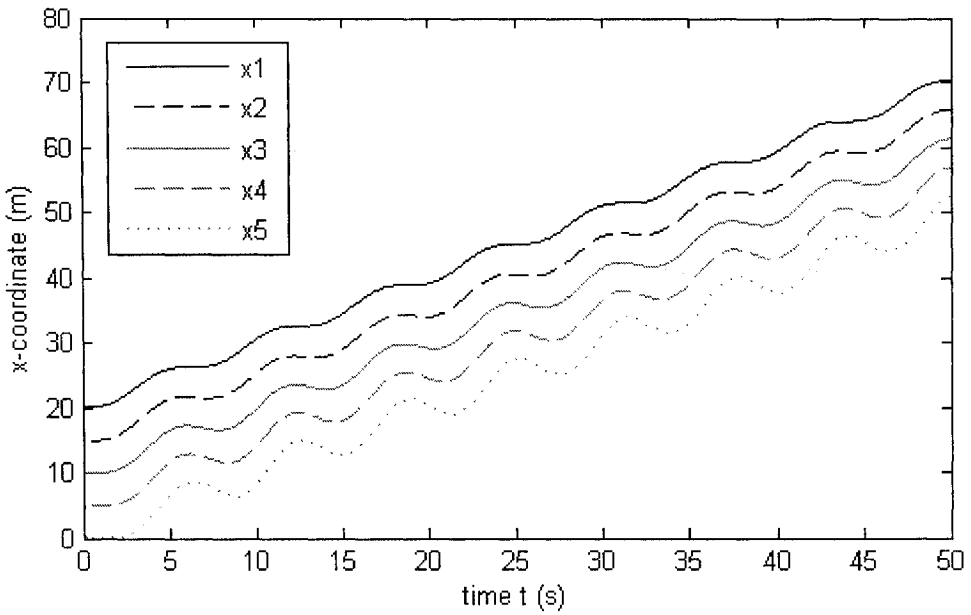

Figure 5 : Trajectories of leader and followers in linear motion with a constant spacing policy and $u = \sin(t)$, $L = 2$, $c = k = 2$.

In general, we can say that this 1D fixed spacing control scheme is not satisfactory: with more followers, it would lead to actuator saturation that would limit acceleration capability of the vehicles and possibly cause collisions. A constant spacing policy is attractive from the point of view of tight formation hold which could, for example, allow very high traffic throughput on an automated highway, but it is difficult to control in a stable manner, at least in this 1D configuration.

4.5 Linear Motion Control with Variable Spacing Policy

This control scheme is characterized by:

- Variable (speed-dependent) inter-vehicle spacing $L_i = hv_i$
- Forward-looking (local) information only, sensed by the i-th vehicle: e_i *and* $v_{i-1} - v_i$
- PD control law:

$$u_i = ke_i + c(v_{i-1} - v_i) \tag{4.5.1}$$

4.5.1 Analysis Using Transfer Function of Spacing Error

Canudas and Brogliato presented the spacing error transfer function that results from this control scheme [1]. Below is a derivation of their result.

From equations for variable (velocity-dependent) inter-vehicle spacing error, we have:

$$e_i = x_{i-1} - x_i - hv_i \tag{4.5.2}$$

Take time derivative:

$$\begin{aligned} \dot{e}_i &= \dot{x}_{i-1} - \dot{x}_i - h\dot{v}_i \\ &= v_{i-1} - v_i - hu_i \end{aligned} \tag{4.5.3}$$

$$\therefore v_{i-1} - v_i = \dot{e}_i + hu_i \quad and \quad v_i - v_{i+1} = \dot{e}_{i+1} + hu_{i+1} \tag{4.5.4}$$

From the control law equations, increase index to $i + 1$:

$$u_{i+1} = ke_{i+1} + c(v_i - v_{i+1}) \tag{4.5.5}$$

Take time derivative:

$$\dot{u}_{i+1} = k\dot{e}_{i+1} + c(u_i - u_{i+1}) \tag{4.5.6}$$

Take time derivative of eq. 4.5.3:

$$\ddot{e}_{i+1} = u_i - u_{i+1} - h\dot{u}_{i+1} \qquad \text{substitute eqs. 4.5.1, 4.5.5 and 4.5.6}$$
$$= [ke_i + c(v_{i-1} - v_i)] - [ke_{i+1} + c(v_i - v_{i+1})] - h[k\dot{e}_{i+1} + c(u_i - u_{i+1})]$$

Remove square brackets and sub eqs. 4.5.4

$$\ddot{e}_{i+1} = ke_i + c(\dot{e}_i + hu_i) - ke_{i+1} - c(\dot{e}_{i+1} + hu_{i+1}) - hk\dot{e}_{i+1} - ch(u_i - u_{i+1})$$

Collect like terms and simplify

$$\ddot{e}_{i+1} = ke_i + c\dot{e}_i + chu_i - ke_{i+1} - c\dot{e}_{i+1} - chu_{i+1} - hk\dot{e}_{i+1} - ch(u_i - u_{i+1})$$
$$= ke_i + c\dot{e}_i - ke_{i+1} - c\dot{e}_{i+1} - hk\dot{e}_{i+1} - ch(u_i - u_{i+1}) + ch(u_i - u_{i+1})$$
$$= ke_i + c\dot{e}_i - ke_{i+1} - c\dot{e}_{i+1} - hk\dot{e}_{i+1}$$

Rearrange:

$$\ddot{e}_{i+1} + ke_{i+1} + c\dot{e}_{i+1} + hk\dot{e}_{i+1} = ke_i + c\dot{e}_i$$

Take Laplace transform with zero initial conditions:

$$(s^2 + hks + cs + k)e_{i+1}(s) = (k + cs)e_i(s)$$

$$\therefore G(s) = \frac{e_{i+1}(s)}{e_i(s)} = \frac{k + cs}{s^2 + (c + hk)s + k} \tag{4.5.7}$$

where h is used to provide *additional damping*.

The magnitude of the transfer function is:

$$|G(j\omega)| = \left|\frac{k + c(j\omega)}{(j\omega)^2 + (c + hk)(j\omega) + k}\right|$$
$$= \frac{|k + c\omega j|}{|k - \omega^2 + (c + hk)\omega j|} \tag{4.5.8}$$

Assuming that $g(t) > 0$ and choosing appropriate c, k and h, this control scheme will lead to the attenuation of spacing errors ($|G(j\omega)|<1$) as we progress down the platoon (as the vehicle index increases) and result in string stability.

Figure 6 shows the transfer function magnitude for specific values of parameters k, c and h. The figure shows that, with these parameter values, the magnitude of the transfer function is 1 when frequency ω is zero and decreases monotonically towards zero as frequency ω increases. This means that, with the given parameter values (similar to the ones used in [1]), the system is string stable for all frequency ω.

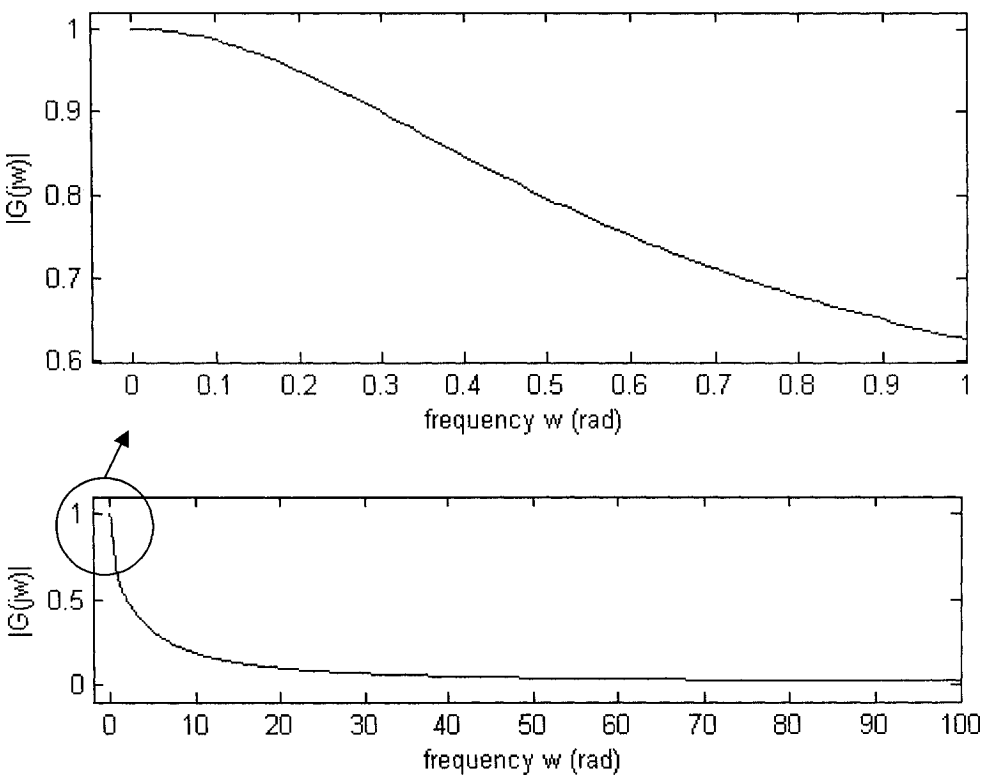

Figure 6 : Magnitude of the spacing error transfer function $|G(j\omega)|$ as a function of frequency ω, with $k = c = 2$, and $h = 1.2$.

Canudas and Brogliato mentioned that string stability in itself does not guarantee collision-free motions [1]. They proposed to explicitly account for vehicle collisions in the future design of controllers.

4.5.2 Analysis Using Lyapunov Function of Spacing Error

For 1D motion with a variable spacing policy, the control law is:

$$u_i = ke_i + c(v_{i-1} - v_i) = \dot{v}_i, \quad k, c > 0$$

For simplicity, let: $v_{i-1} - v_i = z$, $e_i = e$ *and* $v_i = v$, then

$$u_i = ke + cz = \dot{v} \tag{4.5.9}$$

Assume $v_{i-1} = 0$ (no acceleration for predecessor, autonomous system), then

$$\dot{z} = -\dot{v} = -ke - cz \tag{4.5.9}$$

Spacing error defined as:

$$e_i = x_{i-1} - x_i - hv_i, \quad h > 0$$

with time derivative:

$$\begin{aligned} \dot{e}_i &= v_{i-1} - v_i - h\dot{v}_i \\ &= v_{i-1} - v_i - hu_i \end{aligned}$$

$$\begin{aligned} \dot{e} &= z - h\dot{v}_i \\ &= z - hu_i \\ &= z - h(ke + cz) \end{aligned} \tag{4.5.10}$$

Consider the Lyapunov function:

$$V = \frac{1}{2}ke^2 + \frac{1-hc}{2}z^2 \tag{4.5.11}$$

This function is *positive-definite* if $1 - hc > 0$.

$$
\begin{aligned}
\dot{V} &= ke\dot{e} + (1-hc)z\dot{z} \\
&= ke[z - h(ke + cz)] + (1-hc)z[-ke - cz] \\
&= kez - hk^2e^2 - hczke - kze - cz^2 + hczke + hc^2z^2 \\
&= -hk^2e^2 - cz^2 + hc^2z^2 \\
&= -hk^2e^2 - (1-hc)cz^2
\end{aligned}
\tag{4.5.12}
$$

If $1 - hc > 0$, this function is *negative-definite* and the system is *stable*.

It should be noted that $1 - hc > 0$ is a *sufficient* but *not necessary* condition. In fact, h and c were each increased up to the computational limit of the simulation system, without making the formation lose stability.

This analysis may also be valid for 2D motion with local information where $\mathbf{u}_i = k\mathbf{e}_i + c(\mathbf{v}_{i-1} - \mathbf{v}_i)$.

4.5.3 Simulation Using Simulink Model

Several Simulink models were built and executed. The basic model is shown in Appendix B. Solver settings used were identical to the previous model (Section 4.4.2). The simulations had the purpose of verifying the results from the analytical approach, i.e. that a variable (speed-dependent) spacing policy can produce spacing errors that are attenuated down the platoon and that show stability over time.

To allow comparisons, the simulation here uses the same k and c parameters as the ones used in section 4.4.2., the main change being the variable spacing policy defined by the parameter h. The values used are similar to [1]: $k = 2$, $c = 2$, $h = 1.2$, for which the transfer function approach predicts string stability (see figure 6) and the Lyapunov analysis does *not* guarantee stability over time. However, the Lyapunov analysis condition $h < \frac{1}{c}$ did not seem

to represent a time stability limit because simulations that complied with the condition had similar behaviour over time as the simulation presented below: no error amplification over time.

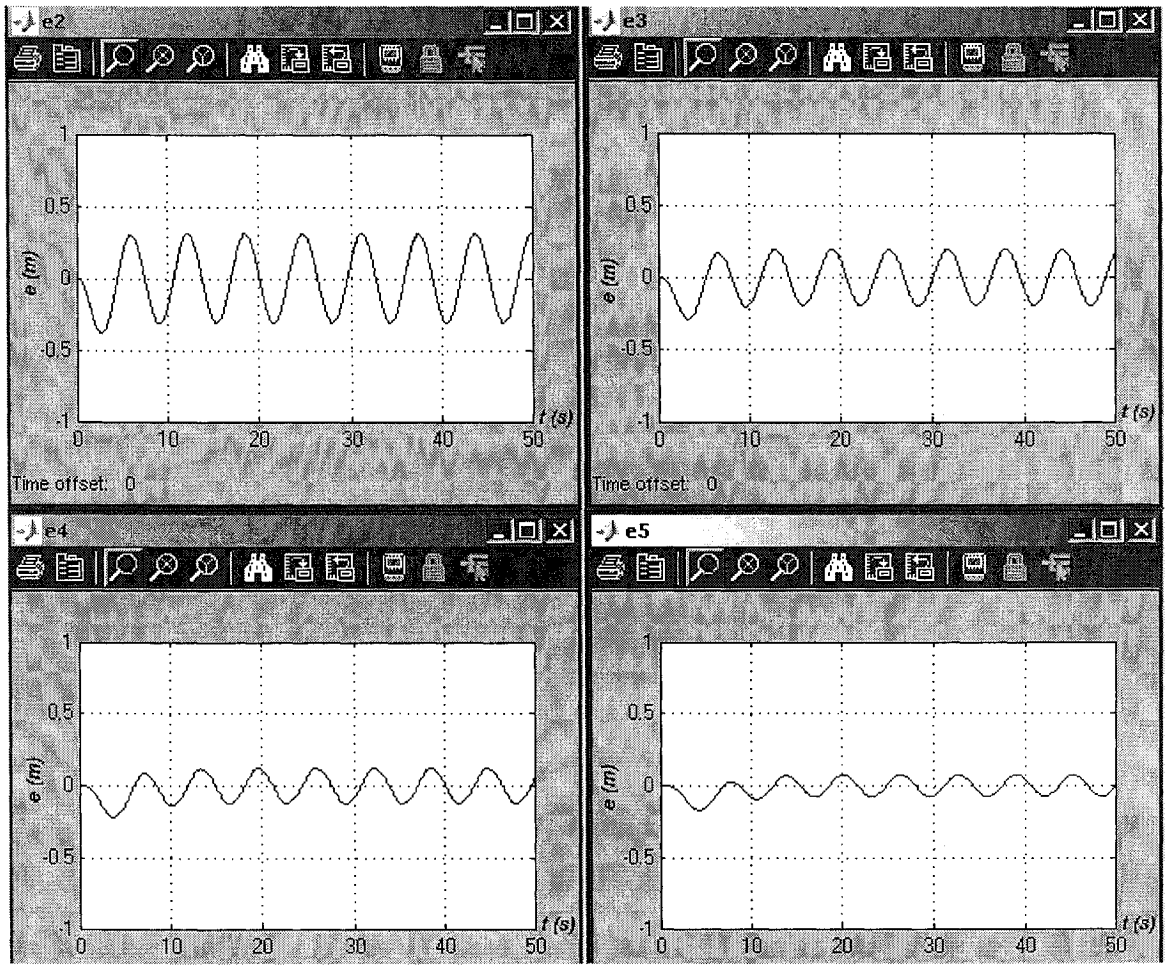

Figure 7 : Follower spacing errors for 1D motion with a variable spacing policy and $v_i(0) = 0$, $u1 = \sin(t)$, $k = c = 2$, $h = 1.2$.

In figure 7, it is interesting to note the smaller amplitude transient regime for vehicle 5 than for its predecessors. A result of diminishing spacing error amplitude of oscillation is a reduction of the amplitudes of acceleration oscillation. As vehicle index increases, it seems that the velocity tends to a constant and the deviations from the leader's trajectory become amplified, but remain bounded (see figure 8).

Note that the slope of the position versus time graphs shown in figure 8 represents each vehicle's velocity versus time. It is clear that abrupt changes in the leader's velocity are quickly attenuated by this control scheme, which was not the case in the constant spacing control scheme (see figure 5).

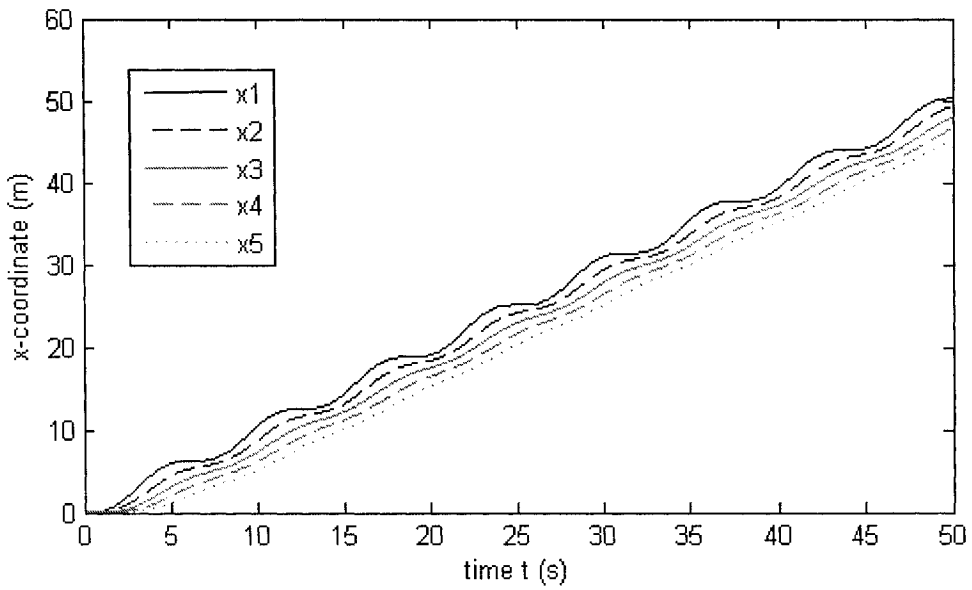

Figure 8 : Positions of leader and followers in 1D motion with a variable spacing policy and $v_i(0) = 0$, $u1 = \sin(t)$, $k = c = 2$, $h = 1.2$.

In fact, cautious drivers also increase their spacing with regard to their predecessor when their velocity increases. The trade-off of this control scheme is increased total space needed to contain a given number of vehicles. Also, the leader's trajectory is adhered to quite loosely by the followers.

5. Simulation Analysis of the Transient Behavior of Strings of Holonomic Vehicles in Planar Motion

5.1 Defining the Leader's Path

In 1D motion, the path followed by all vehicles is a straight line. For planar motion, it is a two-dimensional curve that is tracked. A type of path that is important to analyze is a sinusoid about the x-axis such as shown in figure 9 below. It is known that Fourier series permit to decompose any trajectory into a combination of sinusoids.

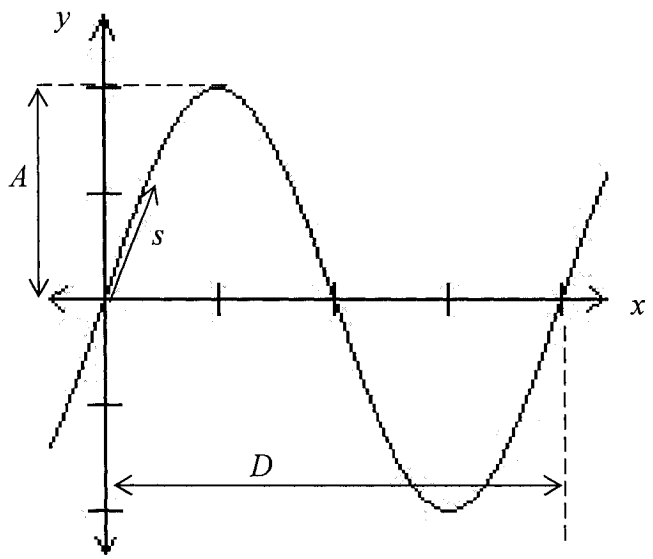

Figure 9 : Sinusoidal path for a 2D (planar) trajectory.

The equation of the path shown above, using Cartesian x-y coordinates, is:

$$y = f(x) = A\sin\left(\frac{2\pi}{D}x\right) \tag{5.1.1}$$

It should be noted that the path is independent of time. This means that the speed at which the vehicle travels along the path remains to be defined.

5.2 Defining the Leader's Trajectory

Given the relationship between horizontal position x and time t, the speed of the vehicle can be obtained and the *trajectory* is defined:

$$x = g(t) \quad \Rightarrow \quad y = f(g(t)) \tag{5.2.1}$$

The trajectory gives the position of the vehicle at any moment in time. From this relationship, we can obtain the vehicle's path as well as its velocity and acceleration, in any convenient set of coordinates such as Cartesian (x-y) or curvilinear (s).

The 2D simulations presented below use the following relationship:

$$x = g(t) = bt - d\cos t + d \quad \Rightarrow \quad \dot{x} = b + d\sin t$$

Where b and d are constants and t is time. Since d is chosen small relative to b, $g(t)$ can be approximated by the linear relationship:

$$x = g(t) = bt \tag{5.2.2}$$

Eq. 5.1.1 can then be written as:

$$y = f(g(t)) = A\sin\left(\frac{2\pi bt}{D}\right) \tag{5.2.3}$$

Differentiating with respect to time gives velocity and acceleration components in the y-direction:

$$\dot{y} = \frac{A2\pi b}{D}\cos\left(\frac{2\pi bt}{D}\right) \tag{5.2.4}$$

$$\ddot{y} = -A\left(\frac{2\pi b}{D}\right)^2 \sin\left(\frac{2\pi bt}{D}\right) \tag{5.2.5}$$

We can see that the magnitudes of velocity and acceleration x-y components are:

$$\dot{x} = b \quad \Rightarrow \quad |\dot{x}| = b \tag{5.2.6}$$

$$\ddot{x} = 0 \quad \Rightarrow \quad |\ddot{x}| = 0 \tag{5.2.7}$$

$$|\dot{y}| \le \frac{A2\pi b}{D} \tag{5.2.8}$$

$$|\ddot{y}| \le A\left(\frac{2\pi b}{D}\right)^2 \tag{5.2.9}$$

The speed v of the vehicle (the time-derivative of path-wise coordinate s) can be obtained from the x-y components:

$$\begin{aligned} v &= \dot{s} \\ &= \sqrt{\dot{x}^2 + \dot{y}^2} \\ &= \sqrt{b^2 + \left(\frac{A2\pi b}{D}\cos\left(\frac{2\pi bt}{D}\right)\right)^2} \end{aligned} \tag{5.2.10}$$

It is useful to note that the velocity **v** of the vehicle is always tangent to the path, pointing in the positive s-direction. For the sinusoidal trajectory described above, the magnitude of velocity **v** (or speed v) is approximately bounded as follows:

$$|\mathbf{v}| = v = \dot{s} \leq \sqrt{b^2 + \left(\frac{A2\pi b}{D}\right)^2} \tag{5.2.11}$$

In the case of acceleration **a**, only the y-component needs to be considered since acceleration in the x-direction is relatively small. Therefore, for the same trajectory, the magnitude of acceleration **a** is approximately bounded as follows:

$$|\mathbf{a}| = |\ddot{y}| \leq A\left(\frac{2\pi b}{D}\right)^2 \tag{5.2.12}$$

It should be noted that maximum speed and acceleration in the trajectory are a function of A, b, d and D. All four parameters must be matched appropriately so that the trajectory does not demand control efforts that are beyond the capability of a specific vehicle. Simulations presented from here on impose a saturation limit of 5 m/s^2 on acceleration in the y and x-direction and the leader's trajectory is chosen not to exceed these limits. No limits are placed in this study on vehicle velocity (this could represent spacecraft moving in free space).

5.3 Constraints on the Leader's Trajectory

In the design of a trajectory for the leading vehicle, we should consider two main constraints:

1. Limitations of the individual vehicle such as top acceleration (for the case of speeding up, slowing down or turning) and top speed;
2. Limitations imposed on the leader's acceleration, speed as well as path, because of its formation of followers.

The first constraint is illustrated by the top speed that is a characteristic of most vehicles and by top acceleration which is commonly described as speeding up or slowing down (acceleration directed along path s) and as turning (acceleration normal to path s). It is important to note that acceleration **a** is a vector quantity defined as the rate of change of velocity **v** (another vector quantity). For most vehicles, the limits on acceleration magnitude vary depending on its direction: for a front-wheel-drive car, braking can usually generate higher acceleration than speeding up; for a boat or airplane, lateral acceleration due to tight turning is normally the source of highest acceleration.

The second constraint is illustrated by human-controlled formation motions where the driver of a leading vehicle such as a car, boat or aircraft, has to impose additional restrictions on acceleration, speed or radius of turn to enable the followers to maintain their formation. If the leading vehicle was traveling alone, it could follow a given path faster, or could follow paths that are unsuitable for an entire formation of vehicles.

Let us consider an omni-directional vehicle. A constraint on the motion of this vehicle could be maximum speed v_{MAX} with the following approximate relationship:

$$|\mathbf{v}| = v = \dot{s} \leq \sqrt{b^2 + \left(\frac{A2\pi b}{D}\right)^2} \leq v_{MAX} \tag{5.3.1}$$

Another constraint could be maximum acceleration a_{MAX}. This limit applies to the total net acceleration of the vehicle, which is the sum of accelerations resulting from speeding up, slowing down or turning.

For the leading vehicle that follows the sinusoidal trajectory described above, acceleration has only a significant y-component:

$$|\mathbf{a}| = |\ddot{y}| \leq A\left(\frac{2\pi b}{D}\right)^2 \leq a_{MAX} \tag{5.3.2}$$

Another type of constraint on parameters of the leader's trajectory results from the "road width" required for a certain formation to follow the leader within a certain tolerance. This constraint will allow for smooth boundaries of a 'roadway' region situated at a distance R on either side of the path of the leader. Figure 10 shows two circles of radius R moving along the sinusoidal path. For the centers of the circles to create smooth paths, the minimum radius of curvature of the sinusoid (r) must be greater than the radius of the circles (R).

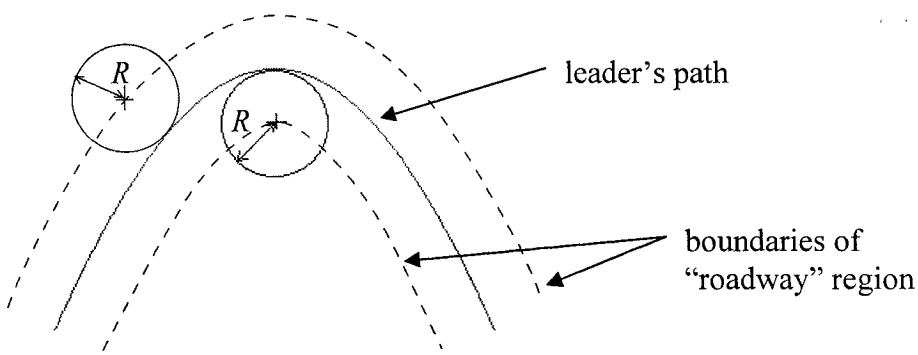

Figure 10 : Maximum of the sinusoidal path showing two circles of radius R used to trace the boundaries of the "roadway" region.

The minimum radius of curvature of the sinusoidal path occurs at a maximum or a minimum of the sinusoid. At the maximum, the acceleration experienced by a particle traveling along the path is directed practically straight down and $v = \frac{dx}{dt}$ for the particle.

At the maximum,

$$a = A\left(\frac{2\pi b}{D}\right)^2 \quad and \quad v = b = \frac{dx}{dt} \tag{5.3.3}$$

Let the sinusoid have curvature of radius r, then

$$a = \frac{v^2}{r} \quad \Rightarrow \quad A\left(\frac{2\pi b}{D}\right)^2 = \frac{v^2}{r}$$

or

$$A\left(\frac{2\pi v}{D}\right)^2 = \frac{v^2}{r}$$

or

$$A\left(\frac{2\pi}{D}\right)^2 = \frac{1}{r} \quad \Rightarrow \quad r = \frac{1}{A}\left(\frac{D}{2\pi}\right)^2 \tag{5.3.4}$$

For a ground vehicle, this radius of curvature r must be larger than roadway half-width R to allow for smooth boundaries of the roadway. To account for the linearization of the displacement in the x-direction (eq. 5.2.1) and to create a certain safety margin, let us adopt the following constraint:

$$R < \frac{r}{2} \quad \Rightarrow \quad R < \frac{1}{2A}\left(\frac{D}{2\pi}\right)^2 \tag{5.3.5}$$

This condition will create a path that will have a smoothly-bounded margin: it models a roadway where the leader traces the centerline and its followers must stay within a set normal distance R to this centerline. Using this model, a narrow roadway allows for smaller radii of curvature (such as in a small winding road) while a wide road allows for only relatively gentle turns (such as a freeway). It should be noted that a narrow roadway, irrespective of its curvature, leaves little room for lateral spacing error of the followers.

In this sense, the "roadway" can be virtual and can represent a margin of error on either side of the leader's trajectory. A ground, water or aerial vehicle would have to stay within this margin of lateral error to maintain formation, i.e. stay within a corridor defined by the "virtual roadway".

5.4 String Stability

One way to extend the concept of string stability to 2D is to expect the followers to:

- attenuate spacing errors *along* path s and position errors *normal* to path s as vehicle index increases (down the platoon), or,
- attenuate the magnitude of the spacing error vector as vehicle index increases.

5.5 Formation Hold

One way to define formation hold is to set an upper limit on acceptable inter-vehicle spacing. For the sake of this study, if inter-vehicle spacing grows to more than double the intended spacing, we will consider the vehicle to have lost formation.

5.6 Possibility of Collisions

It should also be noted that the model defined above cannot detect collisions since all vehicles are modeled as point masses that occupy no space and for a collision to occur, two vehicles would have to have exactly identical positions, which, in this simulation, is highly unlikely.

If the magnitude of the spacing error **e** is comparable to the magnitude of desired inter-vehicle spacing **L**, collisions are *possible*, depending on the directions of both vectors. However, in the analysis that follows, the magnitudes of *inter-vehicle spacing vectors* l_i will be used for collision detection. Collisions will be assumed to occur when inter-vehicle spacing falls below $0.2m$. This creates a circular "safety bubble" around each point mass with a radius of $0.1m$.

5.7 Information (Signal Inputs) Available to Followers

In controlling the motion of a formation of vehicles, it is useful to identify two general types of information:

1. *Local information*, for a given vehicle, which includes the vehicle's absolute position, velocity and acceleration as well as relative positions, velocities and accelerations of vehicles immediately preceding and following the given vehicle. It is assumed that this type of information can be *sensed* directly by the vehicle. The control schemes considered first in this study make use of local information only.
2. *Global information* that characterizes the entire formation of vehicles. This type of information includes a record of the trajectory of the leader up to the

current time. It can also include the absolute position, velocity and acceleration of each vehicle in the formation. It is assumed that this type of information must be *communicated* from vehicle to vehicle and thus is available at a greater cost and may involve greater delays than information sensed locally.

5.8 Set of Initial Conditions

A set of initial conditions was assumed where the platoon is in *perfect linear formation* behind the leader that at this instant has nearly constant velocity (figure 11) and the followers have the same velocity with zero spacing error. If the leader maintains this velocity, all errors will remain zero and all vehicles will continue in uniform motion indefinitely. The perfect linear formation is therefore an *equilibrium state*. When the leader's motion is perturbed (acceleration is introduced at $t = 0$), spacing errors appear and the followers must adjust their motion and hopefully stay close to the equilibrium state of zero spacing error.

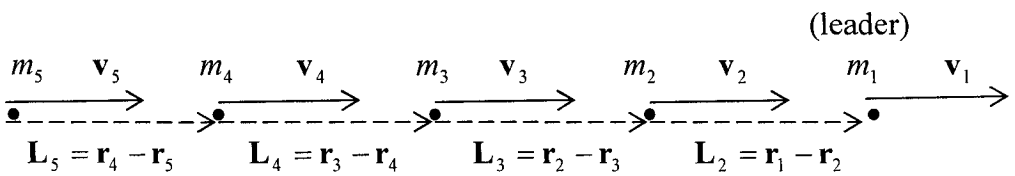

Figure 11 : Platoon with a leader and 4 followers in perfect linear formation.

The start ($t = 0$) of the sinusoidal trajectory shown in figure 9 is a good initial condition for the leader because the leader is moving at nearly constant velocity. From equation 2.1 and 5, we have:

$$\left|\frac{d\mathbf{v}_1}{dt}\right| = \left|\frac{d^2\mathbf{r}_1}{dt^2}\right| = |\mathbf{a}| \cong |\ddot{y}| = \left| -A\left(\frac{2\pi b}{D}\right)^2 \sin\left(\frac{2\pi b t}{D}\right)\right| = 0 \quad if \quad t = 0 \tag{5.8.1}$$

5.9 Planar Control, Local Information, Constant Spacing

Similar to section 4.4, this control scheme is characterized by:

- Constant inter-vehicle spacing distance L
- Forward-looking local information only, sensed by the i-th vehicle: $\mathbf{e}_i$ and $\mathbf{v}_{i-1} - \mathbf{v}_i$
- PD control law: $\mathbf{u}_i = k\mathbf{e}_i + c(\mathbf{v}_{i-1} - \mathbf{v}_i)$, where k and c are constants
- actual accelerations $\ddot{\mathbf{x}}_i$ identical to acceleration commands $\mathbf{u}_i$

Note that here vector quantities have replaced scalar quantities from section 4.4 because here the case of two-dimensional motion is considered.

5.9.1 Definition of Spacing Error

Note that the desired inter-vehicle spacing $\mathbf{L}_i$ has constant magnitude L but variable direction which follows the direction of the velocity of the i-th vehicle:

$$\mathbf{L}_i = \frac{\mathbf{v}_i}{v_i} L \tag{5.8.2}$$

where $\frac{\mathbf{v}_i}{v_i}$ is a unit-vector in the direction of $\mathbf{v}_i$.

In figure 12, the *targeted* displacement of m_{i-1} relative to m_i is $\mathbf{L}_i$. The *actual* displacement of m_{i-1} relative to m_i is $\mathbf{r}_{i-1} - \mathbf{r}_i$.

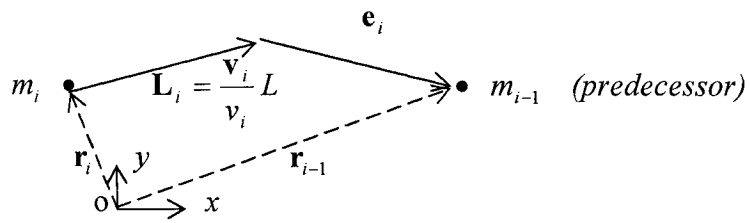

Figure 12 : i-th vehicle and its predecessor in planar motion with local information and constant spacing distance L.

Thus, the error vector is:

$$\mathbf{e}_i = \mathbf{r}_{i-1} - \mathbf{r}_i - \mathbf{L}_i \tag{5.8.3}$$

where $\mathbf{r}_{i-1}$ and $\mathbf{r}_i$ are absolute position vectors of vehicles i-1 and i respectively.

Figure 13 shows the closed-loop block diagram of the i-th vehicle and PD controller.

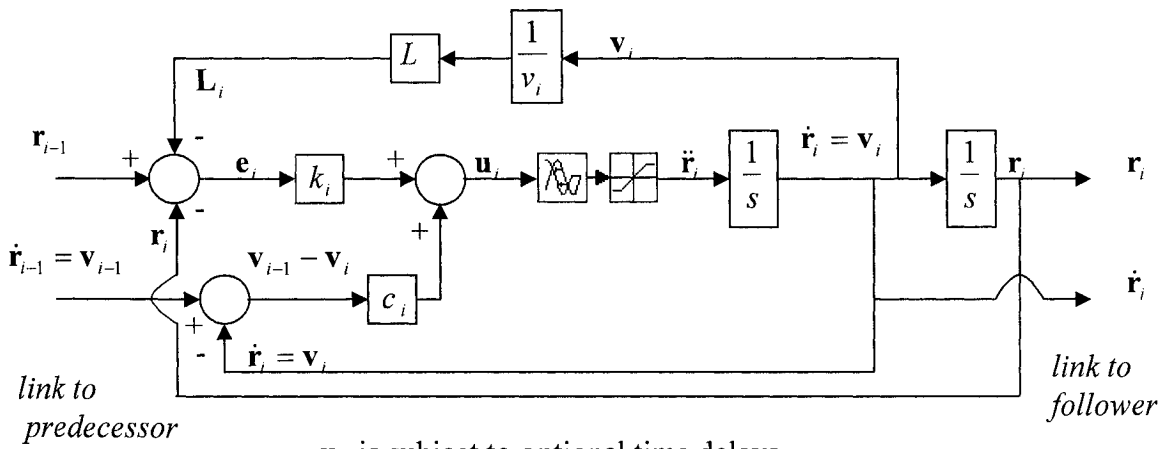

$\mathbf{u}_i$ is subject to optional time delays

$\ddot{\mathbf{r}}_i$ is subject to x and y-saturation constraints

Figure 13 : Block diagram of PD control of i-th vehicle following a constant spacing policy in 2D motion. The vehicle is modeled as a double integrator.

It should be noted that:

$$\begin{aligned}\dot{\mathbf{e}}_i &= \dot{\mathbf{r}}_{i-1} - \dot{\mathbf{r}}_i - \dot{\mathbf{L}}_i = \mathbf{v}_{i-1} - \mathbf{v}_i - \dot{\mathbf{L}}_i \\ &\neq \mathbf{v}_{i-1} - \mathbf{v}_i \\ &\textit{and} \\ \ddot{\mathbf{e}}_i &= \ddot{\mathbf{r}}_{i-1} - \ddot{\mathbf{r}}_i - \ddot{\mathbf{L}}_i = \mathbf{u}_{i-1} - \mathbf{u}_i - \ddot{\mathbf{L}}_i \\ &\neq \mathbf{u}_{i-1} - \mathbf{u}_i\end{aligned} \tag{5.8.4}$$

This is because $\mathbf{L}_i$ is not a constant: it has constant magnitude but variable direction. For this reason, the 1D transfer function analysis of section 4.4 does not apply to 2D motion (for example, equation 4.4.1 does not apply).

5.9.2 Simulation using Simulink Model

The Simulink model used for this simulation is shown in Appendix C. Since delays were introduced on the control variable actuation, a fixed-step solver was used in this simulation to ensure that simulation time-step was small relative to the delays. The same time-step size and solver was used in all simulations discussed in this thesis.

5.9.3 General System Behavior

It is important to note that *deviations from the leader's path are amplified* down the platoon but remain bounded (paths approach a straight line, see figure 14). Because vehicles have local sensing only in this control scheme (they don't know the leader's trajectory), they cannot target the leader's path (or trajectory) and they only aim to keep a certain distance in front of them with regard to their predecessor. Using this spacing policy, *spacing errors are attenuated* down the platoon.

Feedback gains of $k = c = 5$ were chosen as they generated follower paths reasonably close to the leader's path while avoiding the saturation of actuators (accelerations) of the followers (see figures 14 and 15).

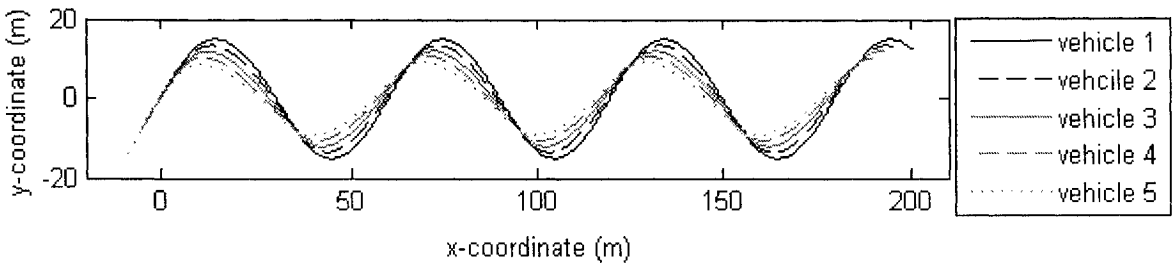

Figure 14 : Paths of leader and followers in planar motion with a constant spacing policy and $A = 15$, $D = 60$, $b = 5$, $d = 0.2$, $L = 4$, $k = c = 5$, $|a_x|, |a_y| \le 5$, *a-delay* $= 0$.

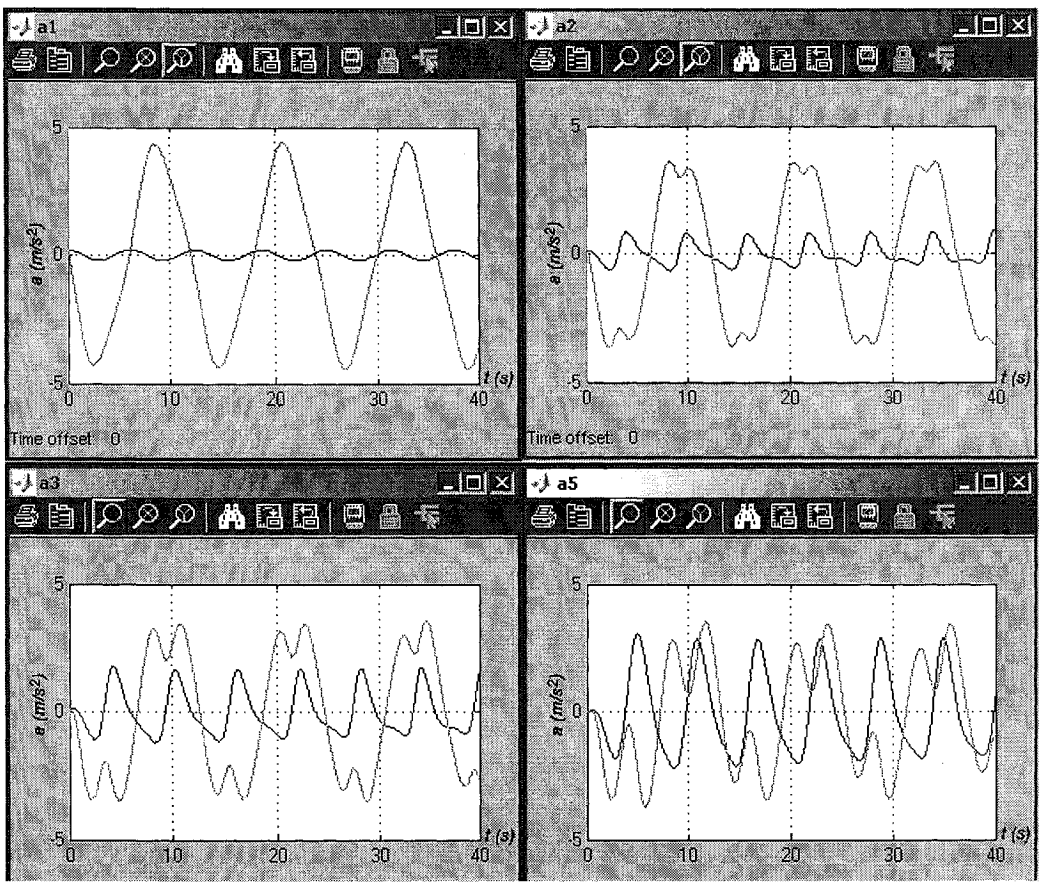

Figure 15 : Accelerations of leader and followers in planar motion with a constant spacing policy, a4 was omitted to save space, black: x-component, grey: y-component, $A = 15$, $D = 60$, $b = 5$, $d = 0.2$, $L = 4$, $k = c = 5$, $|a_x|, |a_y| \le 5$, *a-delay* $= 0$.

One important effect of changing to 2D motion (going from linear to planar motion) is the attenuation with i of spacing errors as defined in section 5.9.1 (see figure 16) in spite of a constant spacing policy (while for linear motion, this spacing policy tended to *amplify* spacing errors, see figure 3). This attenuation is present given large enough desired spacing L. Time stability however is not clear because spacing error amplitudes first drop, then start increasing very gradually with time (see figure 16). It should be noted that, with increased inter-vehicle spacing L, spacing errors attenuate both with i and with t, thus achieving string stability and time stability (see table 1).

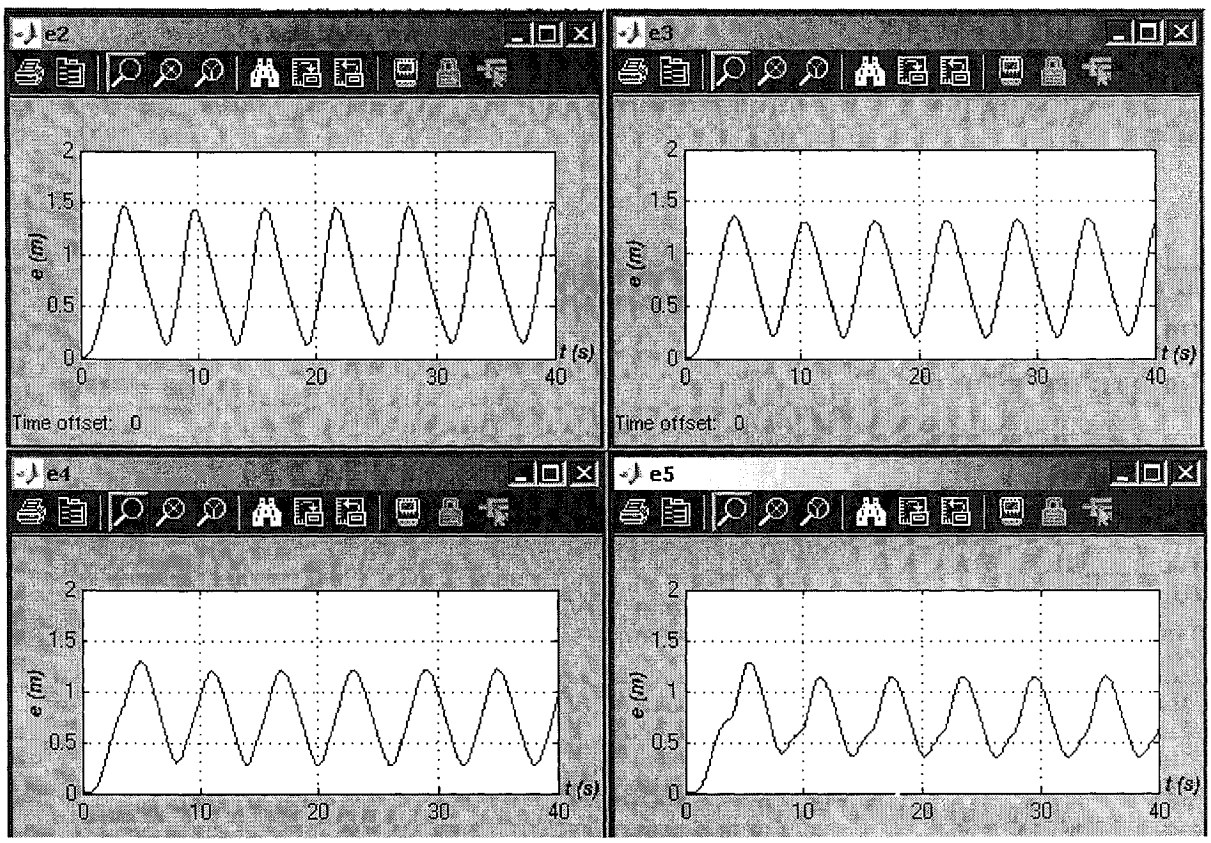

Figure 16 : Follower spacing errors for planar motion with constant spacing policy and $A = 15$, $D = 60$, $b = 5$, $d = 0.2$, $L = 4$, $k = c = 5$, $|a_x|, |a_y| \leq 5$, *a-delay* $= 0$.

One possible explanation for this behavior is an increasing deviation from the leader's path towards the back of the platoon as shown in figure 14. And so, even though the constant spacing policy is quite demanding for the followers, a "path attenuation" effect eases the conditions of motion and enables further followers to achieve smaller spacing errors.

All simulations had an acceleration constraint for the followers. This constraint was set to the approximate maximum acceleration used by the leader in his trajectory. In physical terms, the followers would be equipped with actuators of the same power as the leader. It seems reasonable that vehicles following a leader should be capable of comparable performance (accelerating, decelerating or turning) as their leader.

Figure 15 shows that, with constant spacing, local sensing and no feedback delays, the accelerations used by the followers gradually deviate from those of the leading vehicle: the y-component decreases while the x-component increases. The coupling between the y and x accelerations is a property of motion with DOF greater than 1. It is possible that the two acceleration components are converging to a steady state where both have similar amplitudes and are below the saturation level of $5m/s^2$. If this is true, then the acceleration constraint never becomes active and the trend of decreasing spacing errors continues indefinitely.

5.9.4 Effects of Variations in Simulation Parameters

Varying the Following Distance L:

With *large* following distance L, the followers deviate further from the leader's path (see figure 17). This effect seems intuitive: as a vehicle's following distance goes to infinity, its path should approach a straight line (given the leader's trajectory used in this simulation). Due to this effect, with small enough constant spacing, short platoons could stay close to the leader's path without even knowing where the path is (i.e.: using local sensing only). For long platoons however, the deviation from the path further down the platoon will be significant. In figure 14, the difference in path between the leader and vehicle 2 is small but between the leader and vehicle 5, it is substantial.

There appears to be a limit to how small the spacing can become. Table 1 shows observations on paths, spacing errors and accelerations made for gradually diminishing inter-vehicle spacing L. Note that at $L = 2m$, spacing errors cease to attenuate and that at $L = 1m$, spacing errors amplify down the platoon.

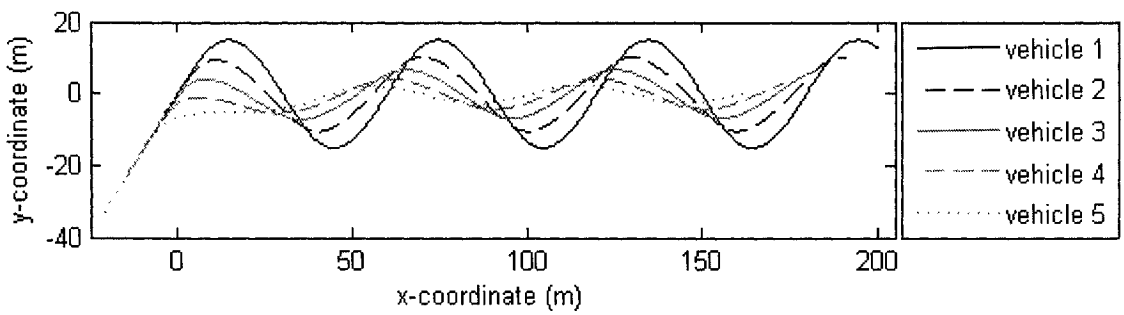

Figure 17 : Paths of leader and followers in planar motion with a constant spacing policy and $A = 15$, $D = 60$, $b = 5$, $d = 0.2$, $L = 10$, $k = c = 5$, $|a_x|, |a_y| \leq 5$, *a-delay* $= 0$.

Table 1 : Effects of varying inter-vehicle spacing in planar motion with a constant spacing policy and $A = 15$, $D = 60$, $b = 5$, $d = 0.2$, benchmark $L = 4$, $k = c = 5$, $|a_x|, |a_y| \leq 5$, *a-delay* = 0.

L (m)	*Paths*	*Inter-vehicle Spacing* l_i *(m)*	*Spacing Errors* e_i *(m)*	*Accelerations* a_i (m/s^2)
10	Large attenuation with *i*	Amplify with *i*	Attenuate with *i* and *t* down to 1.3	Steady at about 2.5
4	Substantial attenuation with *i*	Amplify with *i*	Attenuate with *i* and *t* down to 1.2	Steady at about 3.5
3	Slight attenuation with *i*	attenuate with *t*.	Attenuate with *i* down to 0.85	Steady at about 4
2.0	Almost no change with *i*	Amplify with *i*	Attenuate with *t* down to 0.45	Steady at about 4
1.0	No visible change with *i*	Amplify with *i*	Amplify slightly with *i* up to 0.45	Steady at about 4.2
0.3	Almost no change with *i*	Amplify with *t* and *i*, collisions starting at vehicle 2	Amplify with *i* and *t* up to 0.7	Saturation at vehicle 5

(see notes below)

Notes for interpreting tables:

- all quantities observed vary in a periodic fashion.
- attenuation or amplification with *i* refers to a decreasing or increasing amplitude of the signal as vehicle index *i* increases, i.e.: towards the back of the platoon.
- attenuation or amplification with *t* refers to a decreasing or increasing amplitude of the signal as time *t* increases.

The model confirms an intuitive fact: for very small inter-vehicle spacing, it becomes difficult for vehicles to follow the leader without collisions or jerky accelerations.

Varying the Time-delay of Control Variable (acceleration):

First, a delay in acceleration feedback of 0.05s was introduced (five times the solver step size of 0.01s). The behavior of the system was largely unchanged except for small initial instabilities in acceleration ($t = 0$ to $1s$). A larger delay of 0.15s resulted in a noticeable effect of jerky (fast-changing) acceleration. The effect was amplified down the platoon but attenuated with time (see figure 18).

Note that acceleration constraints are active starting at vehicle 5. These jerky accelerations are caused by spacing error "build-ups" caused by the feedback delays (greater errors had time to form because of the delayed reaction of the control system). In practice, such delays can be caused by a number of factors: controller processing time, internal signal transmission, sensor or actuator lags. The effect is similar to a human driver opening his eyes only at certain intervals to assess the situation and respond to it. The resulting sudden adjustments (jerky accelerations) seem intuitive.

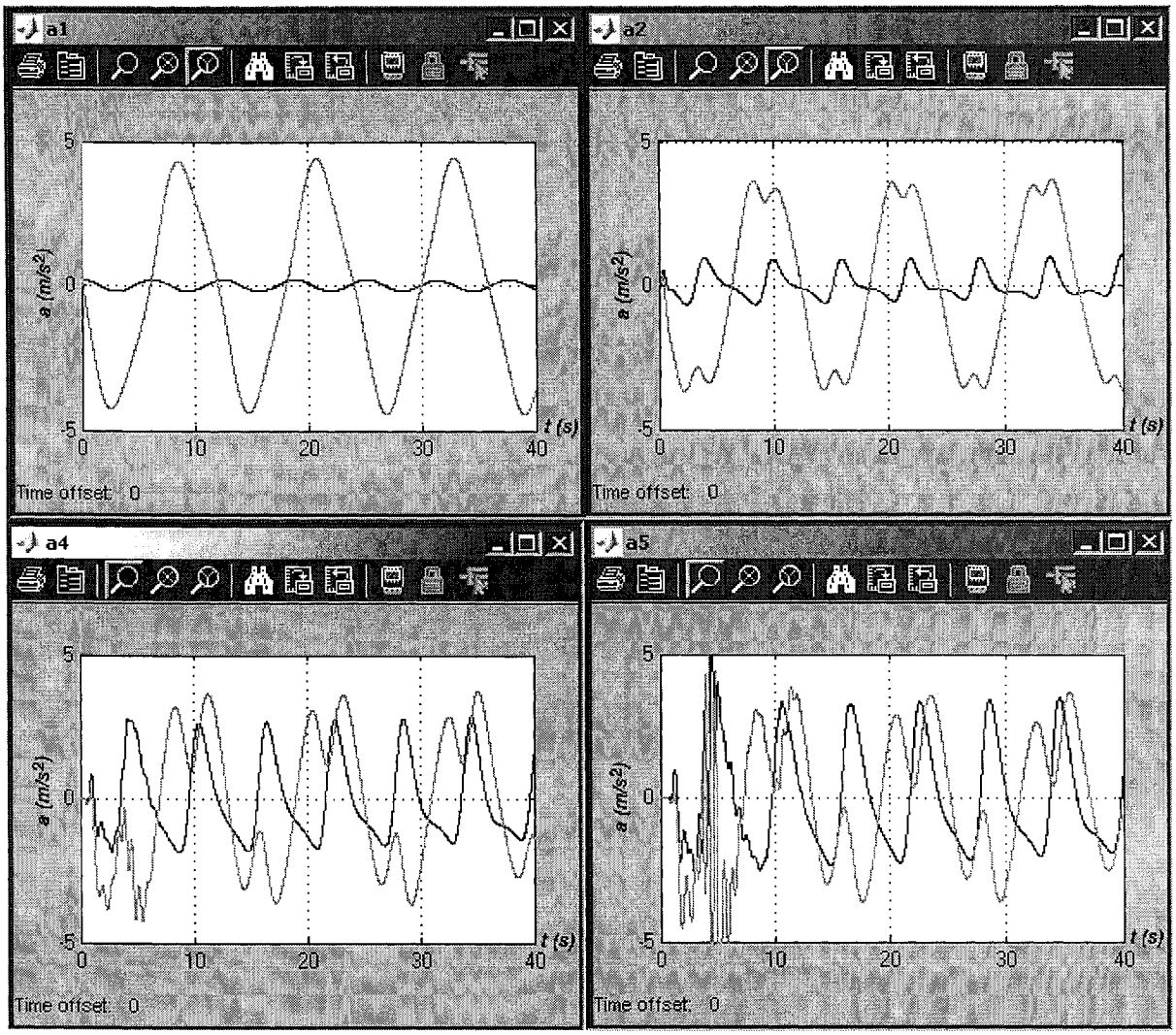

Figure 18 : Accelerations of leader and followers in planar motion with a constant spacing policy, showing the effects of feedback delays, with $A = 15$, $D = 60$, $b = 5$, $d = 0.2$, $L = 4$, $k = c = 5$, $|a_x|, |a_y| \leq 5$, *a-delay* = 0.15.

The more interesting and perhaps less intuitive effect of feedback delays is that the resulting motions continue to attenuate spacing errors with i, in their fundamental frequency, while a new frequency appears in the spacing errors, which is amplified with i (see figure 19). It is difficult to say from these simulations whether, given a large enough number of followers, this new frequency would eventually cause string instability and collisions.

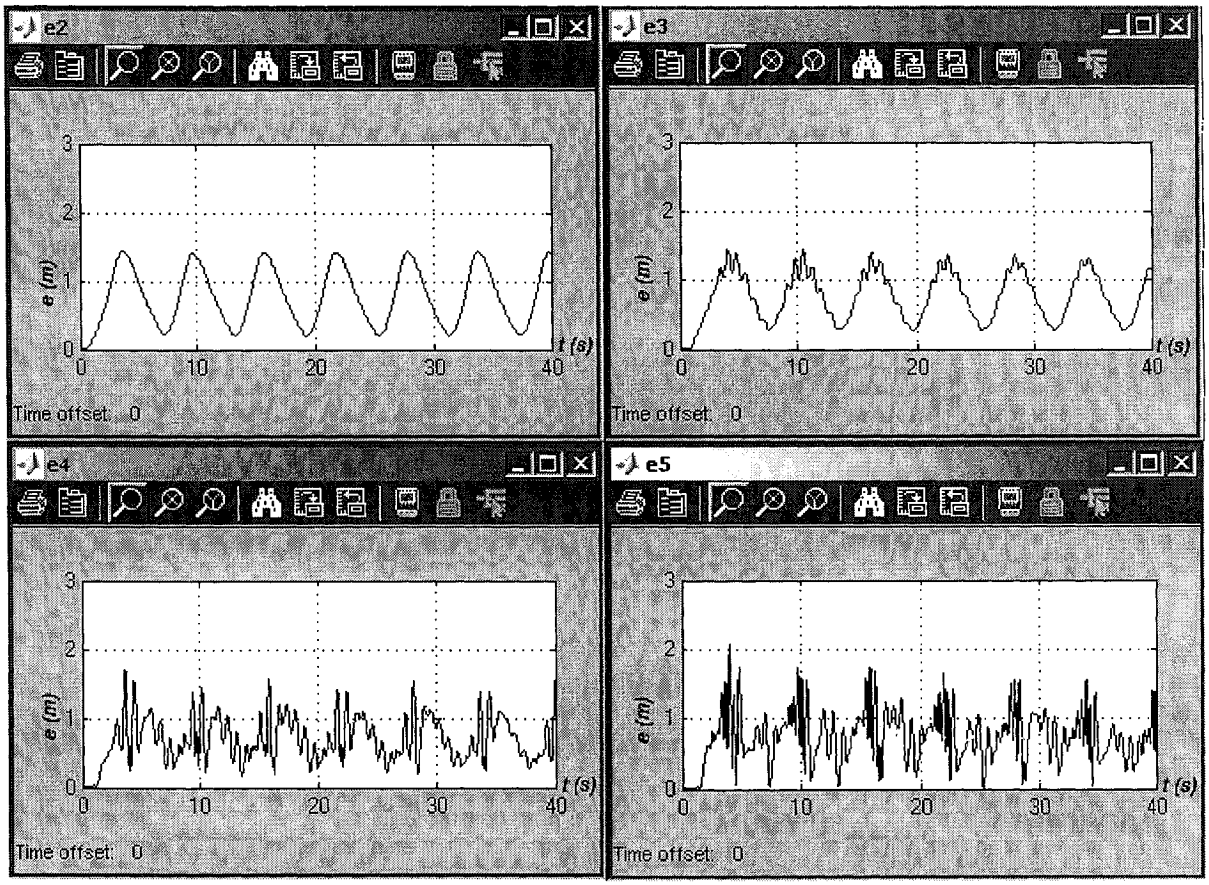

Figure 19 : Follower spacing errors for planar motion with constant spacing policy, showing effects of feedback delays, with $A = 15$, $D = 60$, $b = 5$, $d = 0.2$, $L = 4$, $k = c = 5$, $|a_x|, |a_y| \leq 5$, *a-delay* = 0.18.

The motions of the 5-vehicle platoon remain collision-free up to a delay of 0.2*s*.

A *large delay* in acceleration feedback has more pronounced effects on the paths of the vehicles (figure 20) as well as on the spacing errors (figure 22). It is clear that further followers deviate more and more from the leader's path. Spacing errors also become more pronounced with *i* and vary greatly with *t*.

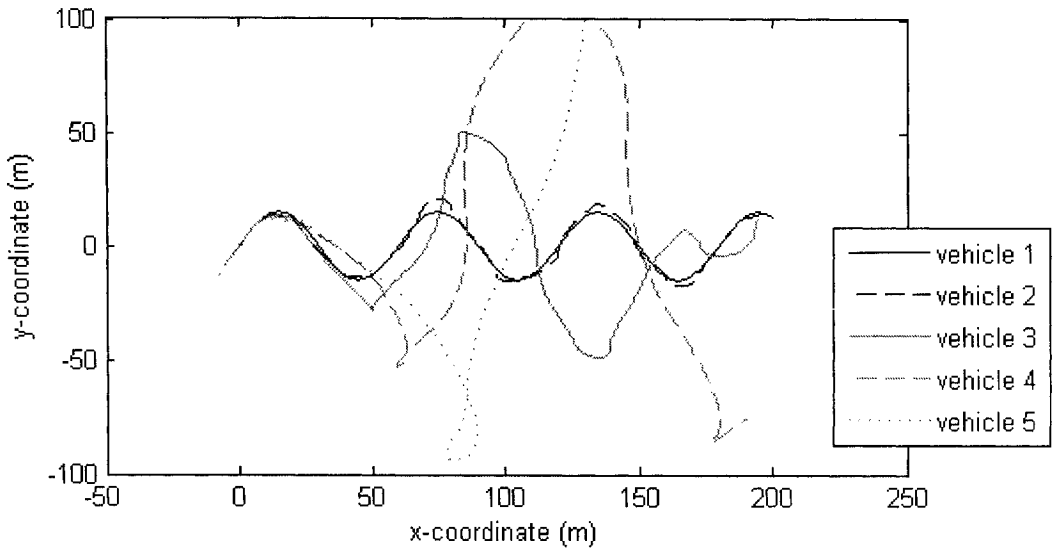

Figure 20 : Paths of leader and followers in planar motion with a constant spacing policy, showing effects of large feedback delay, with $A = 15$, $D = 60$, $b = 5$, $d = 0.2$, $L = 4$, $k = c = 5$, $|a_x|, |a_y| \le 5$, *a-delay* = 0.5.

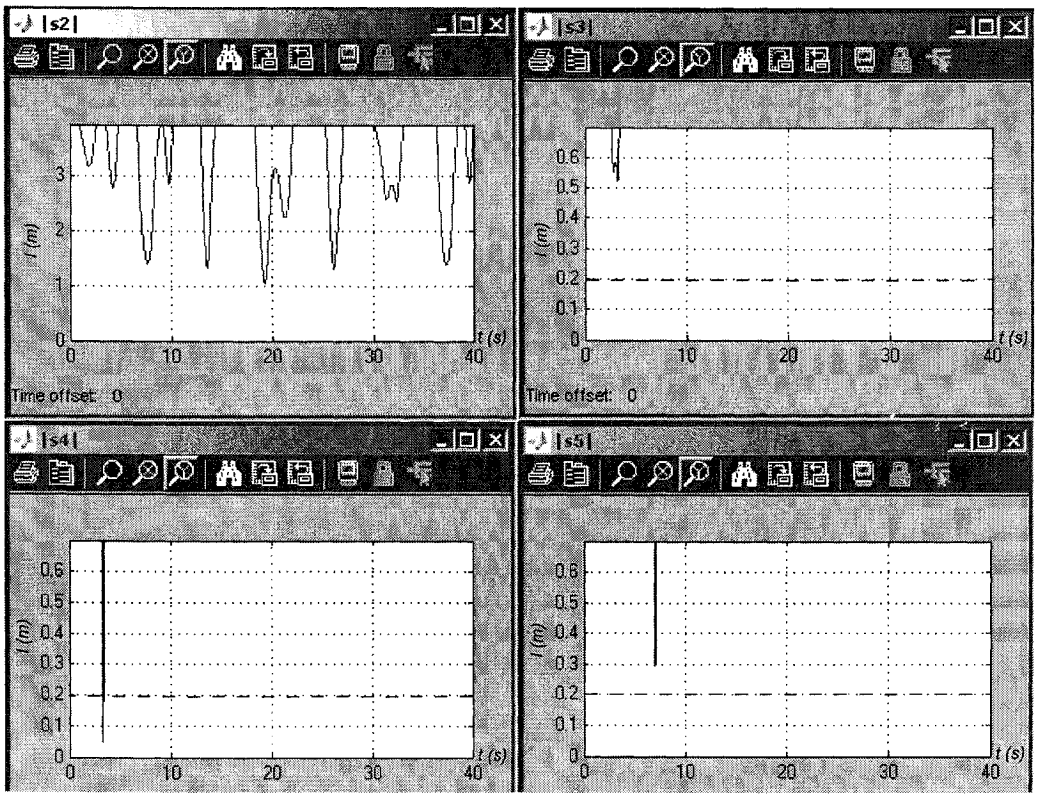

Figure 21 : Follower spacing for 2D motion, constant spacing policy, effects of large feedback delays, with $A = 15$, $D = 60$, $b = 5$, $d = 0.2$, $L = 4$, $k = c = 5$, $|a_x|, |a_y| \le 5$, *a-delay* = 0.5.

From figures 20 and 21, it is clear that vehicles 3, 4 and 5 have lost formation and vehicle 4 has "collided" with vehicle 3 by violating the safety bubble spacing of $0.2m$.

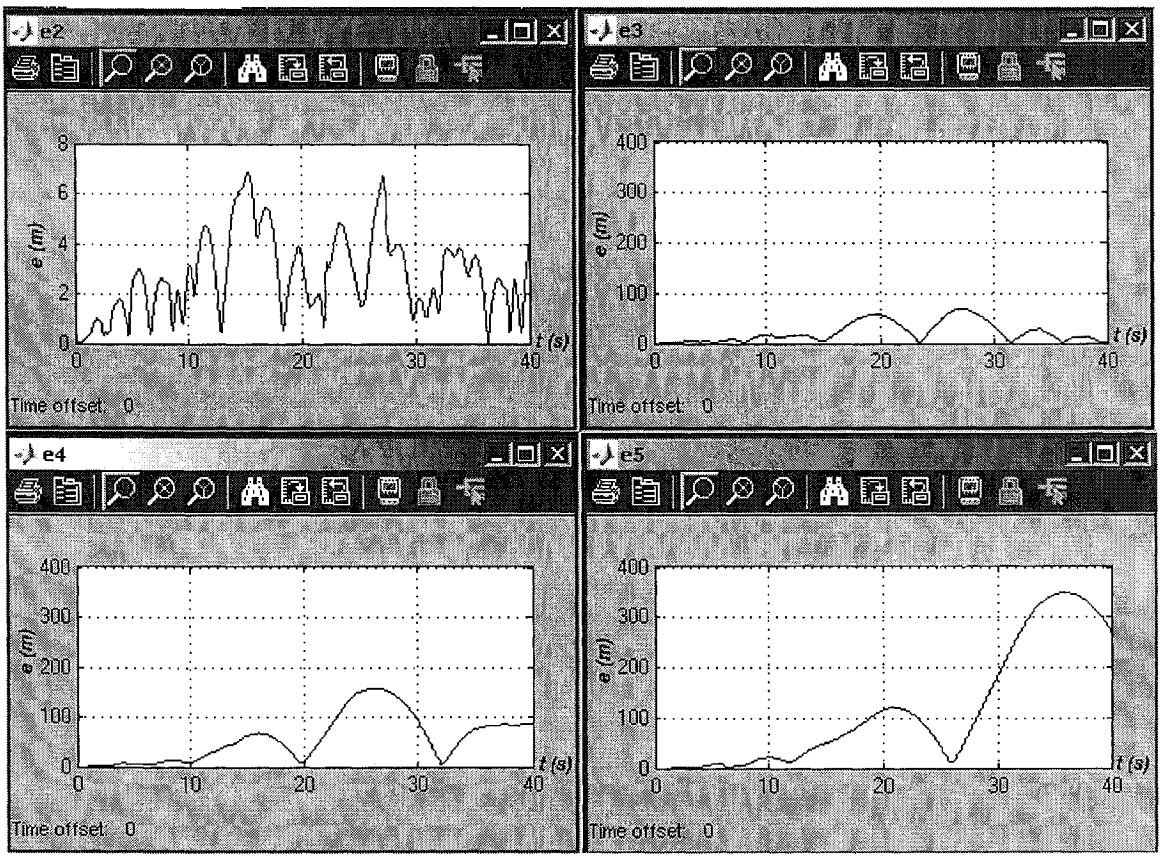

Figure 22 : Follower spacing errors for 2D motion, constant spacing policy, effects of large feedback delays, with $A = 15$, $D = 60$, $b = 5$, $d = 0.2$, $L = 4$, $k = c = 5$, $|a_x|, |a_y| \leq 5$, *a-delay* = 0.5.

From table 2, we can see that while small feedback delays can be tolerated by the system, increasing delays will cause major disruptions including jerkiness, possible collisions and eventually formation loss. These results tend to agree with intuition: if the driver's eyes remain closed for considerable time intervals, his vehicle's proper behavior in the formation will be jeopardized.

Table 2 : Effects of introducing feedback time delays in planar motion with a constant spacing policy and $A = 15$, $D = 60$, $b = 5$, $d = 0.2$, $L = 4$, $k = c = 5$, $|a_x|, |a_y| \leq 5$.

a-delay (s)	*Spacing Errors* e_i *(m)*	*Spacing* l_i *(m)*	*Paths*	*Accelerations* a_i (m/s^2)
0.05	Attenuated with *i* down to 1.3.	Amplified with *i* up to 4.2, slight attenuation with *t*.	Same as with no delay.	Close to saturation.
0.15	Attenuated with *i* down to 1.2, initial disturbances.	Amplified with *i* up to 4.2, slight attenuation with.	Same as with no delay.	Initial jerkiness amplified with *i*, and attenuated with *t*, some saturation at a_5 (see figure 18).
0.18	Amplified and jerkier with *i*, initial peak at around $2m$ for e_5.	Spacing amplified with *i* up to a variation from 3 to 4.5 for l_5.	Same as with no delay.	Jerkiness and saturations starting at a_3 amplifying with *i* and attenuated with *t*.
0.2	Amplified and jerkier with *i* and *t*, up to peaks around 4 for e_5.	Spacing amplified with *i*. Maximum variation from 1.6 to 5.8 for l_5.	Same as with no delay.	High jerkiness and saturations amplified with *i* and *t*.
0.5	Large spacing errors amplified with *i* up to $350m$.	Loss of formation starting at vehicle 2, complete loss of formation for vehicles 4 & 5. *Collision of vehicle 4 with vehicle 3.* (see figure 21)	Deviations from leader's path highly amplified with *i*.	Overwhelming saturations starting at vehicle 2.

Local sensing reduces the amount of time needed to gather information (inputs) and generate a response of the control system. Since feedback delays have a large impact on system behavior with this control scheme, limiting vehicles to local sensing reduces their "reaction time" which improves their chances of successful motion control.

Varying the Feedback Gains *k* and *c*:

This study focuses on the behaviour of a formation of identical vehicles, each vehicle having the same control law. For this reason, feedback gains will be varied in the same way for all vehicles. General system behavior was based so far on simulations using control law gains $k = c = 5$. Below is an analysis of the effects of changing these parameters in three main ways: reducing both, increasing both and making c less than k.

Figure 23 : Follower spacing errors for planar motion with constant spacing policy, showing effects of small feedback gains $k = c = 2$ and $A = 15$, $D = 60$, $b = 5$, $d = 0.2$, $L = 4$, $|a_x|, |a_y| \leq 5$, *a-delay* = 0.

From figure 23, we can see that lowering the gains k and c to 2 (by a factor of 2.5) had clearly adverse effects on system behavior: spacing errors are now amplified with i.

Consequently, accelerations used by the followers also increase with i, reaching saturation at vehicle 5 (see figure 24).

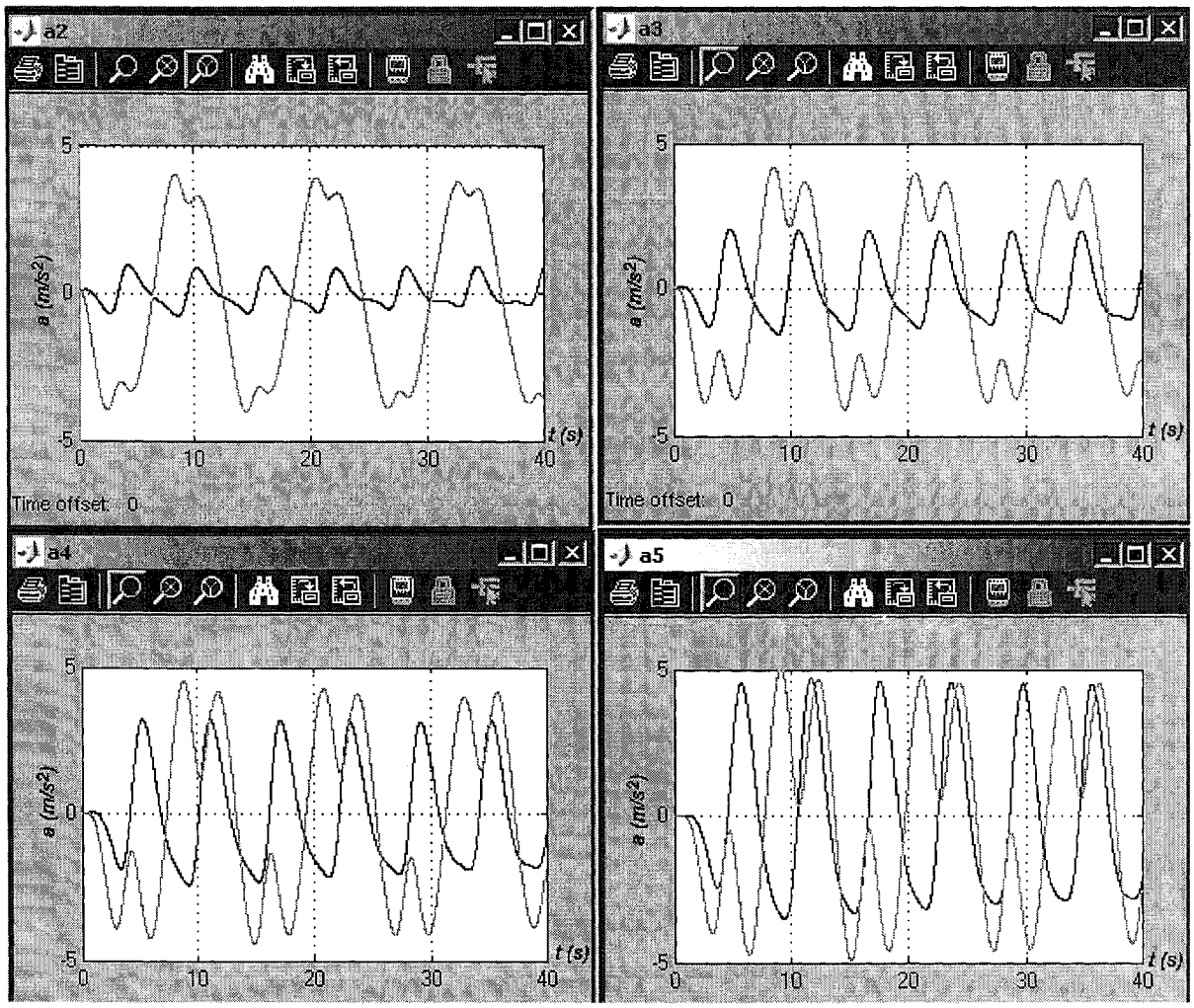

Figure 24 : Accelerations of vehicles in 2D motion, constant spacing policy, effects of small feedback gains $k = c = 2$ with $A = 15$, $D = 60$, $b = 5$, $d = 0.2$, $L = 4$, $|a_x|, |a_y| \leq 5$, *a-delay* = 0.

Very large feedback gains on the other hand do not affect significantly spacing errors (attenuation with i still occurs although slightly decreased), but generate frequent actuator saturation, especially in the y-direction (shown by the high-frequency saturation-to-saturation oscillations of the gray plot in figure 25).

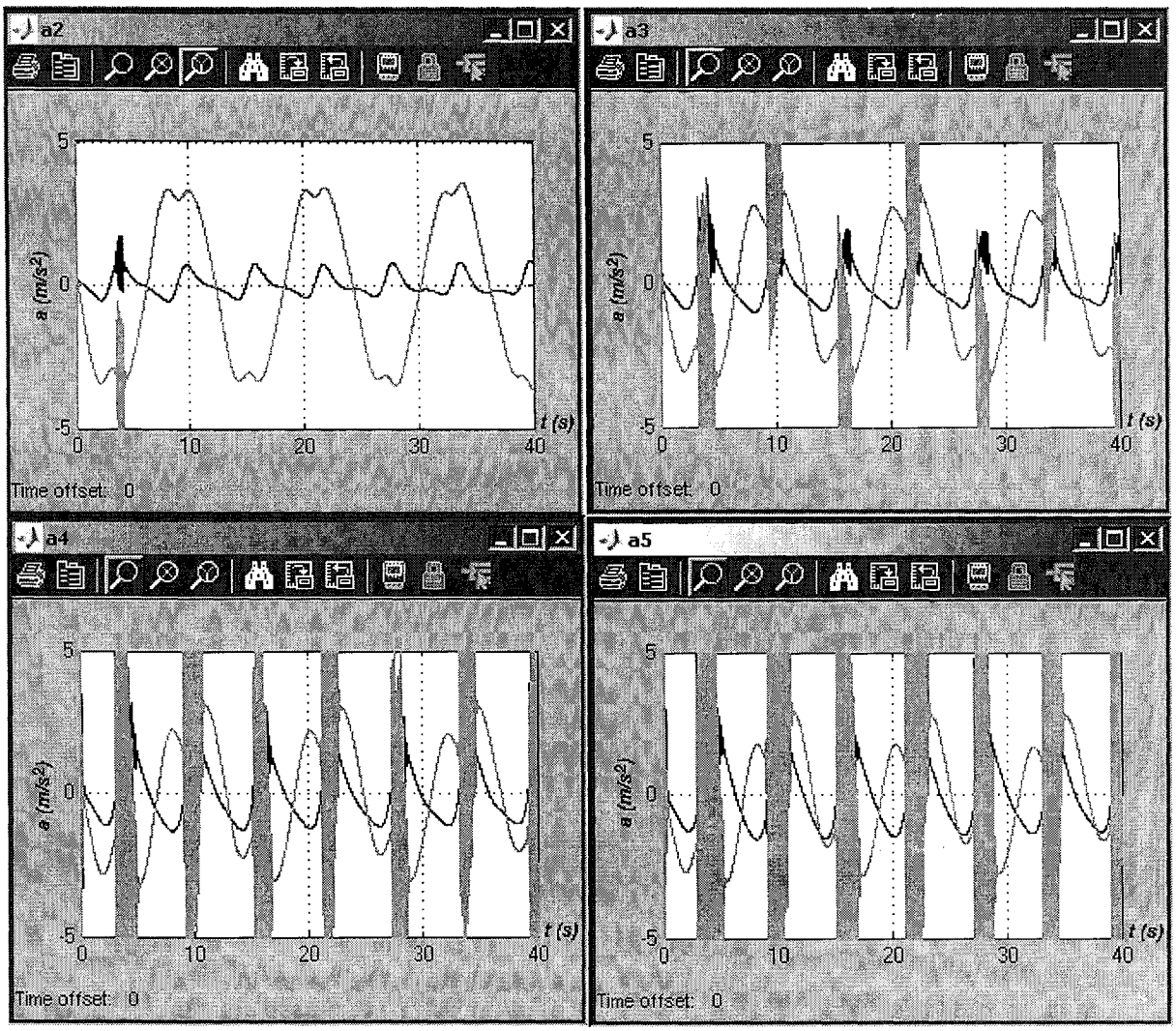

Figure 25 : Accelerations of leader and followers in planar motion with a constant spacing policy, showing the effects of very large feedback gains $k = c = 100$ and $A = 15$, $D = 60$, $b = 5$, $d = 0.2$, $L = 4$, $|a_x|, |a_y| \leq 5$, *a-delay* $= 0$.

It should also be noted that very large feedback gains ($k = c = 100$) have no adverse effect on the paths of the followers (see table 3).

The last parameter variation tested was a decrease in c without changing k. Decreasing c to 2 caused string instability (errors amplified with i, see table 3). It was difficult to predict at what values of k and c string instability would occur first.

Table 3 : Effects of varying feedback gains in planar motion with a constant spacing policy and $A = 15$, $D = 60$, $b = 5$, $d = 0.2$, $L = 4$, benchmark $k = c = 5$, $|a_x|, |a_y| \leq 5$, a-delay = 0.

k	c	*Spacing Errors* e_i *(m)*	*Paths*	*Accelerations* $a_i\ (m/s^2)$
2	2	Amplified up to 2 with *i.*	Increased deviation from path visible at vehicle 4 & 5.	Accelerations amplified with *i*, some saturation at vehicle 5.
10	10	Attenuated with *i* down to 1.3	Improved tracking of leader's path.	Accelerations attenuated with *i.*
100	100	Attenuated with *i* down to 1.4	Tracking of leader's path similar to reference.	Jerky accelerations, frequent saturation in y-direction.
5	2	Initially as low as 0.6 (e_2) but amplified with *i* up to 1.8.	Tracking of leader's path similar to reference.	Saturation from starting at a_3.

It is clear that going from linear to planar motion, the string stability criteria of the platoon have changed. Canudas and Brogliato [1] showed that in linear motion (1 DOF), a constant spacing policy would lead to string instability no matter how k and c were chosen. Using a planar motion (2 DOF) simulation with local sensing and a similar control law using a constant spacing policy, this study has shown that, in a particular situation (such as the one described in section 5.9.3) it is possible to achieve 2D string stability. The simulation also suggests that this stability depends on the various system parameters discussed above, including the values chosen for k and c (see table 3).

While path tracking was not an issue in 1D, it is an important part of 2D motion. It may be useful to think of the string stability achieved in 2D (but not possible in 1D) as resulting from "path attenuation", a possibly useful effect of the additional DOF.

5.10 Planar Control, Local Information, Variable Spacing

Similar to the 1D case from section 4.5, this control scheme for 2D motion is characterized by:

- Variable (speed-dependent) inter-vehicle spacing:

$$\mathbf{L}_i = h\mathbf{v}_i + 0.3m(\frac{\mathbf{v}_i}{v_i}) \tag{5.10.1}$$

  Where $0.3m$ is a minimum standstill ($\mathbf{v}_i \to 0$) spacing that leaves a gap of $0.1m$ between the $0.1m$ radius "safety bubbles" of each vehicle.

- Forward-looking information only, sensed by the i-th vehicle: $\mathbf{e}_i$ and $\mathbf{v}_{i-1} - \mathbf{v}_i$

- PD control law: $\mathbf{u}_i = k\mathbf{e}_i + c(\mathbf{v}_{i-1} - \mathbf{v}_i)$, where k and c are constants.

5.10.1 Definition of Spacing Error

The vector relationships are as shown in figure 12 for the constant spacing policy. The definition of the *targeted* displacement of m_{i-1} relative to m_i is changed: it is now a function of the velocity of m_i and is equal to $h\mathbf{v}_i$. The *actual* displacement of m_{i-1} relative to m_i is $\mathbf{r}_{i-1} - \mathbf{r}_i$. Thus, the error vector is:

$$\mathbf{e}_i = \mathbf{r}_{i-1} - \mathbf{r}_i - \mathbf{L}_i = \mathbf{r}_{i-1} - \mathbf{r}_i - h\mathbf{v}_i - 0.3m\left(\frac{\mathbf{v}_i}{v_i}\right) \tag{5.10.2}$$

5.10.2 Simulink Model

The Simulink model used for this control scheme is shown in Appendix D and is very similar to the model used for the 2D constant spacing policy shown in Appendix C. The main changes are in: *vehicle* subsystem where the spacing error computation and control law are modified and *initial positions of followers* subsystem that uses the new spacing policy.

5.10.3 General System Behavior

The simulation was first performed using a set of parameters similar to the ones used to study the general behavior of the constant spacing control scheme. Parameters *A, D, b, d, k, c, limits on* $|a_x|$ *and* $|a_y|$ as well as the *a-delay* remained unchanged. The only parameter that had to be different was *h*, defining velocity-dependent inter-vehicle spacing. Since the average speed of the leader was around 7 *m/s* (see figure 26), *h* was chosen to match the constant spacing value used in the constant spacing control scheme ($L = 4\ m$):

$$Let \quad hv_{ave} = L = 4m \quad and\ use \quad v_{ave} = 7m/s, \quad then$$

$$h = \frac{L_{ave}}{v_{ave}} = \frac{4m}{7m/s} \cong 0.6s \tag{5.10.3}$$

The tracking of the leader's path by the followers seems improved when compared to the constant spacing control scheme (see figure 27).

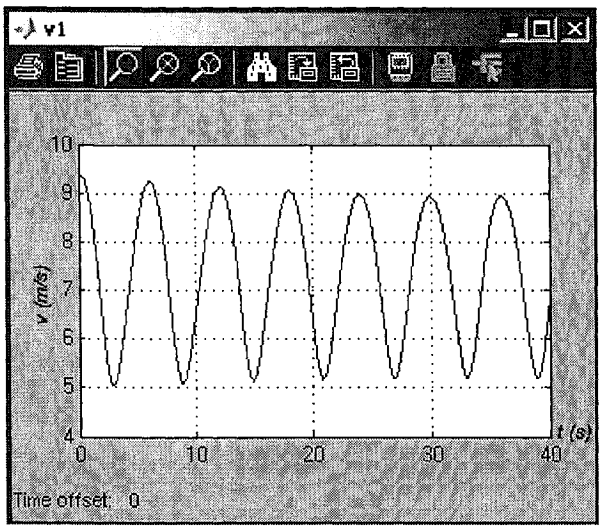

Figure 26 : Magnitude of the leader's velocity with $A = 15$, $D = 60$, $b = 5$, $d = 0.2$.

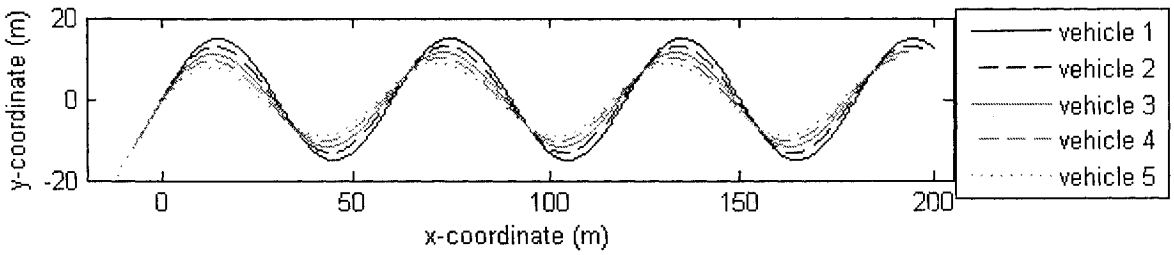

Figure 27 : Paths of leader and followers in planar motion with variable spacing and $A = 15$, $D = 60$, $b = 5$, $d = 0.2$, $h = 0.6$, $k = c = 5$, $|a_x|, |a_y| \leq 5$, *a-delay* $= 0$.

The attenuation of spacing errors is more significant than with a constant spacing policy (down to about $0.9m$ from $1.2m$, see figure 16 and figure 28). This results in lower accelerations used by the followers (see figure 29), attenuated with i down to a y-component amplitude of about $2.5\, m/s^2$ and an x-component amplitude of about $0.09\, m/s^2$ (see figure 30). This is compared to a possible convergence trend to around $3\, m/s^2$ in the previous control scheme (see figure 15).

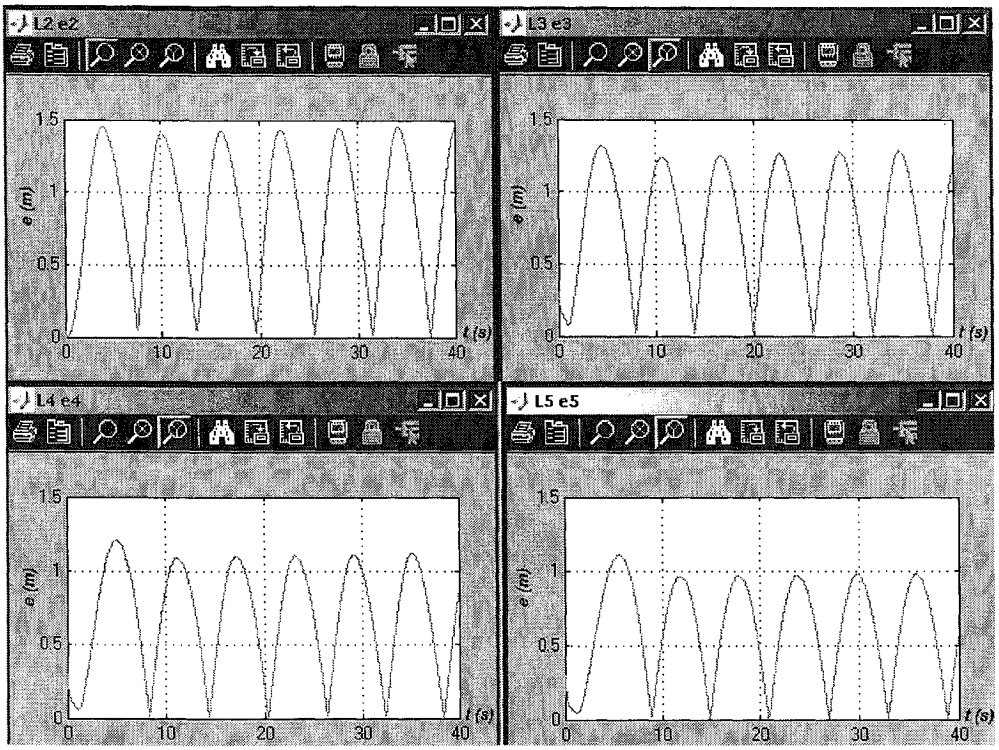

Figure 28 : Follower spacing errors for planar motion with variable spacing policy and $A = 15$, $D = 60$, $b = 5$, $d = 0.2$, $h = 0.6$, $k = c = 5$, $|a_x|, |a_y| \le 5$, *a-delay* = 0.

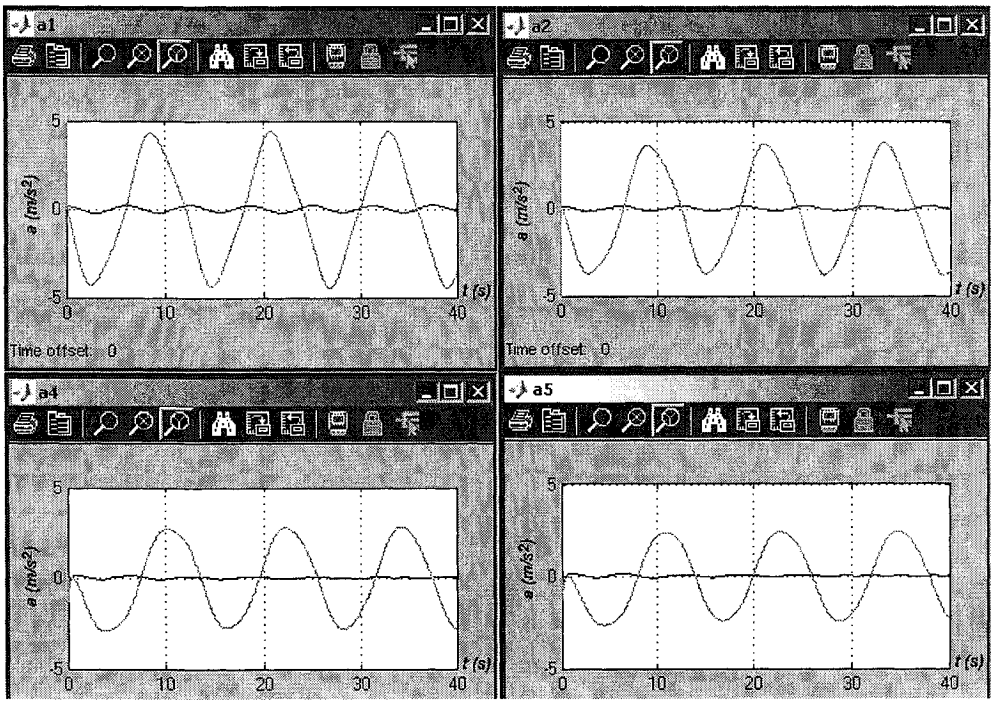

Figure 29 : Accelerations of leader and followers in planar motion with variable spacing policy, a3 was omitted to save space, black: x-component, grey: y-component, $A = 15$, $D = 60$, $b = 5$, $d = 0.2$, $h = 0.6$, $k = c = 5$, $|a_x|, |a_y| \le 5$, *a-delay* = 0.

It is interesting to note the independence of the x and y-components of acceleration in variable spacing, which is different from the constant spacing control scheme that caused increasing similarity between the two components of acceleration down the platoon. It is unclear whether this phenomenon would be observed in practice or whether it is due to simulation peculiarities of the *unit vector* subsystem used in the constant spacing model (see Appendix C).

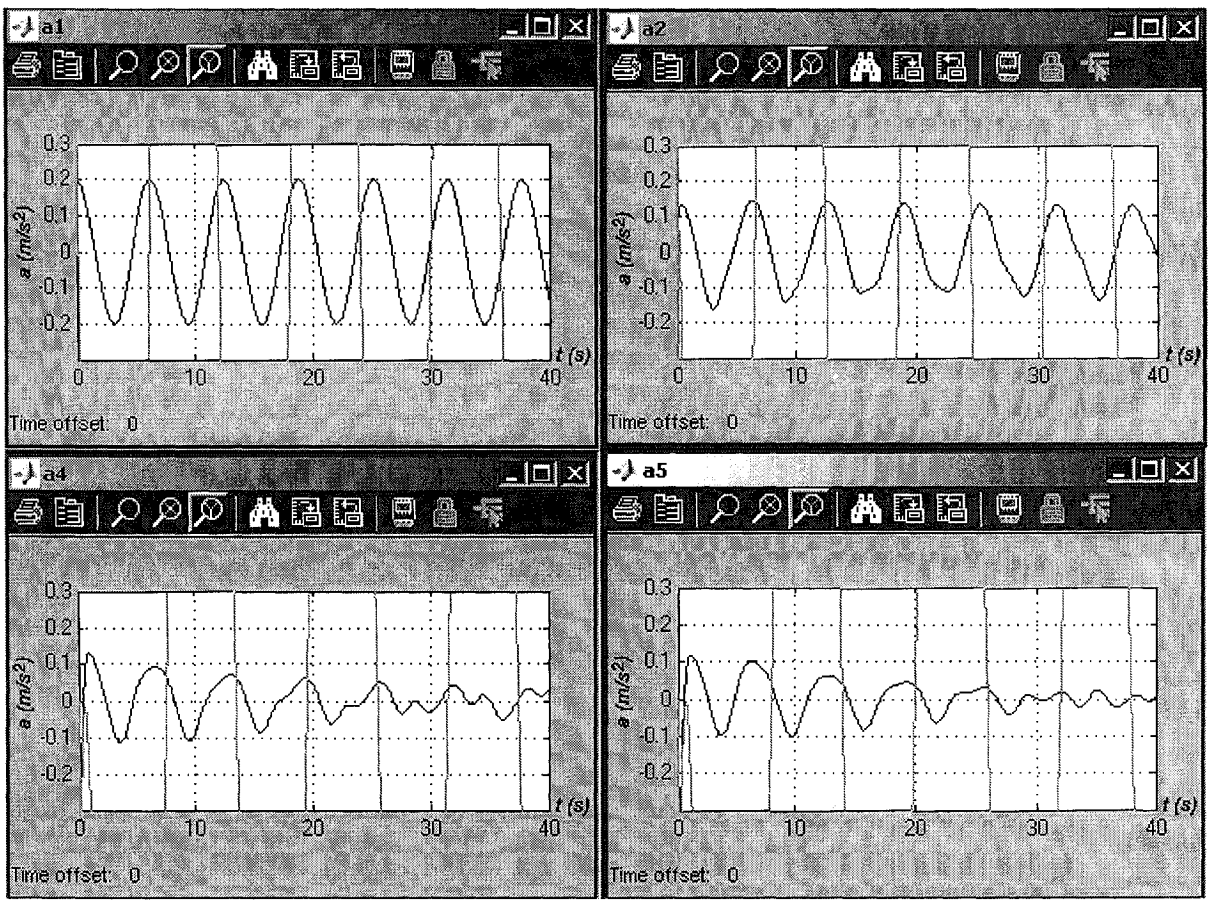

Figure 30 : x-component zoom of accelerations of leader and followers in planar motion with variable spacing policy, a3 was omitted to save space, black: x-component, $A = 15$, $D = 60$, $b = 5$, $d = 0.2$, $h = 0.6$, $k = c = 5$, $|a_x|, |a_y| \leq 5$, *a-delay* = 0.

5.10.4 Effects of Variations in Simulation Parameters

Varying the Spacing Coefficient *h:*

In general, a larger *h* will result in smoother motions (smoother paths, velocities and accelerations) but will cause significant deviations in the followers' paths from the path of the leader (see figure 31).

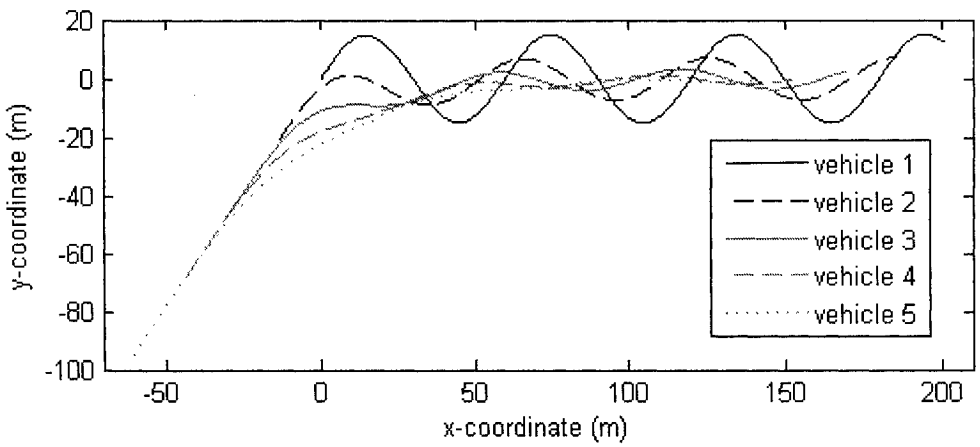

Figure 31 : Paths in planar motion with a variable spacing policy, showing effects of large *h*, with $A = 15$, $D = 60$, $b = 5$, $d = 0.2$, $h = 3$, $k = c = 5$, $|a_x|, |a_y| \leq 5$, *a-delay* $= 0$.

One interesting result is that the magnitude of spacing errors increases as *h* increases and yet, accelerations decrease with *h* (see figure 32 and figure 33). One explanation for this behavior is the fact that accelerations are a function of spacing errors *and* relative velocities. If the relative velocities decrease rapidly with *h*, their effect may be stronger than the effect of increasing errors. Relative velocities may also have opposite sign to errors.

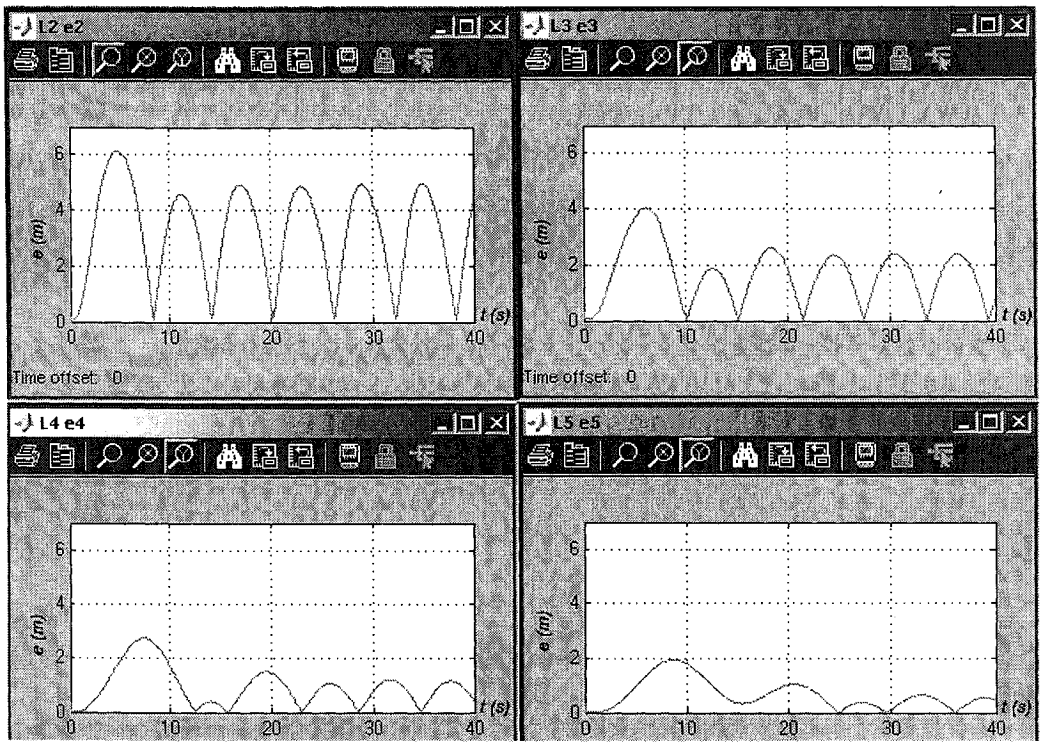

Figure 32 : Spacing errors for planar motion with variable spacing, effects of large *h*, with $A = 15$, $D = 60$, $b = 5$, $d = 0.2$, $h = 3$, $k = c = 5$, $|a_x|, |a_y| \le 5$, *a-delay* = 0.

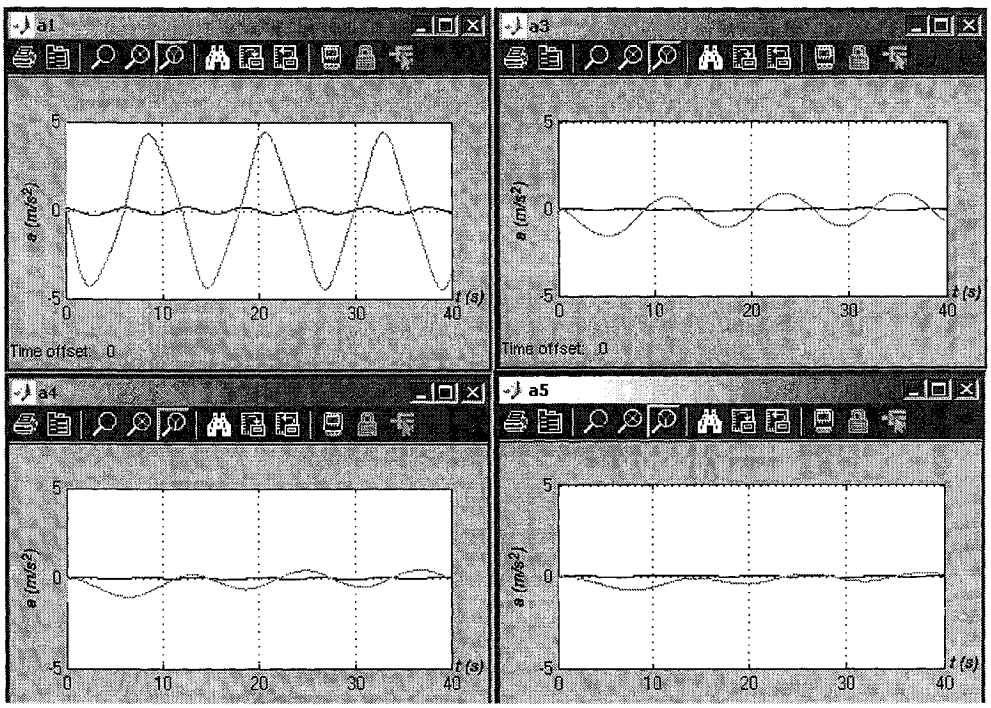

Figure 33 : Accelerations in planar motion with variable spacing policy, showing effects of large *h*, black: x-component, grey: y-component, $A = 15$, $D = 60$, $b = 5$, $d = 0.2$, $h = 3$, $k = c = 5$, $|a_x|, |a_y| \le 5$, *a-delay* = 0.

Table 4 : Effects of varying spacing coefficient h in planar motion with variable spacing policy and $A = 15$, $D = 60$, $b = 5$, $d = 0.2$, $k = c = 5$, $|a_x|, |a_y| \leq 5$, *a-delay* $= 0$.

h (s)	*Paths*	*Spacing* l_i *(m)*	*Spacing Errors* e_i *(m)*	*Accelerations* a_i (m/s^2)
3	Very large attenuation, out of phase	Good formation hold	Significantly larger but also attenuating with *i*	Much greater attenuation with *i.*
1	Slight attenuation	Good formation hold	Larger values but also attenuating down platoon	Greater attenuation with *i.*
0.6	Reference	Reference	Reference	Reference
0.2	Very close path resemblance between leader and followers (see figure 34)	Good formation hold (see figure 36)	Significantly smaller and attenuated with *i.*	Very gradual attenuation with *i.*
0.005	Path resemblance deteriorates		Errors are amplified with *i.*	Gradual amplification with *i.*, near-saturation

Decreasing the spacing coefficient to $0.2s$ has two main effects: extremely close path tracking by the followers (see figure 34) and small spacing errors (see figure 35). Note that no collisions have been possible with all of the h values shown in table 4. Inter-vehicle spacing has stayed above the collision minimum and below the formation loss maximum (see figure 36).

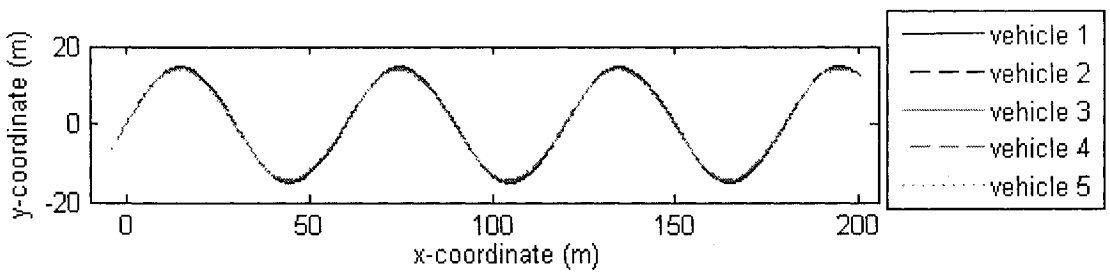

Figure 34 : Paths of leader and followers in planar motion with variable spacing and $A = 15$, $D = 60$, $b = 5$, $d = 0.2$, $h = 0.2$, $k = c = 5$, $|a_x|, |a_y| \leq 5$, *a-delay* $= 0$.

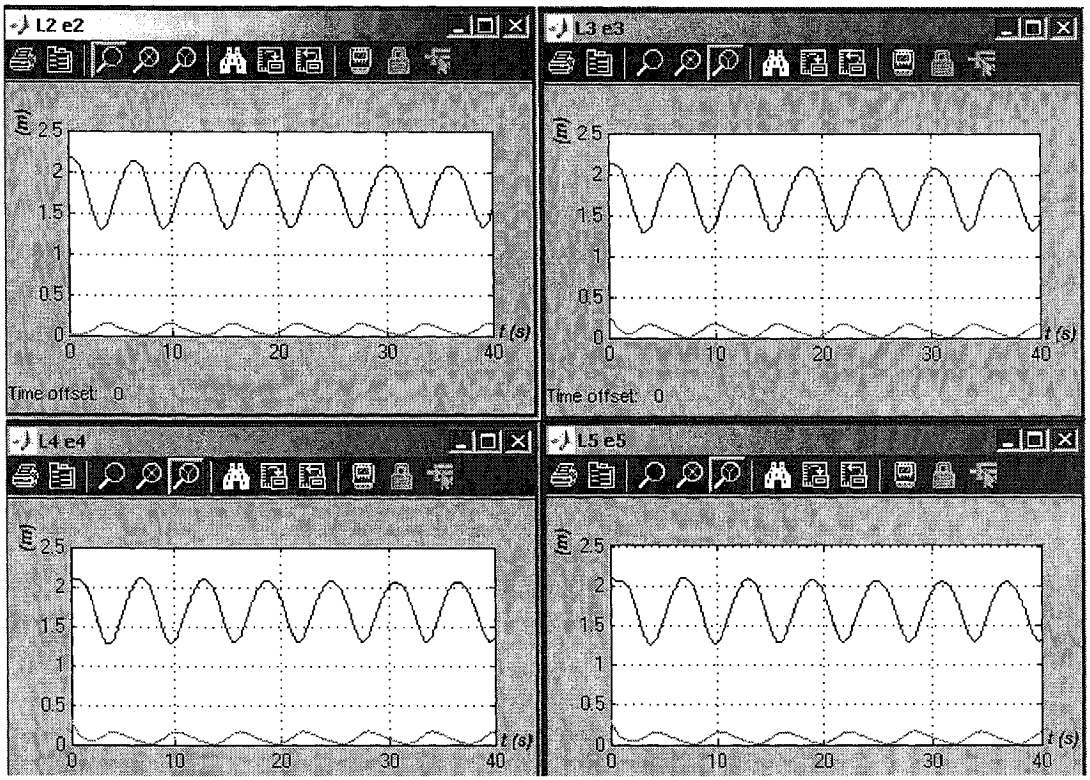

Figure 35 : Desired inter-vehicle spacing L_i (black) and spacing errors e (gray) for 2D motion with variable spacing and $A = 15$, $D = 60$, $b = 5$, $d = 0.2$, $h = 0.2$, $k = c = 5$, $|a_x|, |a_y| \le 5$, *a-delay* $= 0$.

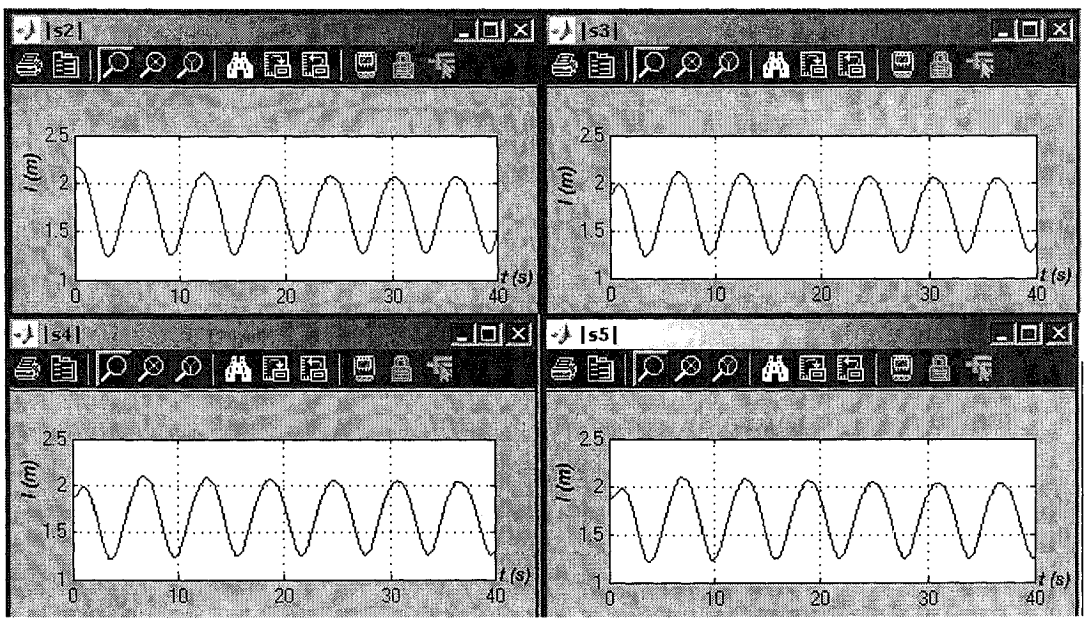

Figure 36 : Inter-vehicle spacing for 2D motion with variable spacing policy and $A = 15$, $D = 60$, $b = 5$, $d = 0.2$, $h = 0.2$, $k = c = 5$, $|a_x|, |a_y| \le 5$, *a-delay* $= 0$.

The resulting accelerations decrease gradually with *i*.

The practical lower limit for *h* is around 0.005 (see table 4). At this *h* value, spacing errors and accelerations begin to amplify with *i*, i.e. clear signs of string instability (see figure 37). Also, inter-vehicle spacing falls below the $0.2m$ collision limit: vehicles 3 and 4 collide with their predecessors.

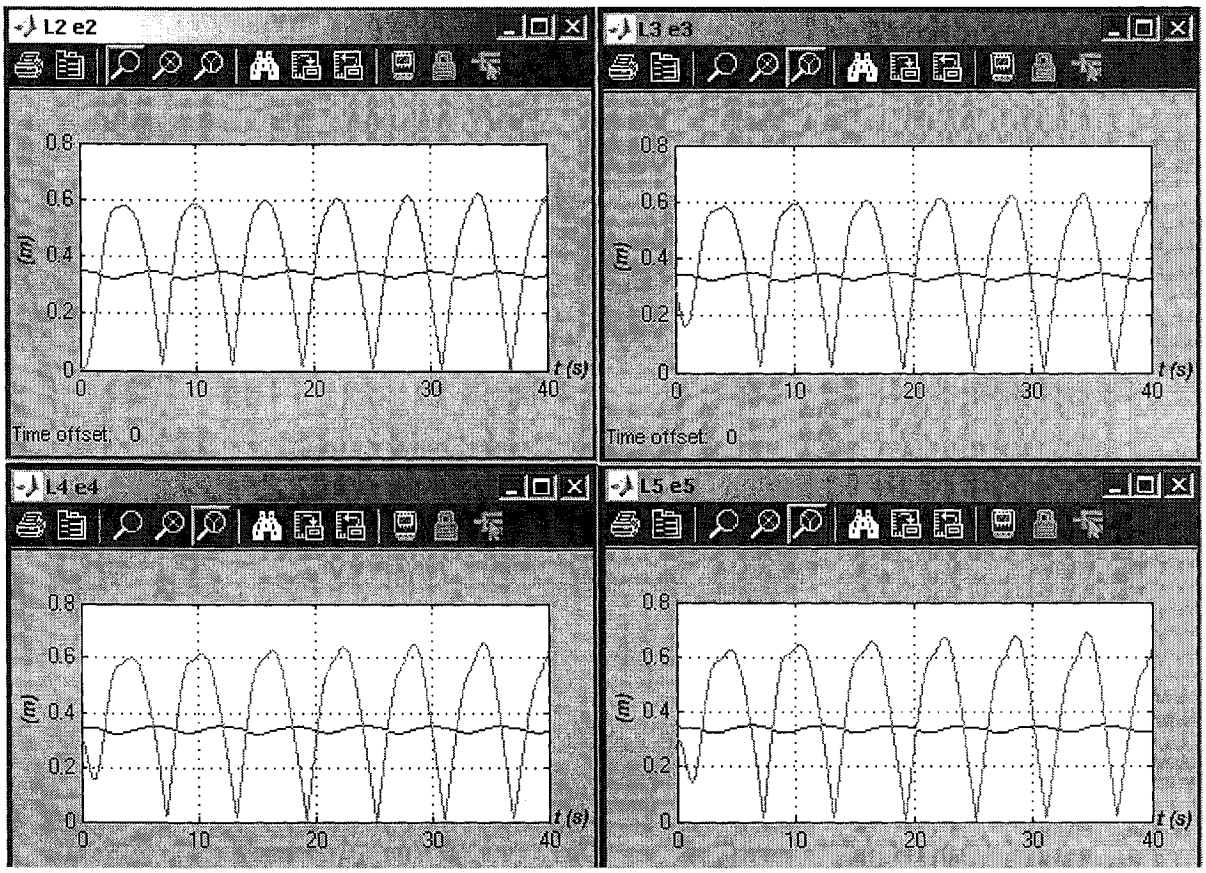

Figure 37 : Effects of very small *h*, black: desired spacing, gray: spacing errors, 2D motion, variable spacing and $A = 15$, $D = 60$, $b = 5$, $d = 0.2$, $h = 0.005$, $k = c = 5$, $|a_x|, |a_y| \le 5$, *a-delay* = 0.

It is interesting to note that variable spacing, because of its improved stability, allows to maintain slightly smaller average inter-vehicle spacing (about 0.4) than the minimum safe spacing achieved by the constant spacing policy (about 1.0, see table 1). Variable spacing would also result in less jerky vehicle motions (smoother acceleration profiles).

Varying the Control Variable (acceleration) Time-Delay:

Table 5 summarizes the effects of gradually increasing time delays introduced into the simulation of the planar variable spacing control scheme. There is a low level of delay (0.05) that causes no noticeable effects. As the delay increases, acceleration is affected first (see figure 38), showing perturbations that amplify down the platoon but attenuate with time. Acceleration saturation is also present starting at vehicle 4. Any perturbation that is amplified down the platoon jeopardizes string stability and so a delay as low as 0.15 s is already a concern. This was also the case in the constant spacing control scheme.

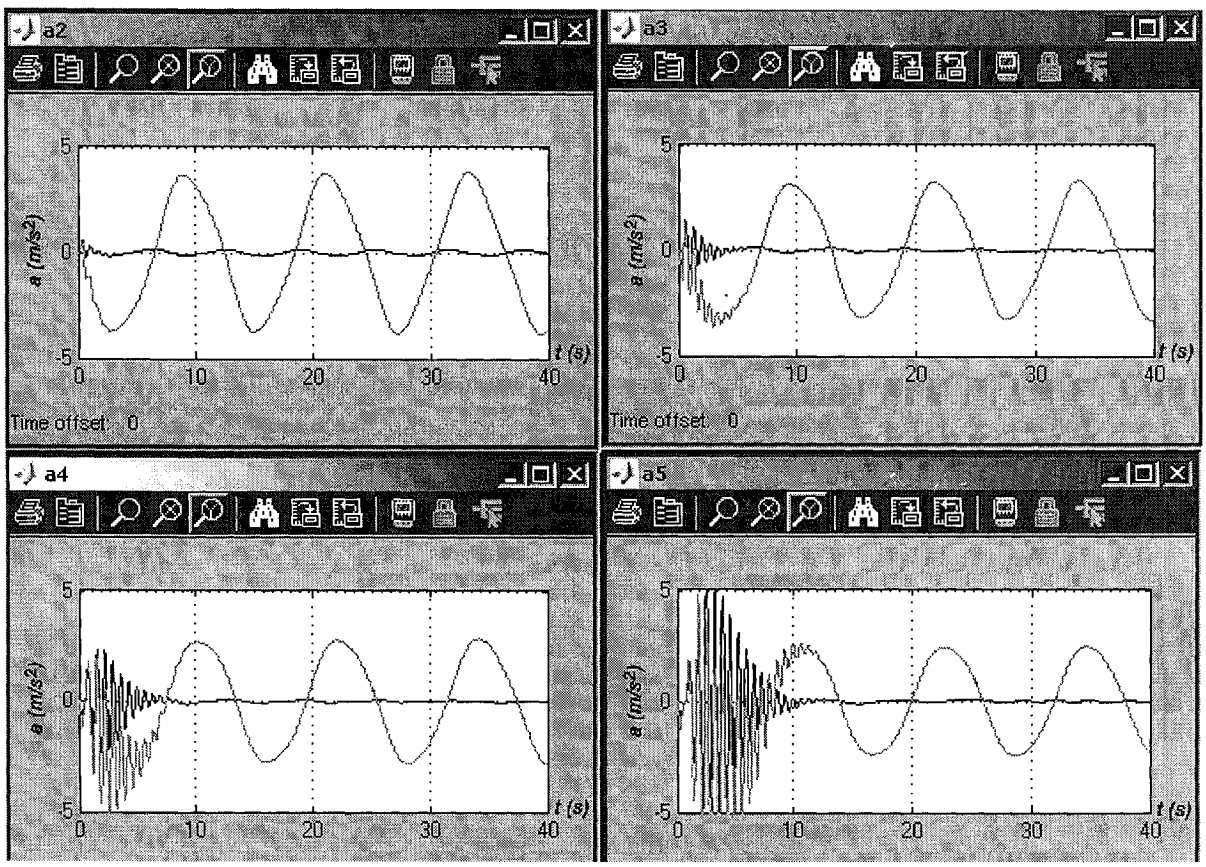

Figure 38 : Effects of feedback delay on accelerations in planar motion with variable spacing policy, a2 was omitted to save space, A = 15, D = 60, b = 5, d = 0.2, h = 0.6, $k = c$ = 5, $|a_x|, |a_y| \leq 5$, *a-delay* = 0.15.

As feedback delays are increased to 0.18s, the effect becomes significant on spacing errors (see figure 39), and very pronounced on accelerations, causing overwhelming actuator saturations down the platoon (see figure 40).

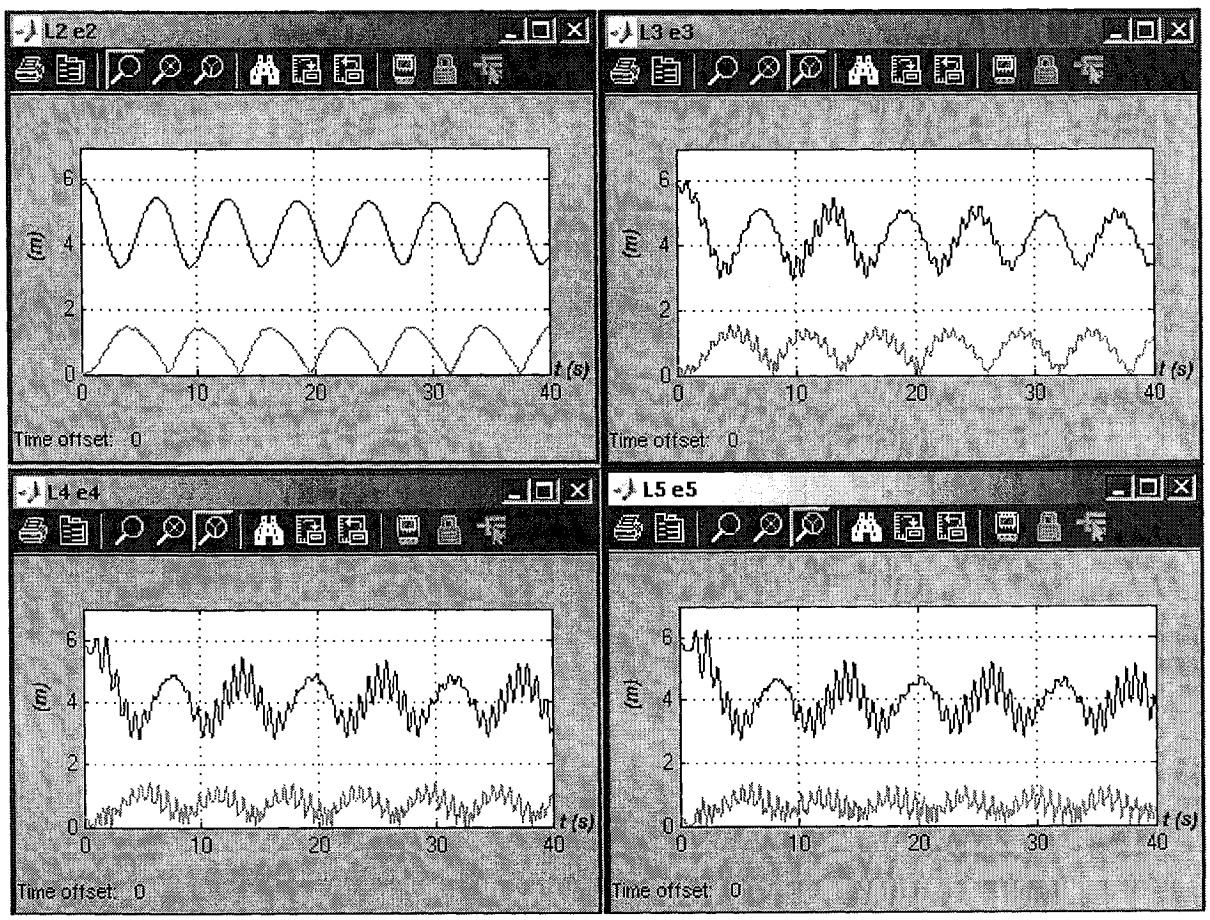

Figure 39 : Effects of feedback delays on spacing errors, planar motion with variable spacing, $A = 15$, $D = 60$, $b = 5$, $d = 0.2$, $h = 0.6$, $k = c = 5$, $|a_x|, |a_y| \leq 5$, *a-delay* = 0.18.

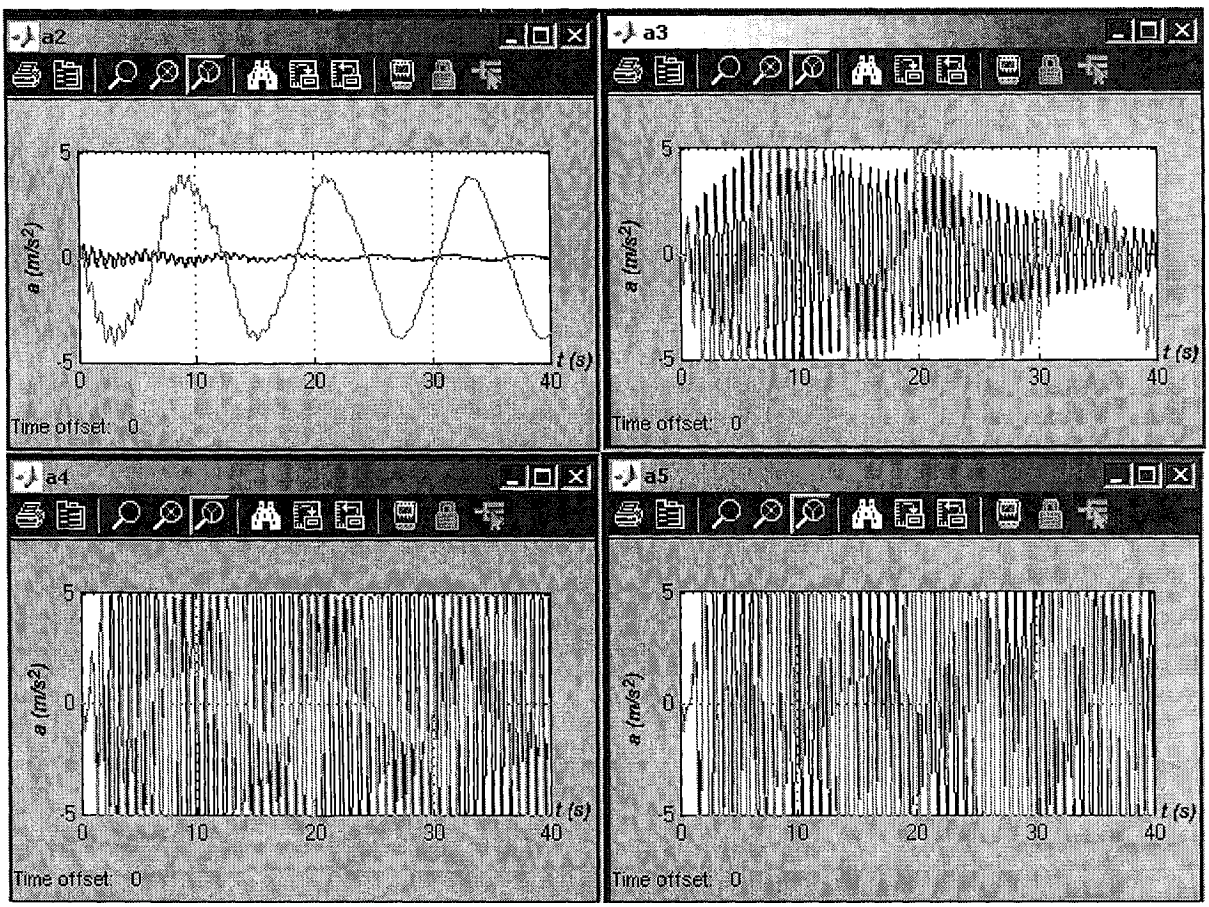

Figure 40 : Effects of delays on accelerations in 2D motion, variable spacing policy, a_1 omitted to save space, A = 15, D = 60, b = 5, d = 0.2, h = 0.6, $k = c$ = 5, $|a_x|, |a_y| \le 5$, *a-delay* = 0.18.

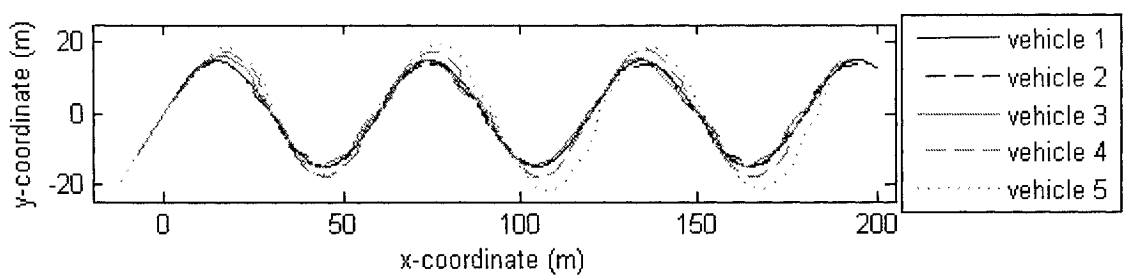

Figure 41 : Effects of delay on vehicle paths in planar motion with variable spacing policy and A = 15, D = 60, b = 5, d = 0.2, h = 0.6, $k = c$ = 5, $|a_x|, |a_y| \le 5$, *a-delay* = 0.4.

Table 5 : Effects of introducing feedback time delays in planar motion with a variable spacing policy and $A = 15$, $D = 60$, $b = 5$, $d = 0.2$, $h = 0.6$, $k = c = 5$, $|a_x|, |a_y| \leq 5$.

a-delay (s)	*Spacing Errors* e_i *(m)*	*Spacing* l_i *(m)*	*Paths*	*Accelerations* a_i (m/s^2)
0.05	Attenuated to 1.1 with *i*.	Same as with no delay.	Same as with no delay	*y* : attenuated with *i* down to 2.4, increasing with *t* *x* : attenuated with *i* down to 2.4, decreasing with *t*
0.15	Small initial high frequency perturbations, attenuated with *i* down to 1.0 and amplified slightly with *t*.	Small initial high frequency perturbations, attenuated with *i* and *t*.	Same as with no delay	Initial high frequency perturbations (see figure 38) attenuated with *t*. Amplitude amplified slightly with *t*.
0.18	High frequency perturbations amplified with *i*, fundamental frequency attenuated with *i* and *t* down to 1.3 (see figure 39)	High frequency perturbations amplified with *i*, fundamental frequency attenuated with *i*	Same as with no delay	Jerkiness starting at vehicle 2, amplified with *i* and attenuated with *t* (see figure 40).
0.4	Errors amplified with *i* up to 10	Amplified with *i*, loss of formation starting at vehicle 4	Important deviations from the path, (see figure 41)	Overwhelming saturations starting at vehicle 2
0.5	Amplified with *i* up to 95	Loss of formation hold starting at vehicle 3, *possible collisions* starting at vehicle 4	Complete deviations from path and out of phase starting at vehicle 4.	Overwhelming saturations starting at vehicle 2

Comparing table 5 for delays with variable spacing to table 2 for delays with constant spacing, both schemes have similar tolerance for feedback delays (although the variable spacing scheme is able to tolerate slightly longer delays without causing collisions).

Varying the Feedback Gains

Reducing feedback gains caused an improvement in leader tracking as well as reduced spacing errors. It is surprising to note that higher accelerations are used by the followers (peaks of 3.3, see table 6 instead of 2.5, see figure 29).

The choice of feedback gains $k = 5$ and $c = 2$ improve platoon control: better path tracking, smaller spacing errors, slightly larger accelerations used by followers. A detailed controller design might verify that these are the best feedback gains for this control scheme.

Table 6 : Effects of varying feedback gains in planar motion with a variable spacing policy and $A = 15$, $D = 60$, $b = 5$, $d = 0.2$, $h = 0.6$, $L = 4$, $|a_x|, |a_y| \leq 5$, a-delay = 0.

k	c	*Spacing Errors* e_i *(m)*	*Spacing* l_i *(m)*	*Paths*	*Accelerations* a_i (m/s^2)
2	2	Attenuated down to 0.4 with *i*	Attenuated with *i* and *t*.	Same as reference	Attenuated with *i* to 3.0 (*y*), 0.04 (*x*), amplified with *t*.
5	5	Reference	Reference	Reference	Reference
10	10	Attenuated down to 1.1 with *i*	Attenuated with *i* and *t* down to 4.1.	Slightly worse tracking of the leader's path	Attenuated with *i* to 2.3 (*y*), 0.02 (*x*), amplified with *t*.
100	100	Attenuated down to 1.2 with *i*	Attenuated with *i* and *t* down to 4.0	Slightly worse tracking of the leader's path	Attenuated with *i* to 2.1 (*y*), 0.06 (*x*), amplified with *t*.
5	2	Attenuated down to 0.19	Attenuated with *i* and *t* down to 5.0	Slightly improved tracking of leader's path	Attenuated with *i* to 3.1 (*y*), 0.01 (*x*), amplified with *t*.

In general, it is not a clear advantage to use a variable spacing policy rather than a constant spacing policy, for a 2D local sensing control scheme. The simulation study shows that both have their advantages and their drawbacks.

5.11 Planar Control, Global Information

The goal of this control scheme is to ensure that all vehicles following the leader follow the leader's path in a specified formation and within a certain tolerance. To achieve this, the knowledge of past and present leader position, i.e. knowledge of leader trajectory so far, becomes a necessity. It will be assumed, for the purpose of this study, that the leader's position can be communicated, in reasonable time, to all followers. Each follower will associate this information with a time value and store it to create a record of the leader's trajectory so far.

The communication method would probably be a kind of broadcast. Another communication pattern could be a transmission of this information from vehicle to vehicle, allowing for greater privacy of communication, but likely causing greater communication delays.

The spacing policy is a constant path-wise distance L.

The PD control law is:

$$\mathbf{u}_i = k\mathbf{e}_i + c\dot{\mathbf{e}}_i \tag{5.11.1}$$

5.11.1 Global Information 2D Test Formation

The formation that will be analyzed here is again a single file platoon of followers. The desired location of each follower is on the leader's path, at a certain path-wise distance behind the actual location of the leading vehicle. For the first follower, the desired location is at a certain path-wise distance behind the position of the leader (see figure 42).

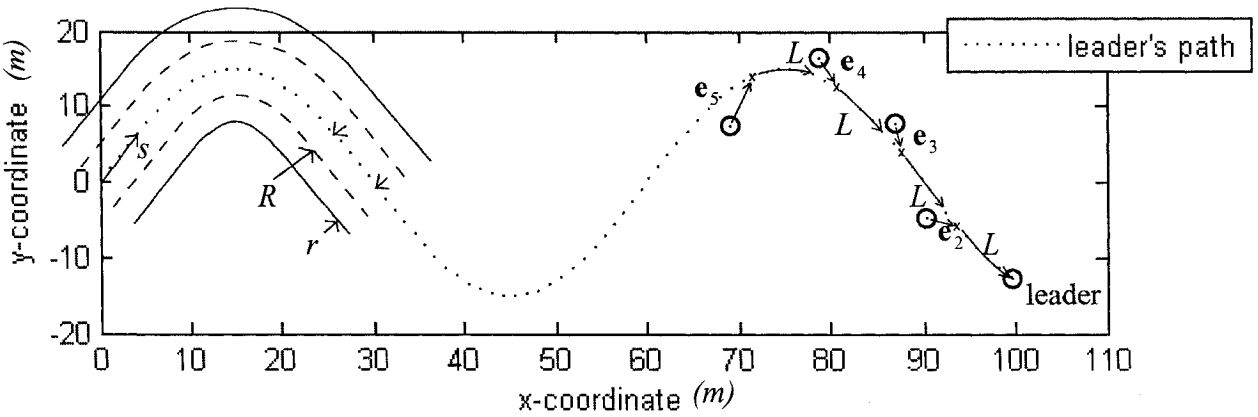

Figure 42 : Single-file formation and spacing errors, one leader and four followers

5.11.2 Global Information Spacing Policy

From the analysis presented in previous sections, it is unclear whether a variable spacing policy is superior to a fixed spacing policy in a 2D motion. The fixed spacing policy makes efficient use of space but its stability needs to be studied. For this reason, a fixed spacing policy has been tested in the global information control scheme.

Since the leader's past trajectory is known to all followers, this control scheme makes extensive use of the leader's path. The path-wise direction is the longitudinal direction along the path coordinate s and the fixed spacing distance is measured along this path. This is different from the straight-line spacing prescribed in the train-like-vehicle (TLV) control scheme developed by Canudas in [15]. Path-wise spacing eliminates singularities that occurred in certain configurations of the TLV.

5.11.3 Definition of Spacing Error

One type of spacing error is a vector from a vehicle's actual position to its desired position on the leader's path (see figure 42) and can be expressed as follows:

$$\mathbf{e}_i = \mathbf{r}_i^d - \mathbf{r}_i \quad \text{for} \quad i = 2,3,4,5 \tag{5.11.2}$$

where:

$\mathbf{r}_i^d = (x_i^d, y_i^d)$ is the desired position of the *i*-th vehicle, a path-wise distance L behind the normal position $\mathbf{r}_{i-1}^n = (x_{i-1}^n, y_{i-1}^n)$ of the preceding vehicle (see figure 43).

$\mathbf{r}_i = (x_i, y_i)$ is the actual position of the *i*-th vehicle

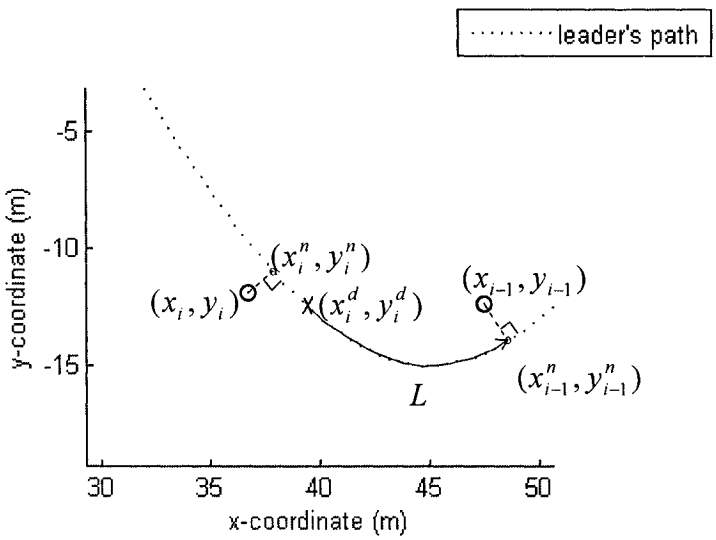

Figure 43 : Determination of desired position $\mathbf{r}_i^d = (x_i^d, y_i^d)$ for *i*-th vehicle.

The normal position (x_i^n, y_i^n) is the closest point on the path to the vehicle's actual position (x_i, y_i). Assuming that the vehicle is less than R away from the path of the leader and using the fact that the slope of segment $\mathbf{r}_i^n - \mathbf{r}_i$ is the negative reciprocal of the slope of the path at x_i^n, the coordinates of the normal position (x_i^n, y_i^n) can be determined as follows:

$$\frac{rise}{run} = \frac{y_i - y_i^n}{x_i - x_i^n} = \frac{y_i - f(x_i^n)}{x_i - x_i^n} = \frac{-1}{\frac{d\,f(x_i^n)}{dx}}$$

where $f(x_i^n) = y(x_i^n)$ (path function) (5.11.3)

and $x_i - R < x_i^n < x_i + R$

Given the vehicle's actual position (x_i, y_i), eq. (5.11.3) could be solved for x_i^n.

If the distance from the vehicle to the leader's path is *small*, the path can be approximated by a line tangent to the path at x_i:

$$y_i^{nl} = q(x_i)x_i^n + p(x_i)$$

where $q(x_i) = \frac{d\,f(x_i)}{dx} = \frac{d\,y(x_i)}{dx}$

When $x_i^n = x_i$,

$$y_i^{nl} = y(x_i) = \frac{d\,y(x_i)}{dx}x_i + p(x_i)$$

$$p(x_i) = y(x_i) - \frac{d\,y(x_i)}{dx}x_i \qquad (5.11.4)$$

$$\therefore y_i^{nl} = x_i^n \frac{d\,y(x_i)}{dx} + y(x_i) - \frac{d\,y(x_i)}{dx}x_i$$

The slope of segment $\mathbf{r}_i^{nl} - \mathbf{r}_i$, where $\mathbf{r}_i^{nl} = (x_i^n, y_i^{nl})$, is the negative reciprocal of the slope of the linearized path. This allows the coordinates of the normal position (x_i^n, y_i^n) to be determined as follows:

$$\frac{rise}{run} = \frac{y_i - y_i^{nl}}{x_i - x_i^n}, \text{ using eq.(5.11.4)}$$

$$\frac{-1}{\frac{d\,y(x_i)}{dx}} = \frac{y_i - \left[x_i^n \frac{d\,y(x_i)}{dx} + y(x_i) - \frac{d\,y(x_i)}{dx} x_i \right]}{x_i - x_i^n}, \quad \text{solving for } x_i^n$$

$$-x_i + x_i^n = \frac{d\,y(x_i)}{dx}\left[y_i - x_i^n \frac{d\,y(x_i)}{dx} - y(x_i) + \frac{d\,y(x_i)}{dx} x_i \right]$$

$$x_i^n \left\{ 1 + \left[\frac{d\,y(x_i)}{dx} \right]^2 \right\} = x_i + \frac{d\,y(x_i)}{dx}\left[y_i - y(x_i) + \frac{d\,y(x_i)}{dx} x_i \right]$$

$$\therefore x_i^n = \frac{x_i + \frac{d\,y(x_i)}{dx}\left[y_i - y(x_i) + \frac{d\,y(x_i)}{dx} x_i \right]}{1 + \left[\frac{d\,y(x_i)}{dx} \right]^2} \qquad (5.11.5)$$

The same x_i^n value can then be used in the real path equation to give a good approximation of the normal point (x_i^n, y_i^n) and distance n_i (see figure 44). In practice, look-up tables can be used to compute $y(x_i)$ and $\frac{d\,y(x_i)}{dx}$.

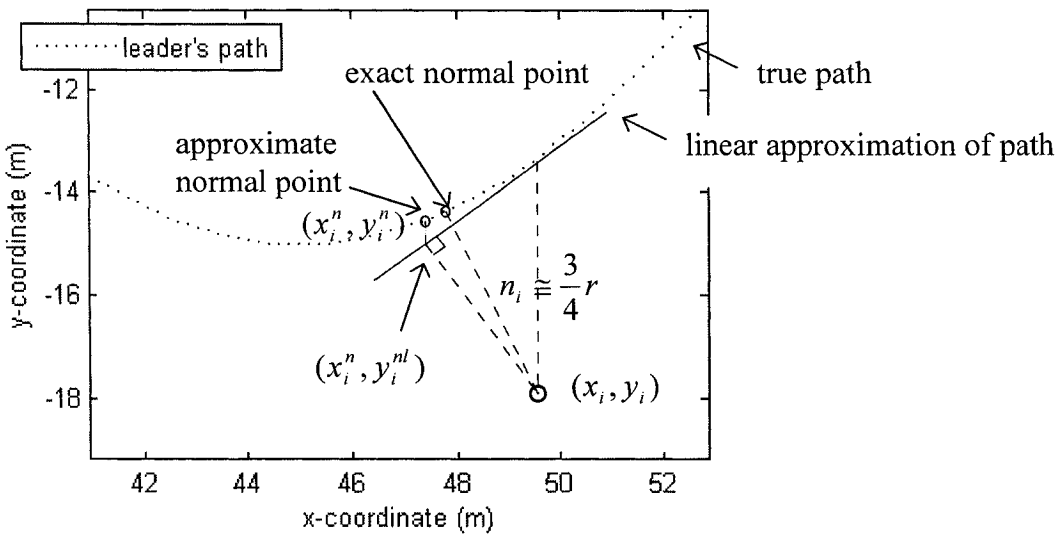

Figure 44 : Finding the normal point using a linear approximation of the leader's path.

5.11.4 Finding Desired Position

The desired position $\mathbf{r}_i^d = (x_i^d, y_i^d)$ is located a path-wise distance L behind the normal point of the predecessor $\mathbf{r}_{i-1}^n = (x_{i-1}^n, y_{i-1}^n)$. To obtain an exact solution for the desired x-coordinate x_i^d, it is necessary to solve the following integral:

$$L = \int_{x_i^d}^{x_{i-1}^n} \sqrt{1 + \left[\frac{d\,y(x)}{dx}\right]} \, dx \tag{5.11.6}$$

There is no readily available analytical solution method for this equation.

Using look-up tables that relate x to s and vice-versa, x_i^d can be computed as follows:

$$\begin{aligned} & x_{i-1}^n \;\Rightarrow\; \text{lookup table } x \text{ to } s \;\Rightarrow\; s_{i-1} \\ & s_{i-1} - L = s_d \;\Rightarrow\; \text{lookup table } s \text{ to } x \;\Rightarrow\; x_i^d \end{aligned} \tag{5.11.7}$$

The corresponding y_i^d can then be computed using any practical relation between the x and the y coordinates (in practice, this could also be a look-up table). The desired position of the i-th vehicle is thus determined: $\mathbf{r}_i^d = (x_i^d, y_i^d)$.

5.11.5 Set of Initial Conditions

As in the previous sections, the platoon will initially be in a state of equilibrium with zero spacing errors and a constant velocity of the leader (a perfect straight line formation, see figure 11). As long as the leader maintains constant velocity (magnitude and direction), so will the followers and spacing errors will be zero indefinitely (equilibrium).

5.11.6 Simulation Using Simulink Model

The data for the lookup tables is generated by a separate Simulink program called "pathgenerator" (see Appendix E). The data produced by this program was used to construct lookup tables that approximate the following mappings: $x \to y$, $x \to s$, $s \to x$, $x \to \frac{dy}{dx}$.

The straight line and constant speed trajectory that precedes the start of the simulation was added to the look-up tables separately within the Matlab workspace by concatenating two arrays. Based on the look-up table data, a graph of the leader's path is shown in figure 45 and graphs of the leader's x and y-coordinates over time are shown in figure 46.

It is important to note that the leader travels at constant speed along the initial straight portion of the path and enters the sinusoidal path with variable x and y velocities beginning at time $t = 0$. In other words, perturbation is introduced into the motion of the platoon at time $t = 0$.

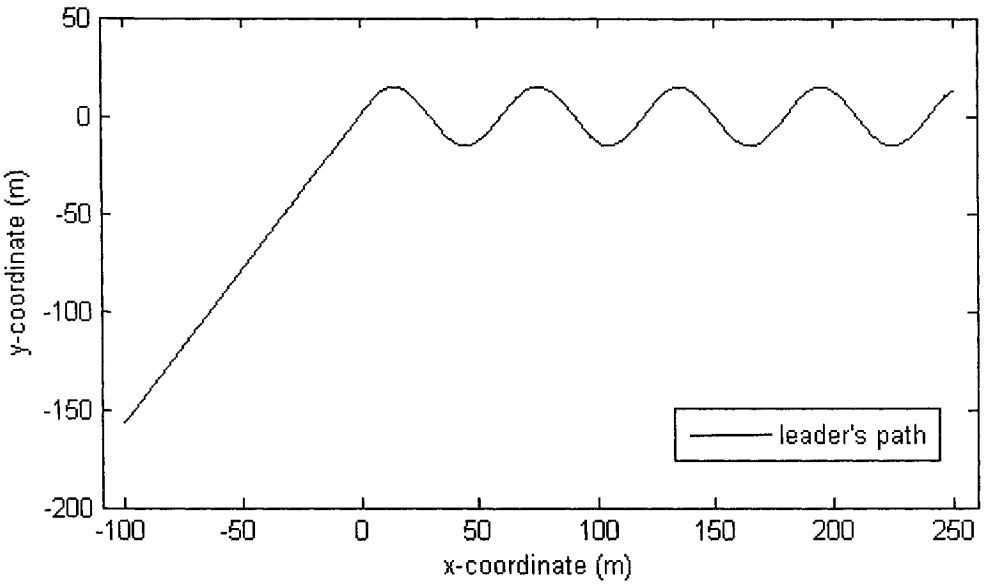

Figure 45 : Graph of the leader's path, control scheme using global information.

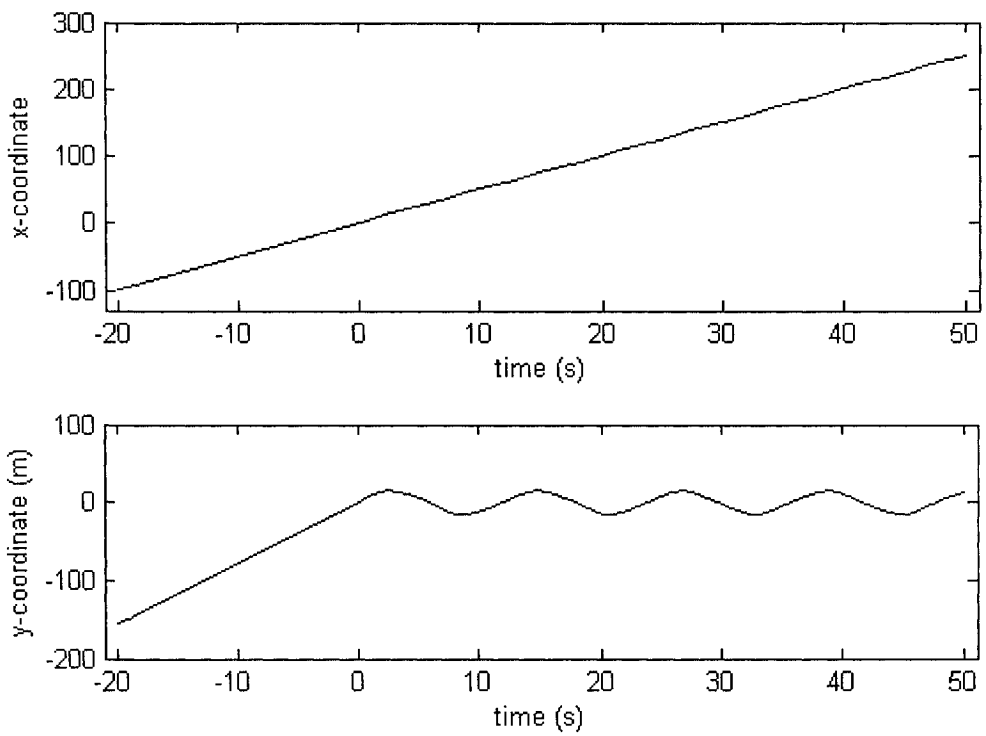

Figure 46 : Graph of the leader's x and y-coordinates over time, control scheme using global information.

The various components of the Simulink model are shown in Appendix E

5.11.7 General System Behavior

To allow for comparison with the local sensing 2D control scheme, similar parameters were used for this simulation: $A = 15$, $D = 60$, $b = 5$, $d = 0.2$, $k = c = 5$, $L = 4$, $\max|a| = 5$ and a-delay = 0. The leader's trajectory remained unchanged. In the simulated platoon motion, the followers adhere to the leader's path reasonably well (see figure 47).

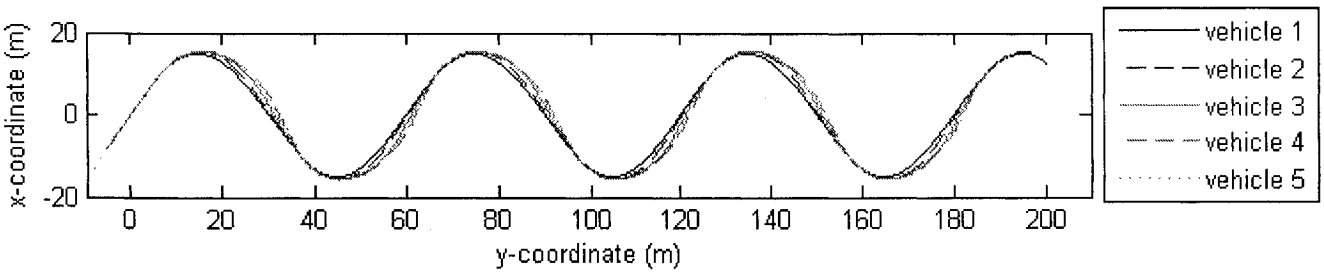

Figure 47 : Paths of leader and followers, control scheme using global information, $A = 15$, $D = 60$, $b = 5$, $d = 0.2$, $k = c = 5$, $L = 4$, $\max|a| = 5$, a-delay = 0.

Unfortunately, the spacing errors (path-wise e_i^s and normal n_i) do not show stable behavior. Figure 48 shows that path-wise errors amplify down the platoon (as i increases) and have an unclear behavior as time increases. Also, vehicle 5 loses formation temporarily at time $t = 7s$. Figure 49 shows that normal spacing errors start by amplifying down the platoon and then level out. As time increases, normal spacing errors seem to amplify which would be a sign of instability.

It seems that the path-wise interconnection of this control scheme along with adherence to the leader's path through global information bring back the instability that exited in the 1D constant spacing control scheme.

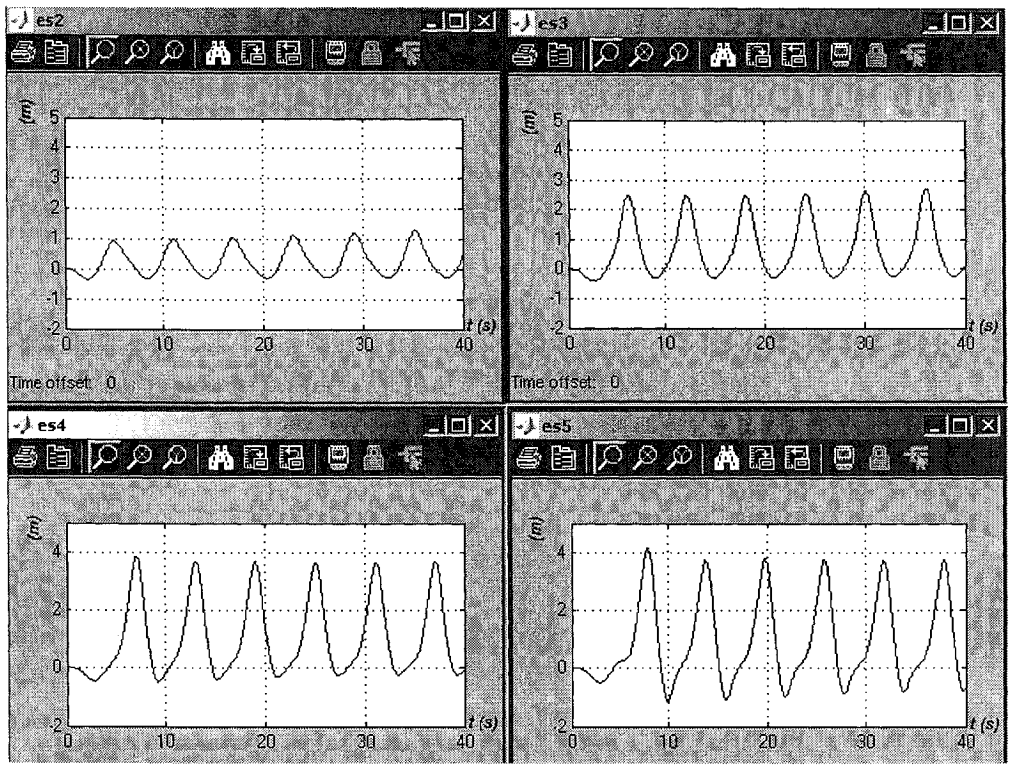

Figure 48 : Path-wise errors, control scheme using global information, $A = 15$, $D = 60$, $b = 5$, $d = 0.2$, $k = c = 5$, $L = 4$, $\max|a| = 5$, a-delay $= 0$.

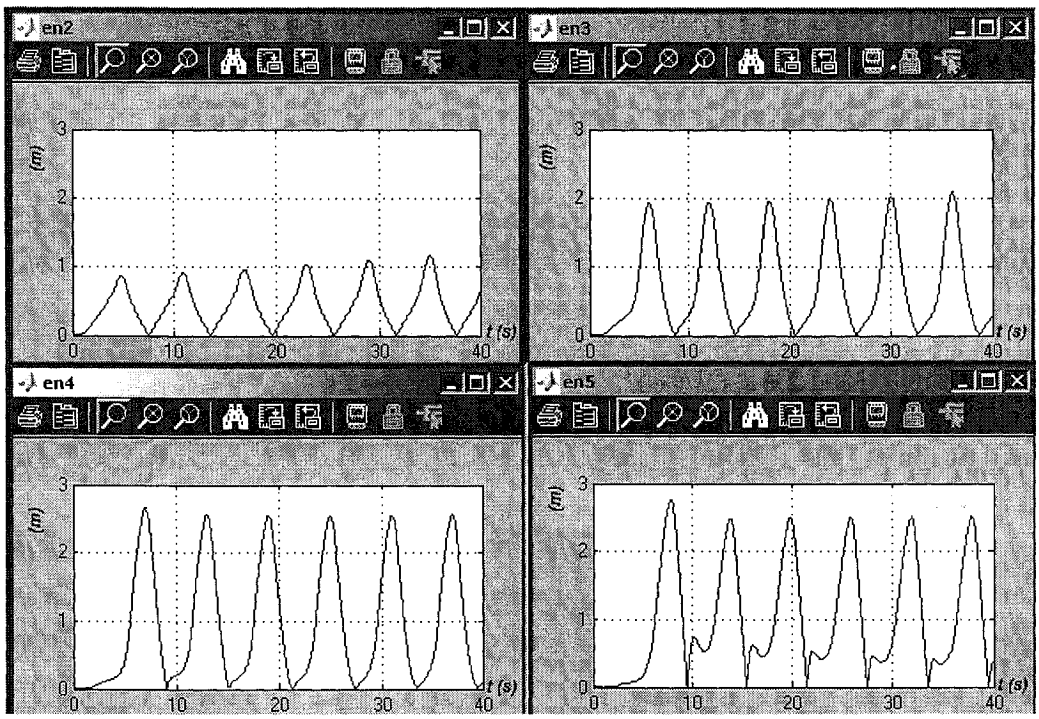

Figure 49 : Normal spacing errors, control scheme using global information, $A = 15$, $D = 60$, $b = 5$, $d = 0.2$, $k = c = 5$, $L = 4$, $\max|a| = 5$, a-delay $= 0$.

The normal spacing error should not exceed the road half-width R which, according to equation 5.3.5, is limited to:

$$R = \frac{1}{2A}\left(\frac{D}{2\pi}\right)^2 \quad \text{with } A = 15,\ D = 60$$

$$R \cong 3$$

Therefore, in a relatively small platoon of 5 vehicles, formation loss is already an issue with path-wise spacing exceeding the $2L$ limit and normal spacing error comes close to the roadway half-width of $3m$, with vehicle 5 having a normal error maximum around 2.8 m. To achieve string stability, as defined for 2D in section 5.4, the global information control scheme would have to adopt a variable spacing policy, or a better set of control parameters would need to be found.

6. Conclusions

When dealing with the motion of a platoon or string of vehicles, stability must be considered with respect to two variables: time t (traditional sense) and vehicle index i (string stability). The second dimension is especially important for platoons with large numbers of vehicles. In this thesis, only platoons of identical vehicles with identical controllers were considered.

Stability over time can be studied using transfer function root locus methods for linear systems or Lyapunov function methods. In this thesis, a Lyapunov function analysis predicted time stability for a certain range of parameters for both constant and variable spacing policies in the 1D control schemes studied. This was confirmed by computer simulations.

Stability with respect to vehicle index was studied using the spacing error transfer function. This was done for 1D motion and predicted string *instability* for a constant spacing policy and string stability for a variable spacing policy for a certain domain of parameters. In general, platoon stability is easier to achieve for a variable spacing policy.

In all cases, analytical methods are difficult to apply to some features of platoon models. For this reason, the behavior of 2D motion and the effects of actuator saturation or feedback delays were studied using computer simulations.

Although string stability cannot be achieved with a constant spacing policy in 1D motion, in 2D motion simulations, with local sensing only, a stable behavior was achieved with the same constant spacing policy. This could be due to a "path attenuation" effect where followers deviate substantially from the leader's path.

If the platoon is traveling through a space free of obstacles, this control scheme is very appealing. It appears that string stability is created by introducing lateral perturbations. Perhaps 1D string stability could also be achieved with constant spacing if a sufficiently large lateral perturbation was introduced into the leader's trajectory and a 2D control scheme was used. This control scheme would not guarantee, however, adherence to the leader's path for major changes in direction of the leader.

If adherence to the leader's path is important, global information sharing becomes a necessity so that followers know the location of the leader's path. Based on the simulation performed in this thesis, adherence to the leader's path eliminates the stabilizing path attenuation effect and string stability is not achieved with a constant spacing policy and the longitudinally interconnected control scheme used in the simulation.

In general, for a constant spacing policy, a balance must be achieved between adherence to the leader's path, system interconnectedness, spacing policy and platoon stability. The results of computer simulations in 2D motion indicate that a constant spacing policy and longitudinal interconnection of vehicles make it difficult to achieve platoon stability while adhering to the path of the leader. Platoon stability is achieved more easily if deviations from the leader's path are tolerated or if platoon members are disconnected from each other by appropriate use of information broadcast by the leader.

In a global information control scheme, the desired position of each follower can be determined solely based on the leader's position. This disconnects the platoon completely and the issue of string stability no longer exists [15]. The drawback of such a control scheme is that individual vehicles no longer react to the relative position of their predecessor which increases the possibility of collisions or formation loss.

7. Directions for Further Study

The results presented in this thesis are valid only for the particular test trajectory used in the simulations. Many other trajectories would have to be tested to verify these results for a general trajectory. Sinusoidal trajectories are however relevant test trajectories given that Fourier series permit the decomposition of arbitrary trajectories into a combination of sinusoidal components.

The global information control scheme could be studied in more detail and a set of control parameters could possibly be found that achieve platoon stability in spite of a constant spacing policy, longitudinal interconnection of vehicles and path-adherence requirements. Also, different heuristics could be used in the planar control schemes to define vehicle coordinates, motions and spacing errors and how they are used in the control law. Perhaps this would lead to improved performance.

Another step that could be taken to better understand string stability of long formations is to model 3D motion. Perhaps new effects would be discovered such as the path attenuation observed in this study in going from 1D to 2D motion.

To investigate how particular vehicle dynamics affect the behavior of long formations, a comprehensive vehicle model could replace the basic point mass representation used above. Because the stability of any system is guaranteed only with respect to a specific set of coordinates, the particular vehicle model and the coordinates used to describe its motion and control as well as the motion of the entire formation are likely to have an impact on the results of such a study.

Lastly, as with all theoretical and simulated investigations, the ultimate test of feasibility of any control scheme would be to use real automated vehicles to conduct a series of physical trials. These could be ground vehicles moving along a flat surface, or, if larger resources are available, automated watercraft, submarines or aerial vehicles.

References

[1] Canudas de Wit, C., and Brogliato, B., "Stability Issues for Vehicle Platooning in Automated Highway Systems," http://www-lag.ensieg.inpg.fr/canudas/publications/vechicle_control/String_stability_CCA99.pdf, 1999, accessed October 26, 2004, pp. 6.

[2] Swaroop, D., and Hedrick, J.K., "Constant Spacing Strategies for Platooning in Automated Highway Systems," *Transactions of the ASME,* Vol. 121, 1999, pp. 462-470.

[3] Baillieul, J., and Suri, A., "Information Patterns and Hedging Brockett's Theorem in Controlling Vehicle Formations," *42nd IEEE Conference on Decision and Control, Dec 9-12 2003,* Vol. 1, Institute of Electrical and Electronics Engineers Inc, Maui, HI, United States, 2003, pp. 556-563.

[4] Cassandras, C.G., and Li, W., "A Receding Horizon Approach for Solving Some Cooperative Control Problems," *Proceedings of the 41st IEEE Conference on Decision and Control,* IEEE, 2002, pp. 3760-3765.

[5] Slotine, J.E., and Li, W., "Applied Nonlinear Control," Prentice Hall, Englewood Cliffs, New Jersey, 1991, pp. 459.

[6] Merkin, D.R., "Introduction to The Theory of Stability," Springer, New York, 1997,

[7] Zhang, J., Suda, Y., and Iwasa, T., "Vector Liapunov function approach to longitudinal control of vehicles in a platoon," *JSME International Journal, Series C: Mechanical Systems, Machine Elements and Manufacturing,* Vol. 47, No. 2, 2004, pp. 653-658.

[8] No, T.S., Chong, K.-T., and Roh, D.-H., "A Lyapunov function approach to longitudinal control of vehicles in a platoon," *IEEE Transactions on Vehicular Technology,* Vol. 50, No. 1, 2001, pp. 116-125.

[9] Swaroop, D., and Hedrick, J.K., "String Stability of Interconnected Systems," *IEEE Transactions on Automatic Control,* Vol. 41, No. 3, 1996, pp. 349-357.

[10] Boskovic, J.D., Li, S., and Mehra, R.K., "Formation flight control design in the presence of unknown leader commands," *2002 American Control Conference, May 8-10 2002,* Vol. 4, Institute of Electrical and Electronics Engineers Inc, Anchorage, AK, United States, 2002, pp. 2854-2859.

[11] Caicedo, R.E., Valasek, J., and Junkins, J.L., "Preliminary Results of One-Dimensional Vehicle Formation Control Using a Structural Analogy," *2003 American Control Conference, Jun 4-6 2003,* Vol. 6, Institute of Electrical and Electronics Engineers Inc, Denver, CO, United States, 2003, pp. 4687-4692.

[12] Liu, X., Goldsmith, A., and Mahal, S.S., "Effects of communication delay on string stability in vehicle platoons," *2001 IEEE Intelligent Transportation Systems Proceedings, Aug 25-29 2001,* Oakland, CA, 2001, pp. 625-630.

[13] Papadimitriou, I., and Tomizuka, M., "Lateral control of platoons of vehicles on highways: The autonomous following based approach," *International Journal of Vehicle Design,* Vol. 36, No. 1, 2004, pp. 24-37.

[14] Suryanarayanan, S., Tomizuka, M., and Suzuki, T., "Design of Simultaneously Stabilizing Controllers and its Application to Fault-Tolerant Lane-Keeping Controller Design

for Automated Vehicles," *IEEE Transactions on Control Systems Technology,* Vol. 12, No. 3, 2004, pp. 329-339.

[15] Canudas de Wit, C., and NDoudi-Likoho, A.D., "Nonlinear Control for a Convoy-like Vehicle," *Automatica,* Vol. 36, 2000, pp. 457-462.

[16] Chen, X., Serrani, A., and Ozbay, H., "Control of leader-follower formations of terrestrial UAVs," *Proceedings of the 42nd IEEE Conference on Decision and Control,* IEEE, 2003, pp. 498-503.

[17] Fredslund, J., and Mataric, M.J., "A General Algorithm for Robot Formations Using Local Sensing and Minimal Communication," http://www.daimi.au.dk/%7Echili/Formations/journalpaper.pdf, 2001, accessed August 24, 2004, pp. 9.

[18] Bendersky, D.A., and Santos, J.M., "Robot Formations as an Emergent Collective Task using Target-following Behavior," http://tornado.dia.fi.upm.es/caepia/numeros/21/bendersky.pdf, 2004, accessed August 24, 2004, pp. 10.

[19] Jadbabaie, A., Lin, J., and Morse, A.S., "Coordination of Groups of Mobile Autonomous Agents Using Nearest Neighbor Rules," *IEEE Transactions on Automatic Control,* Vol. 48, No. 6, 2003, pp. 988-1001.

[20] Lee, J., Huang, R., and Vaughn, A., "Strategies for Path-Planning for a UAV to Track a Ground Vehicle," http://vehicle.me.berkeley.edu/Publications/AVC/strategies_ains2003.pdf, 2003, accessed August 16, 2004, pp. 6.

[21] Wang, D., and Qi, F., "Trajectory Planning for a Four-Wheel-Steering Vehicle," *Proceedings of the 2001 IEEE International Conference on Robotics and Automation,* IEEE, 2001, pp. 3320-3325.

[22] Fraichard, T., "Dynamic Trajectory Planning with Dynamic Constraints: a 'State-Time Space' Approach," *Proceedings of the IEEE/RSJ Int. Conf. on Intelligent Robots and Systems,* 1993, pp. 1393-1400.

[23] Connolly, T.R., and Hedrick, J.K., "Longitudinal Transition Maneuvers in an Automated Highway System," *Journal of Dynamic Systems, Measurement, and Control,* Vol. 121, 1999, pp. 471-478.

[24] Halle, S., Laumonier, J., and Chaib-draa, B., "A Decentralized Approach to Collaborative Driving Coordination," *Proceedings of the 7th IEEE International Conference on Intelligent Transportation Systems*, 2004, pp. 6.

[25] Bae, H.S., and Gerdes, C.J., "Parameter Estimation and Command Modification for Longitudinal Control of Heavy Vehicles," Vol. 2004, 2000, pp. 8.

[26] Inalhan, G., Tillerson, M., and How, J.P., "Relative Dynamics and Control of Spacecraft Formations in Eccentric Orbits," *Journal of Guidance, Control, and Dynamics,* Vol. 25, No. 1, 2002, pp. 48-59.

[27] Gill, E., Steckling, M., and Butz, P., "Gemini: A Milestone Towards Autonomous Formation Flying," *ESA Workshop on On-Board Autonomy*, Noordwijk, 2001, pp. 5.

[28] Bauer, F.H., Hartman, K., and How, J.P., "Enabling Spacecraft Formation Flying through Spaceborne GPS and Enhanced Automation Technologies," *12th International Technical Meeting of the Satellite Division of the Institute of Navigation*, 1999, pp. 369-384.

[29] Singh, S.N., "Adaptive feedback linearizing nonlinear close formation control of UAVs," *2000 American Control Conference, Jun 28-Jun 30 2000,* Vol. 2, Institute of Electrical and Electronics Engineers Inc., Piscataway, NJ, USA, Chicago, IL, USA, 2000, pp. 854-858.

[30] Boskovic, J.D., and Mehra, R.K., "Multiple Model-Based Adaptive Reconfigurable Formation Flight Control Design," *Proceedings of the 41st IEEE Conference on Decision and Control,* IEEE, 2002, pp. 1263-1268.

[31] Healey, A.J., "Application of formation control for multi-vehicle robotic minesweeping," *40th IEEE Conference on Decision and Control (CDC), Dec 4-7 2001,* Vol. 2, Institute of Electrical and Electronics Engineers Inc, Orlando, FL, 2001, pp. 1497-1502.

[32] Lofland Gould, L., and Heppner, F., "The Vee Formation of Canada Geese," *The Auk,* Vol. 91, 1974, pp. 494-506.

[33] Huth, A., and Wissel, C., "The Simulation of the Movement of Fish Schools," *Journal of Theoretical Biology,* Vol. 156, 1992, pp. 365-385.

Appendices

Appendix A : Simulink Model, Linear Motion, Constant Spacing

Filename: onedirconstspace.mdl

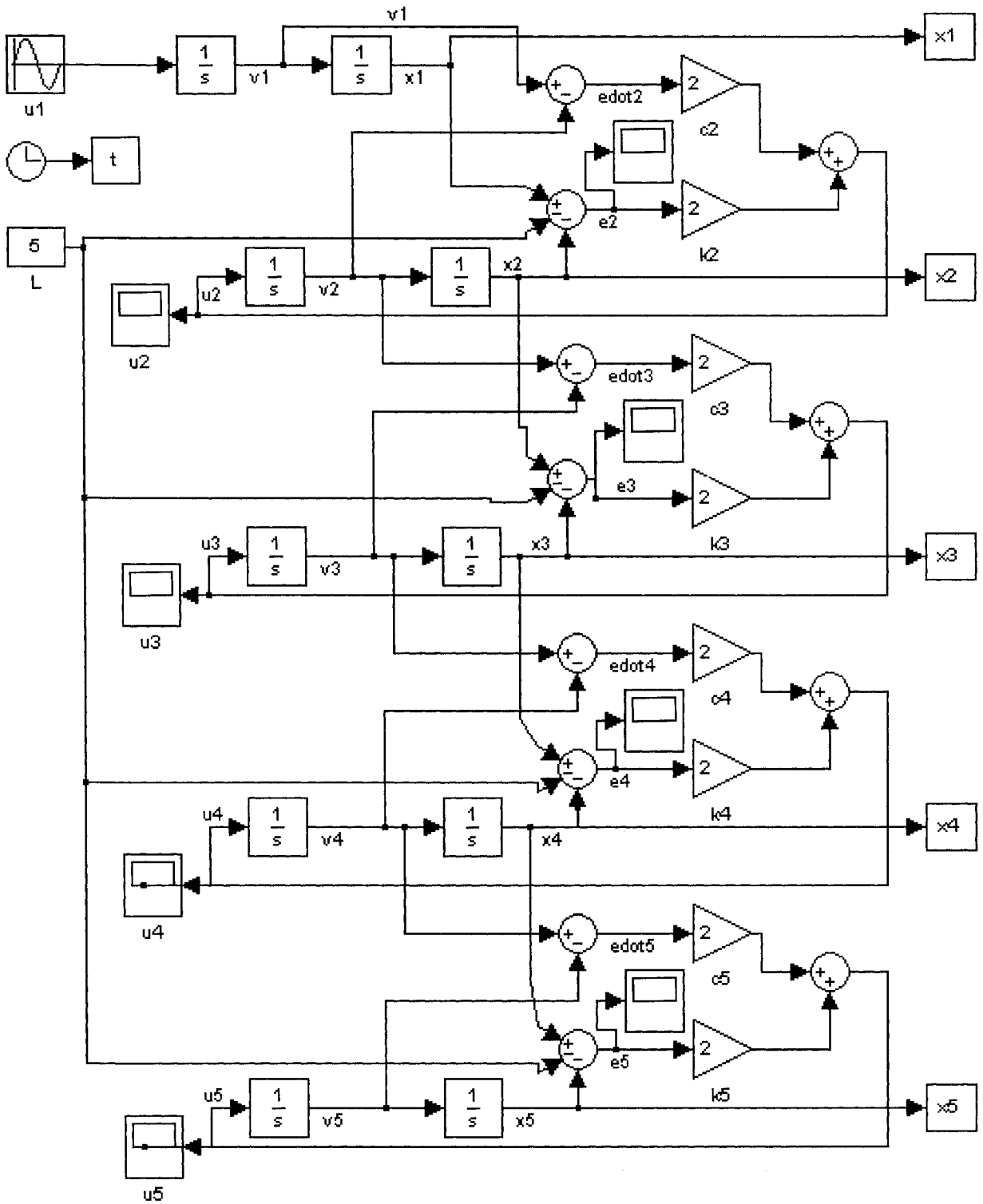

5-vehicle platoon model
with constant spacing L,
proportional/derivative feedback,
forward looking information only.
Constant feedback gains.
u1 = sin (2pi t)
at t=0,
v1 = v2 = v3 = v4 = v5 = 0
[x1, x2, x3, x4, x5] = [20, 15, 10, 5, 0]
See [1] section 4.1

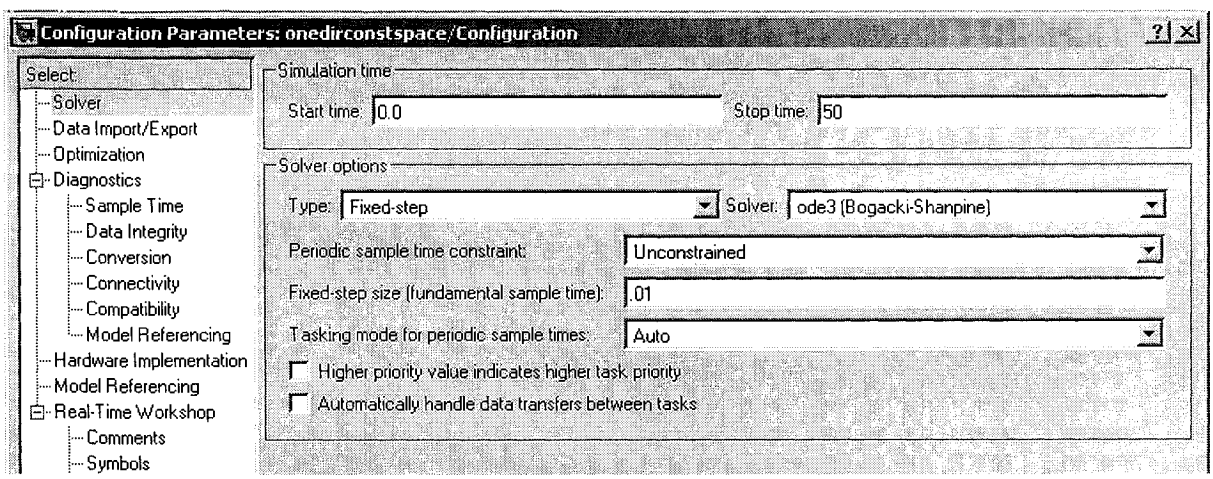

Appendix B : Simulink Model, Linear Motion, Variable Spacing

Filename: onedirvarspace.mdl

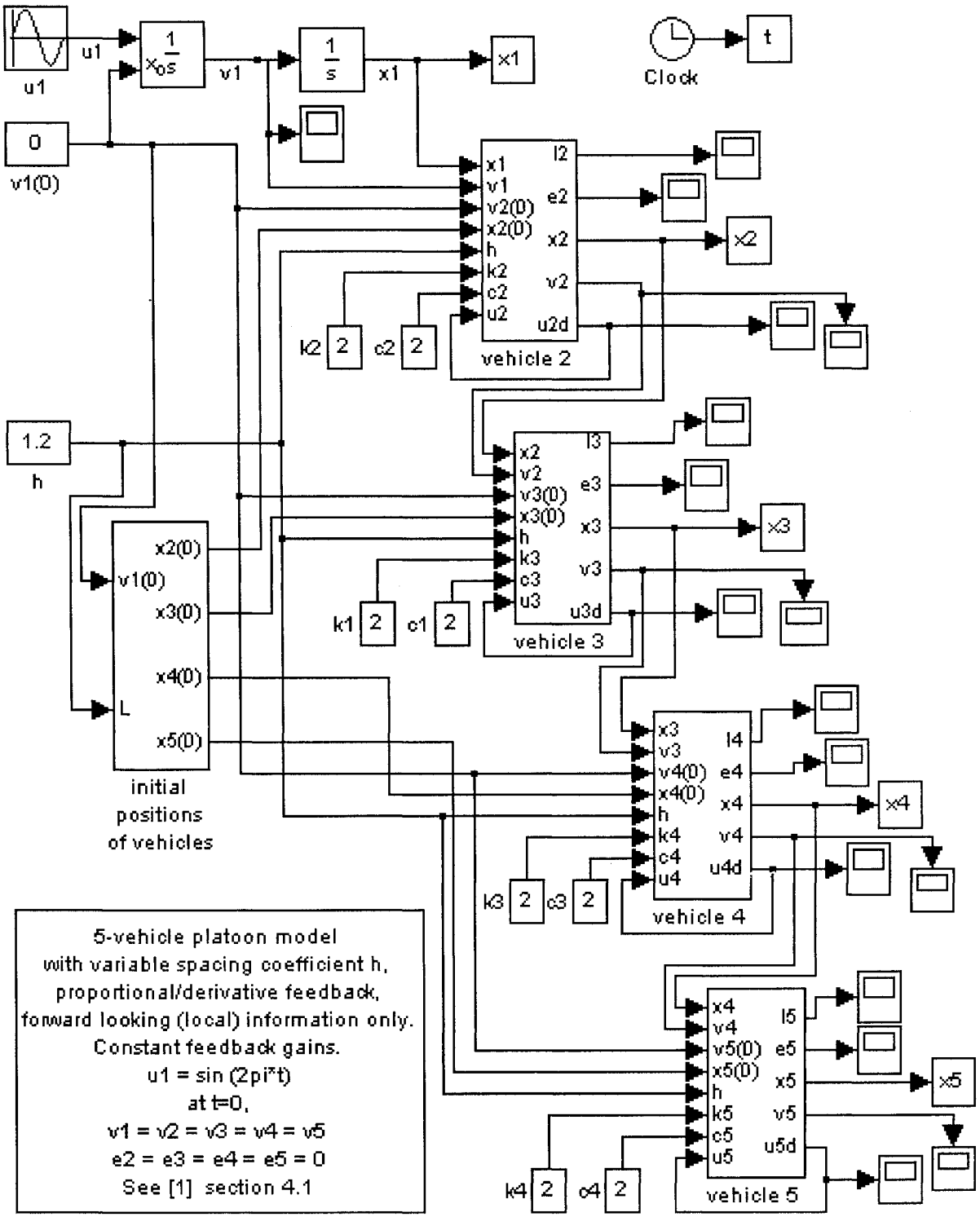

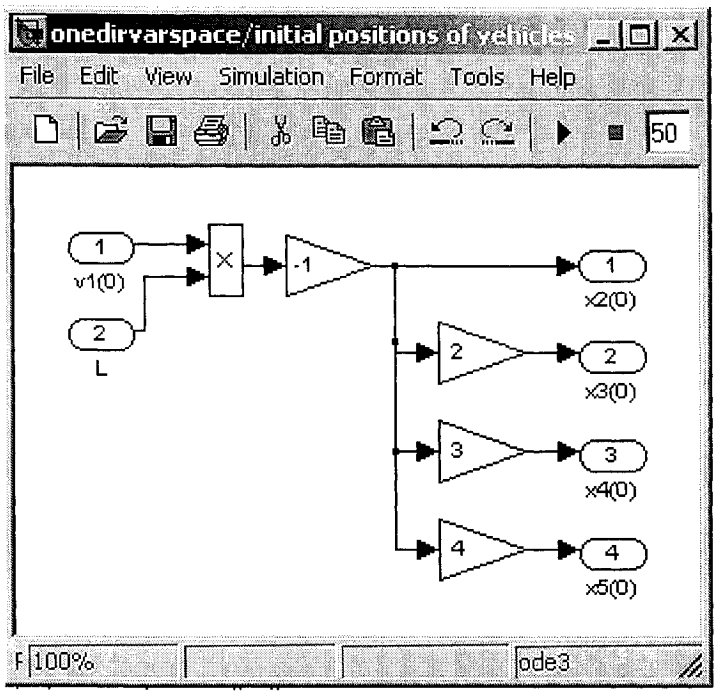

Initial Position of Vehicles subsystem

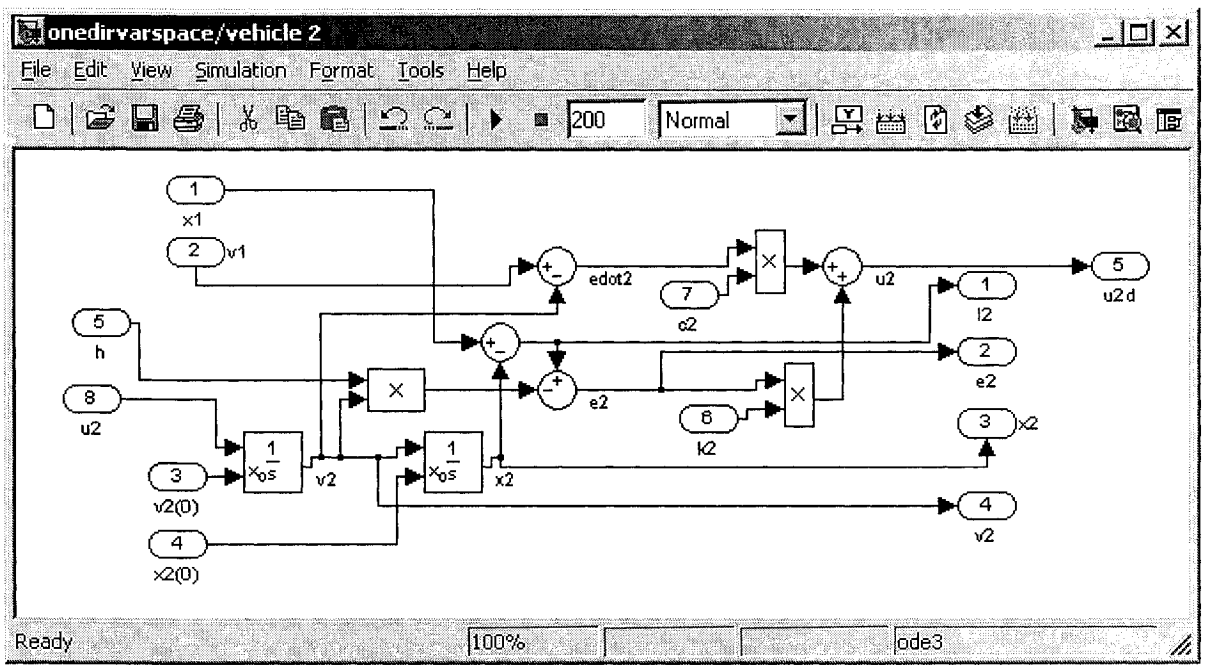

Vehicle 2 Subsystem

Appendix C : Simulink Model, Planar Motion, Local Information, Constant Spacing

Filename: onedirconstspace2dxdot.mdl

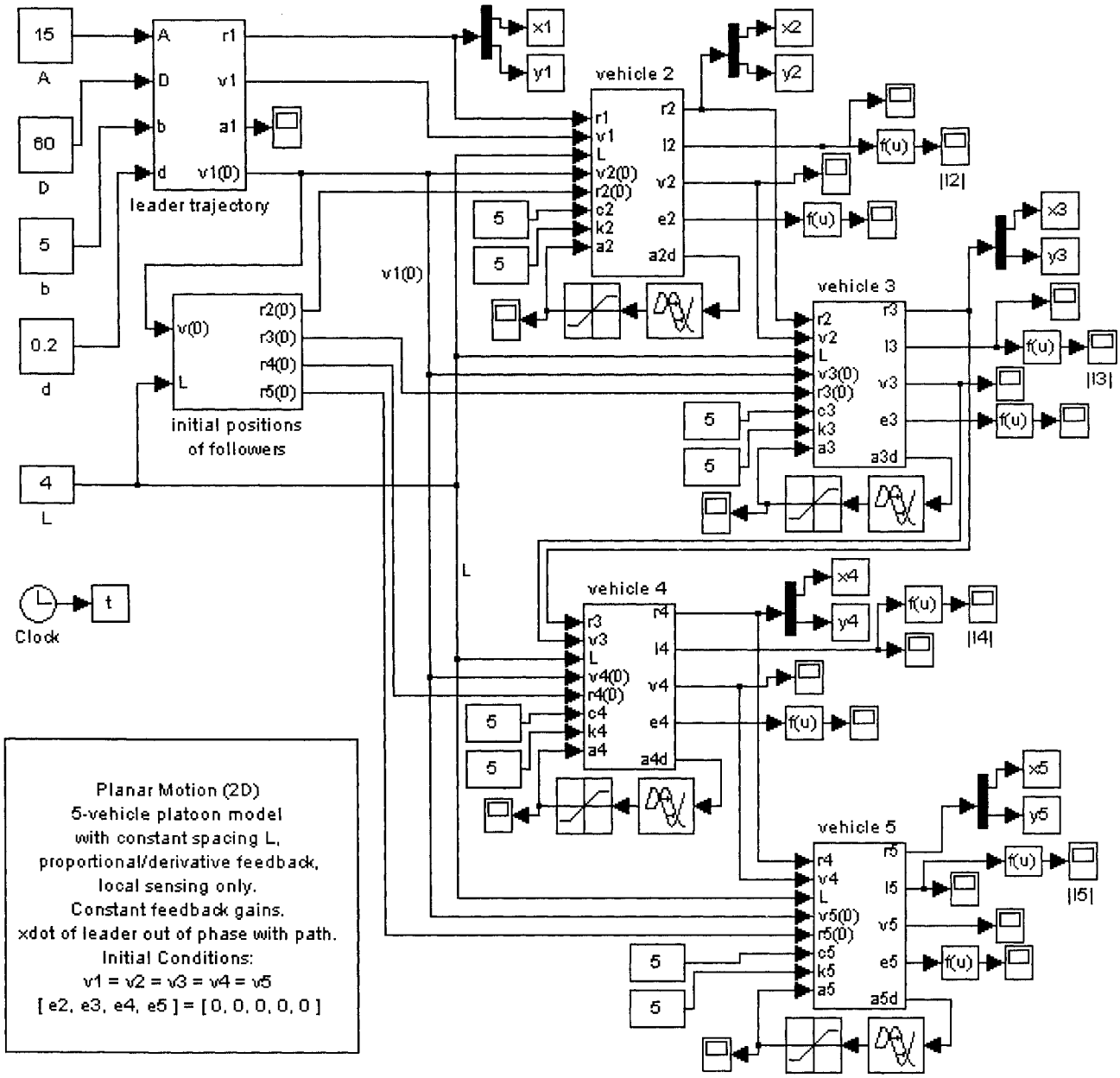

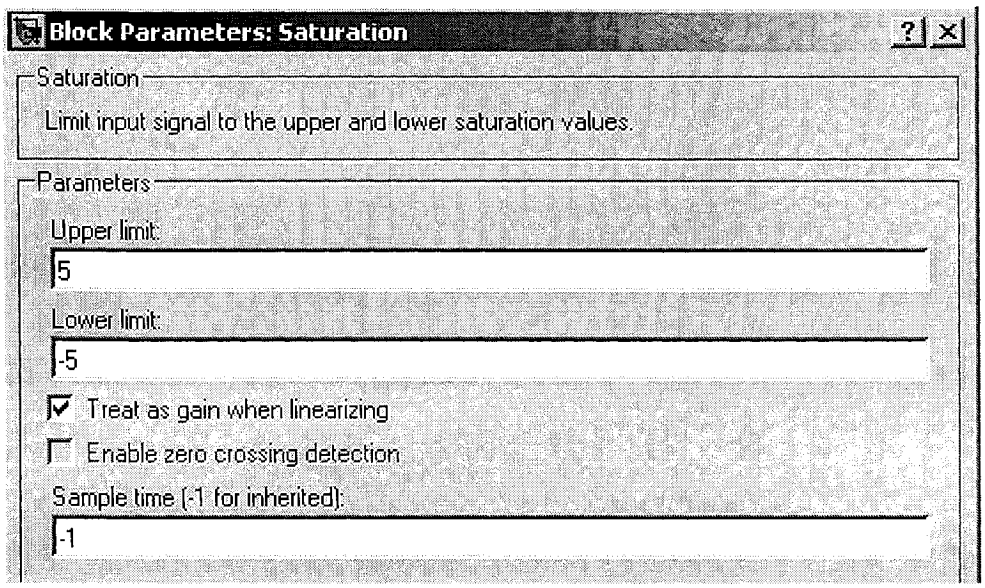

Saturation block used for limiting acceleration, showing typical setting

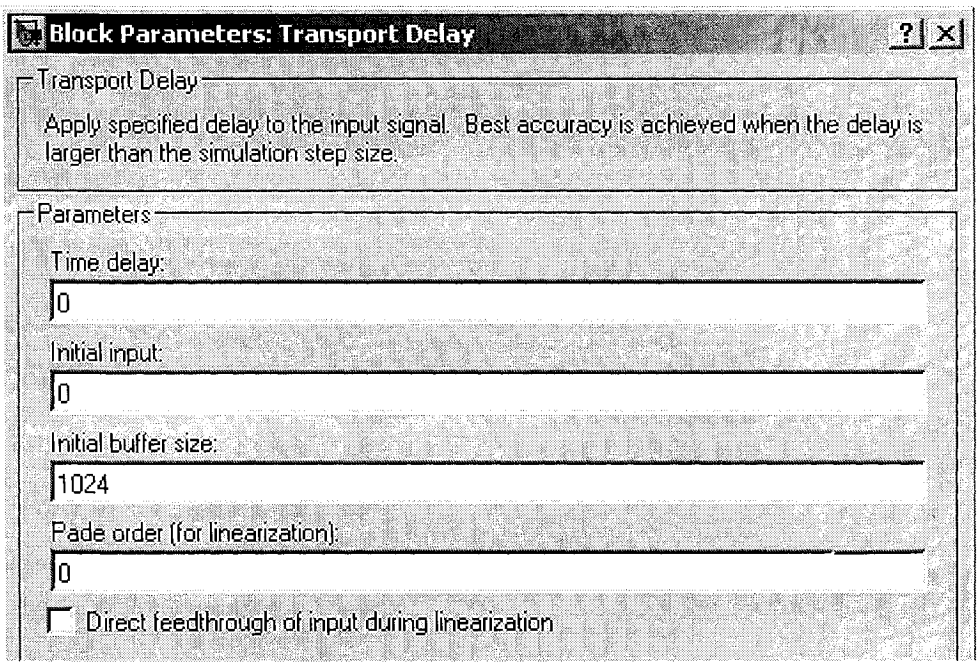

Time-delay block used for feedback loop delay, showing zero delay setting

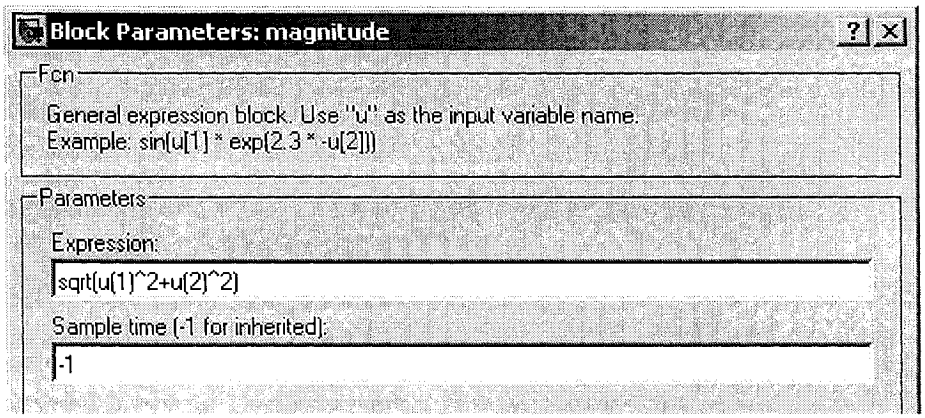

User-defined block used to compute the magnitude of a 2D vector (*f(u)* on block diagrams)

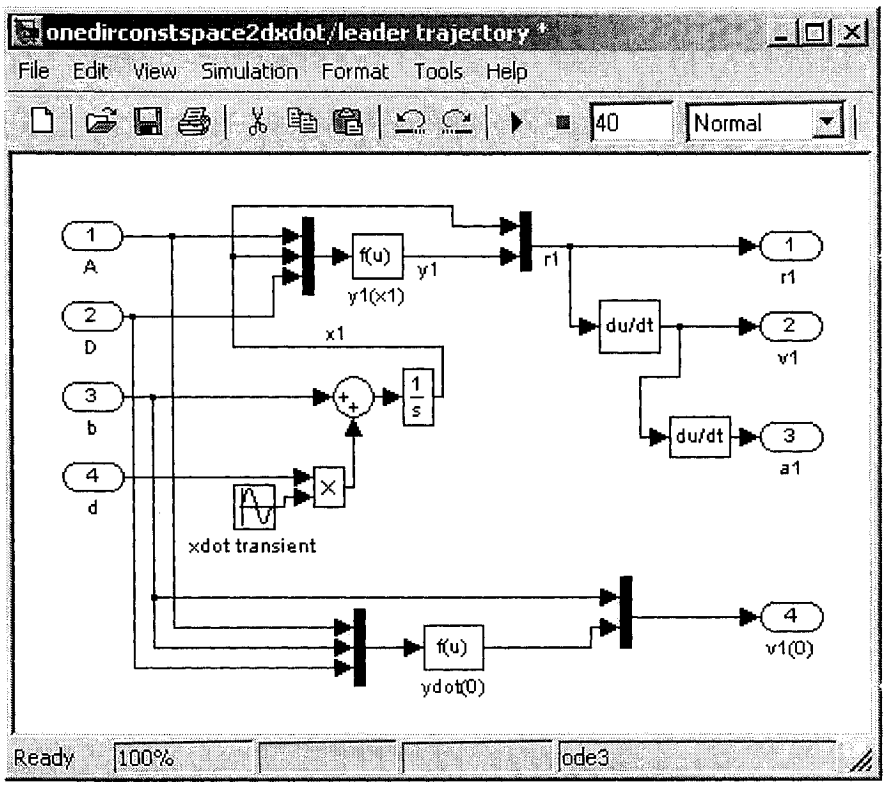

Leader Trajectory subsystem

Note: *xdot transient* = sin(*t*)

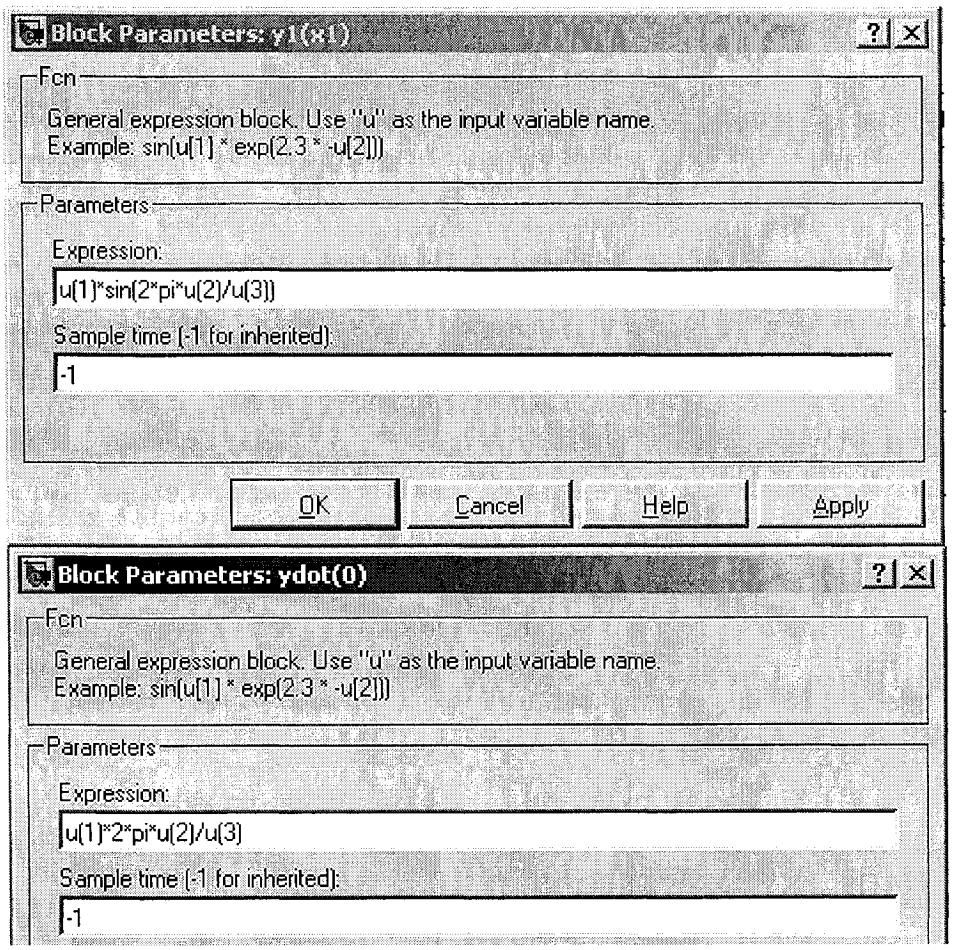

User-defined blocks used in *Leader Trajectory* subsystem

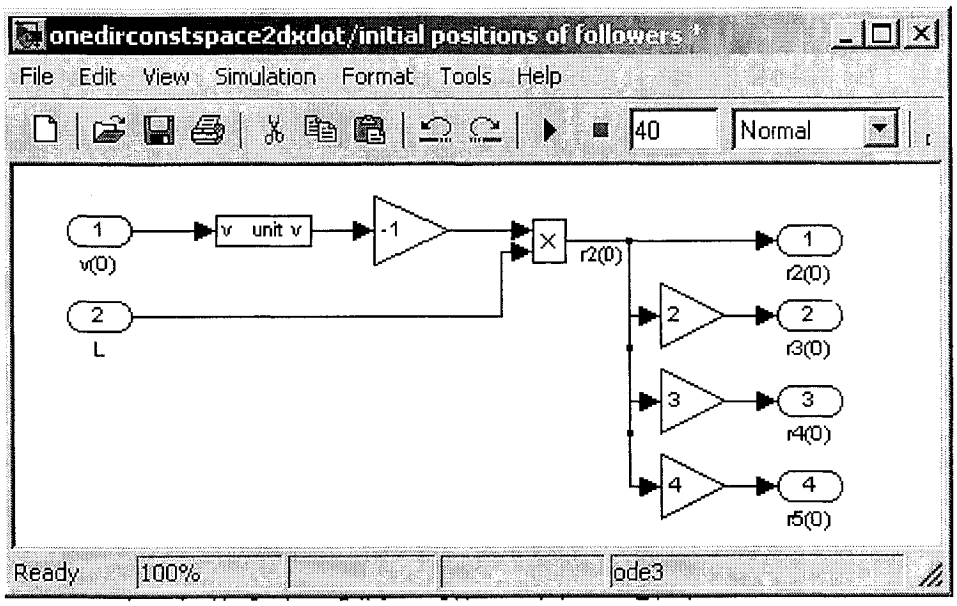

Initial Positions of Followers Subsystem

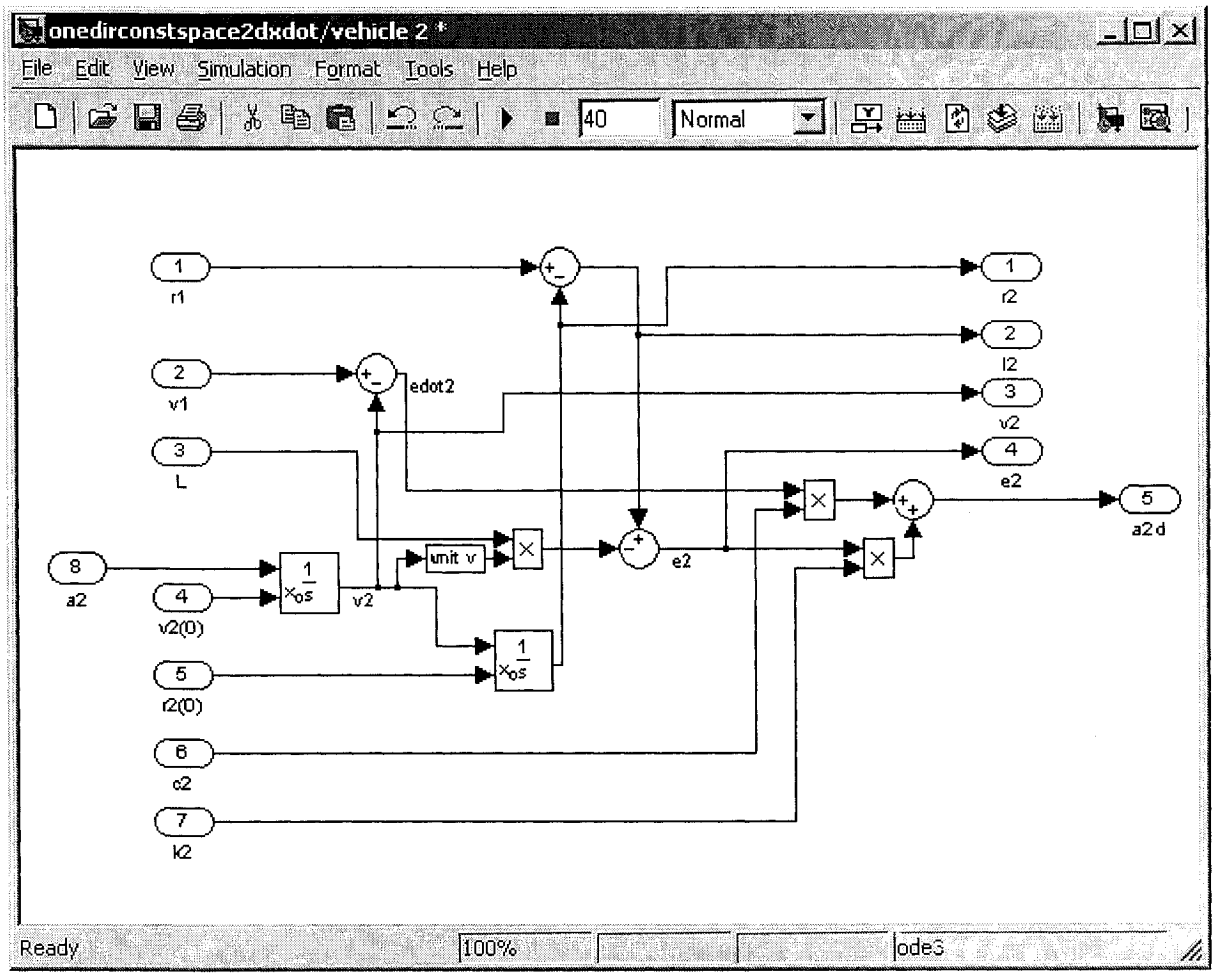

Vehicle subsystem example: *Vehicle* 2

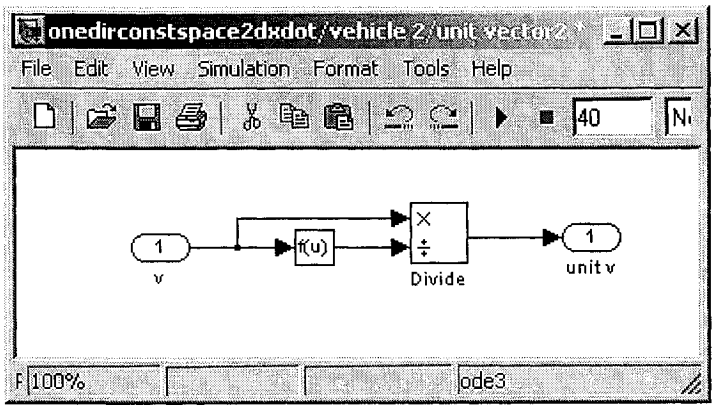

Unit Vector subsystem: accepts a 2D vector and outputs a unit vector in the direction of the original vector.

Appendix D : Simulink Model, Planar Motion, Local Information, Variable Spacing

Filename: onedirvarspace2dxdot.mdl

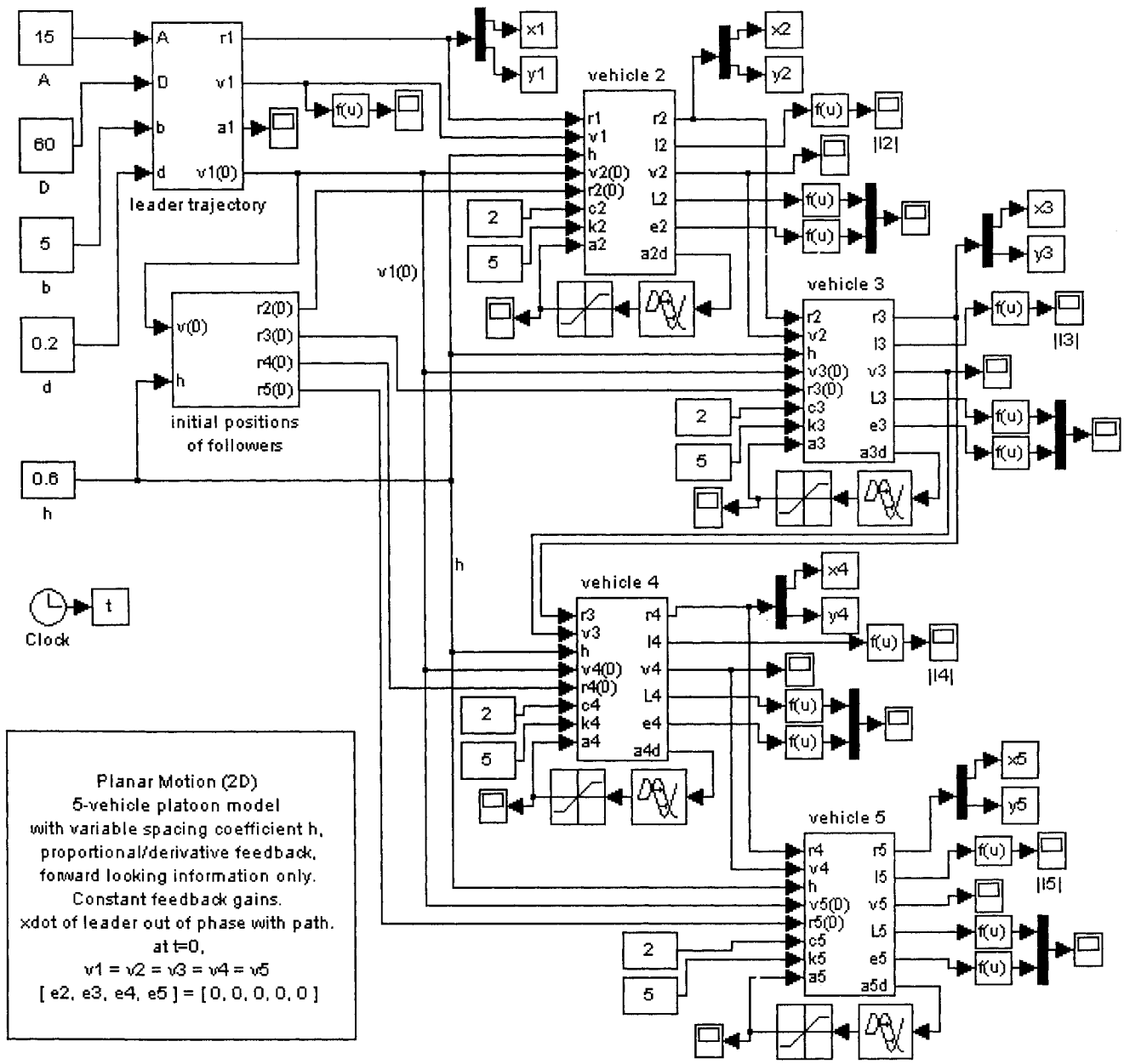

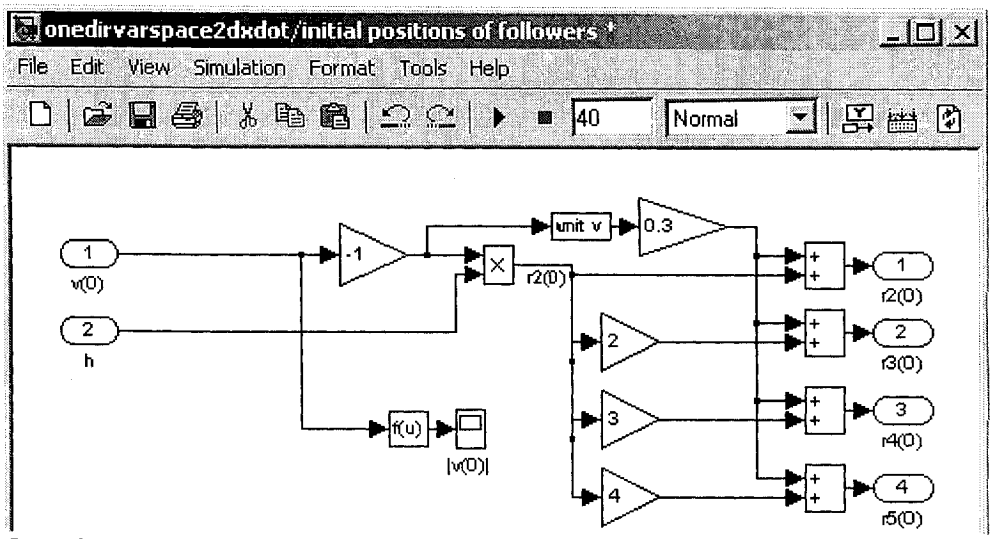

Initial Positions of Followers subsystem

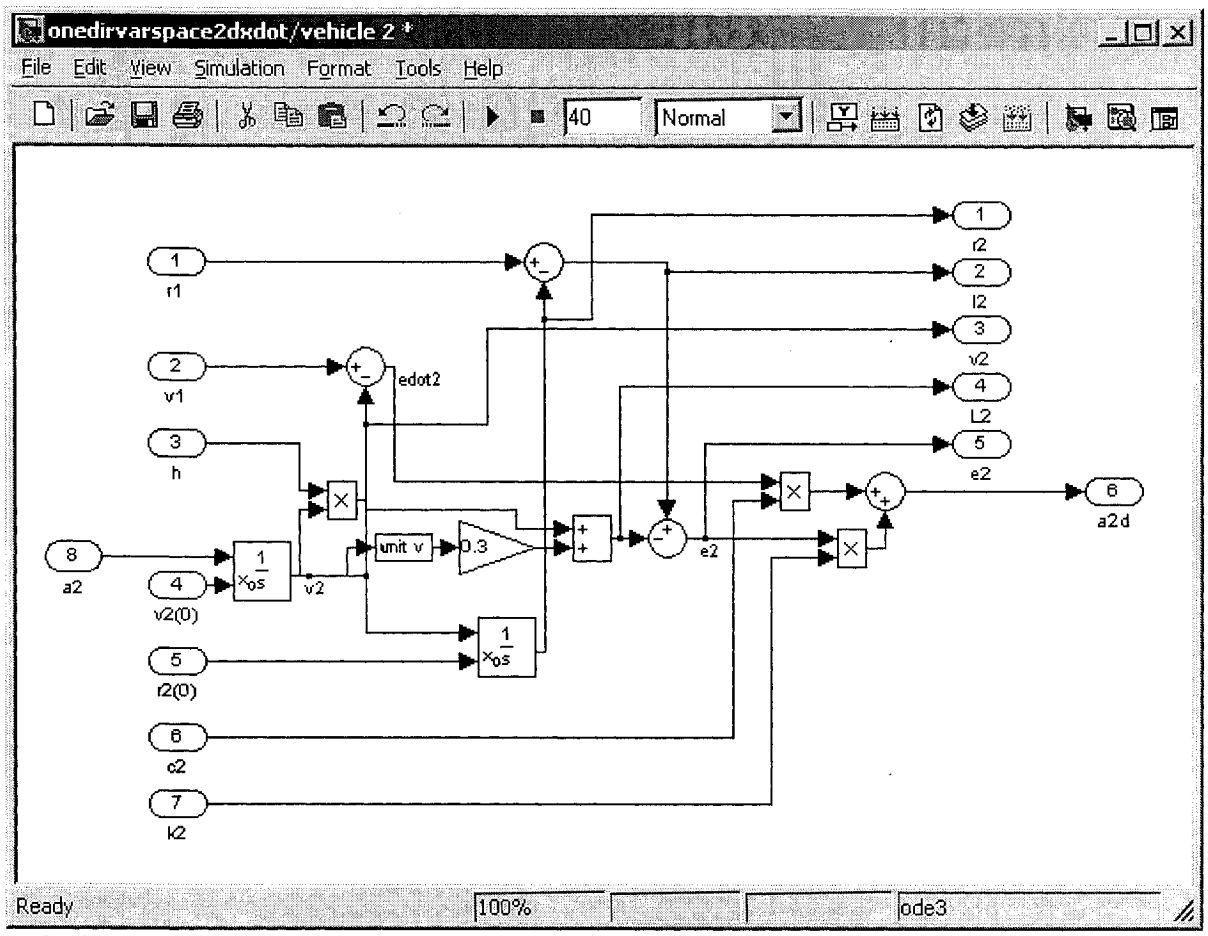

Vehicle 2 subsystem (all followers used the same model)

Note: all other subsystems and user-defined blocks were the same as in the Simulink model for 2D motion with constant spacing (filename: onedirconstspace2dxdot.mdl).

Appendix E : Simulink Model, Planar Motion, Global Information

Filename: pathgenerator.mdl

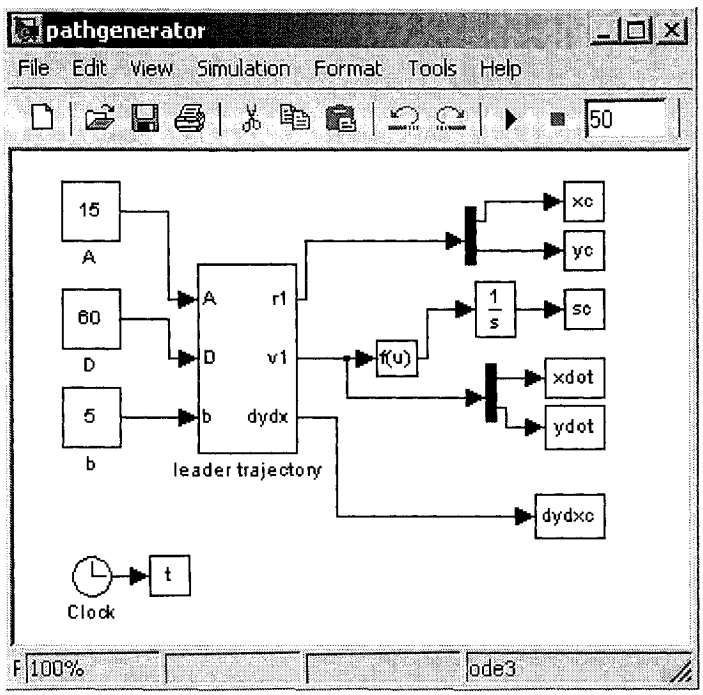

The f(u) block calculates the magnitude of the velocity vector. The result is then integrated to give path-wise distance *s*.

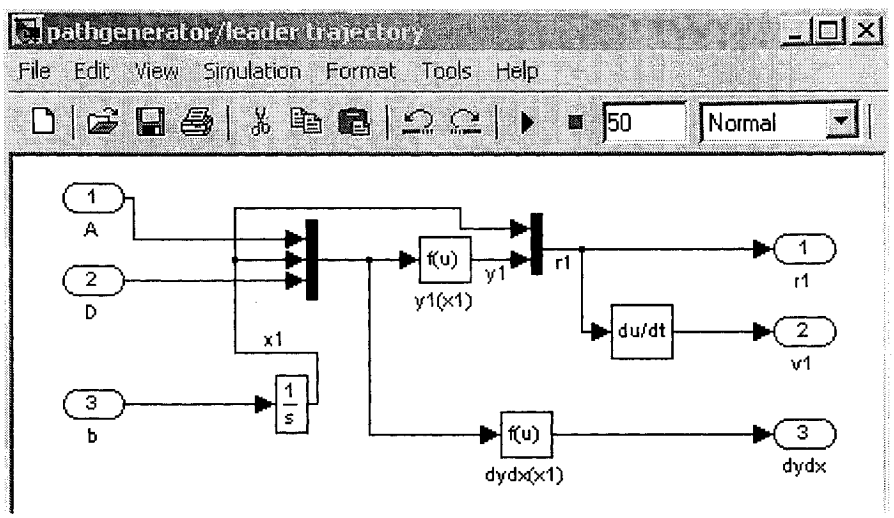

Leader Trajectory subsystem

Filename: globalconstspace2D.mdl

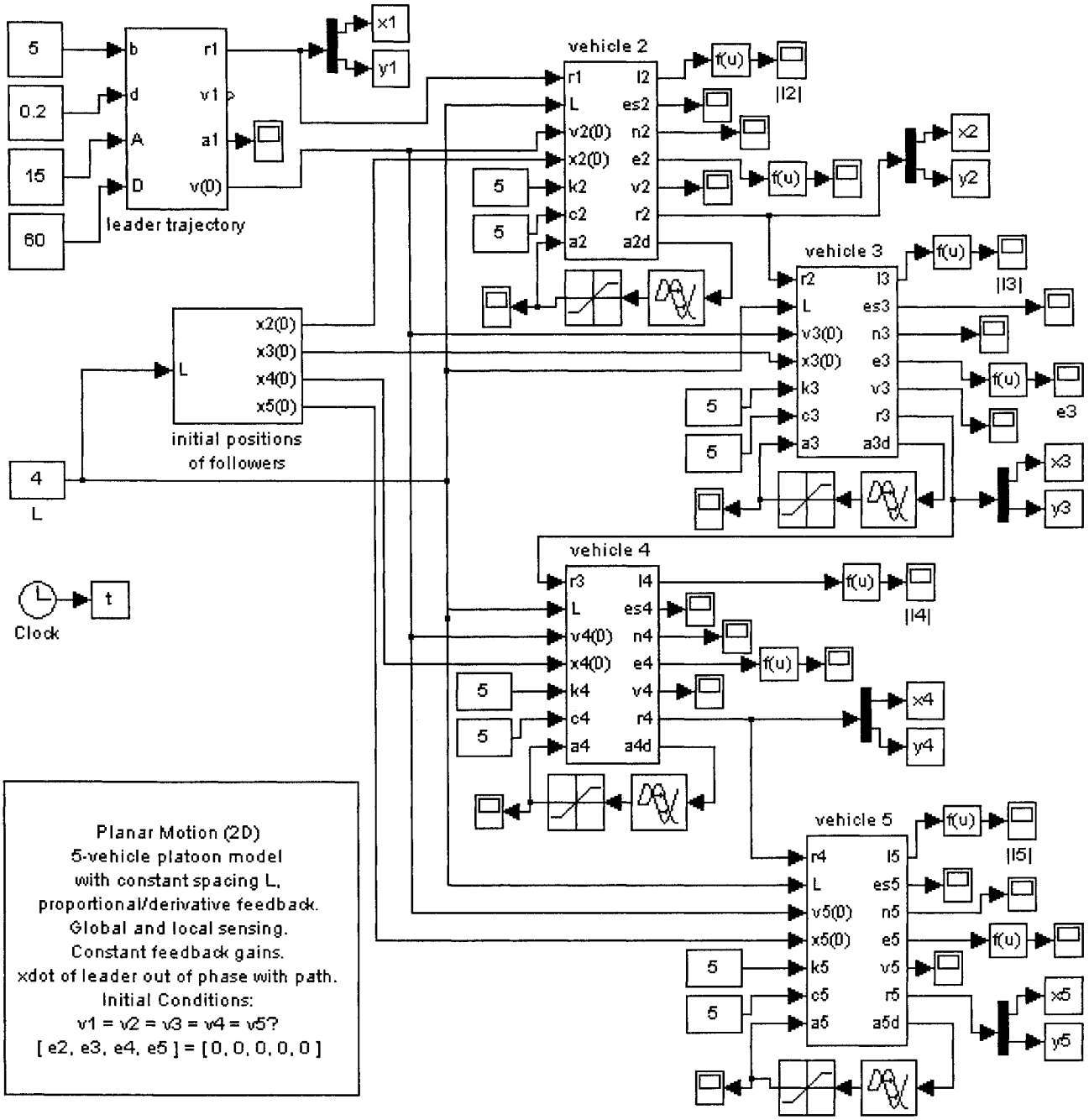

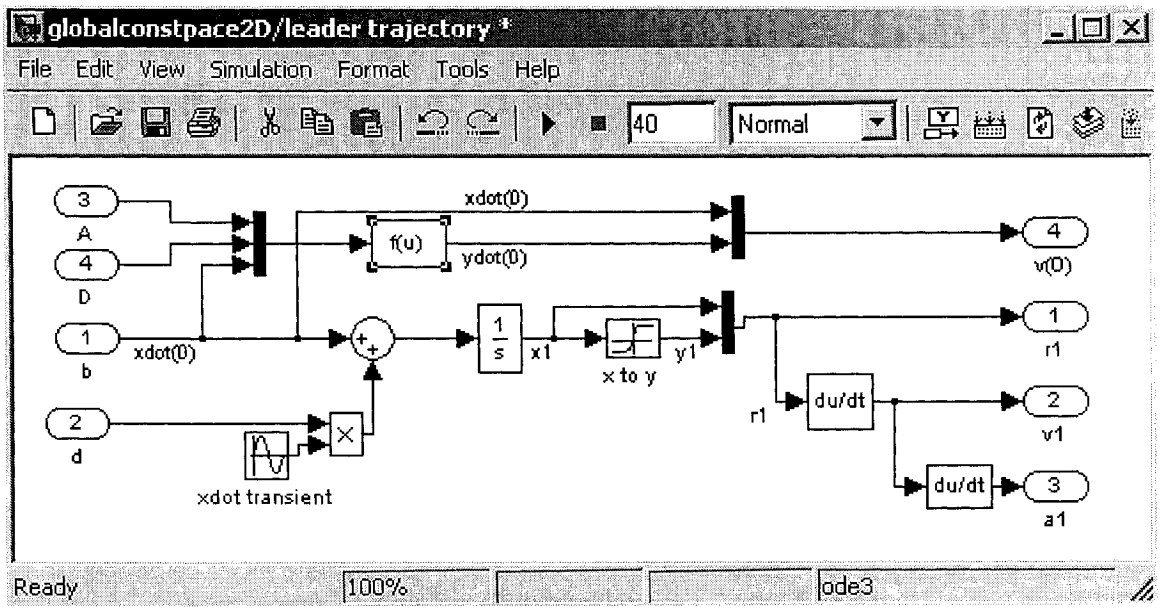

Leader Trajectory subsystem, where f(u) = 2*pi*A*b/D.

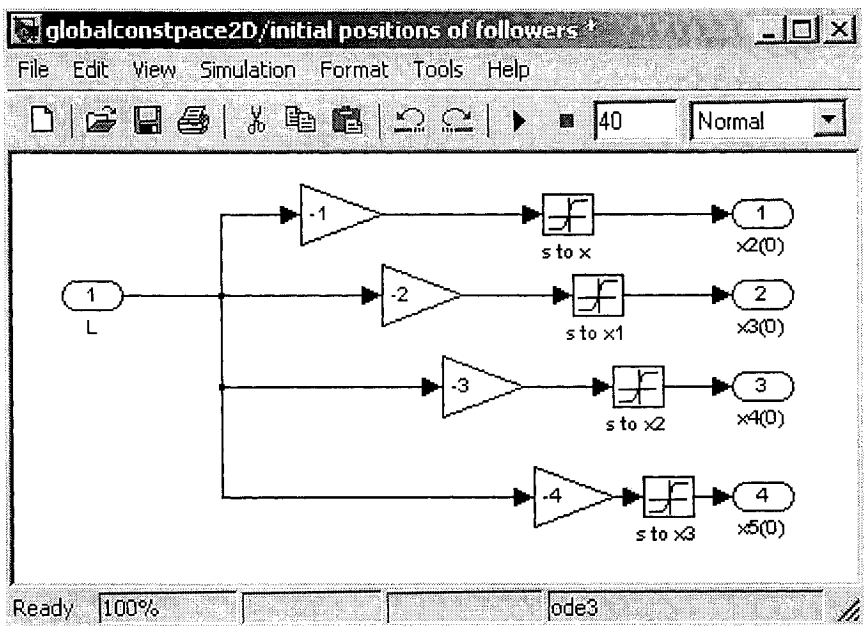

Initial Positions of Followers subsystem, all look-up tables are identical (different names are imposed by the Simulink environment)

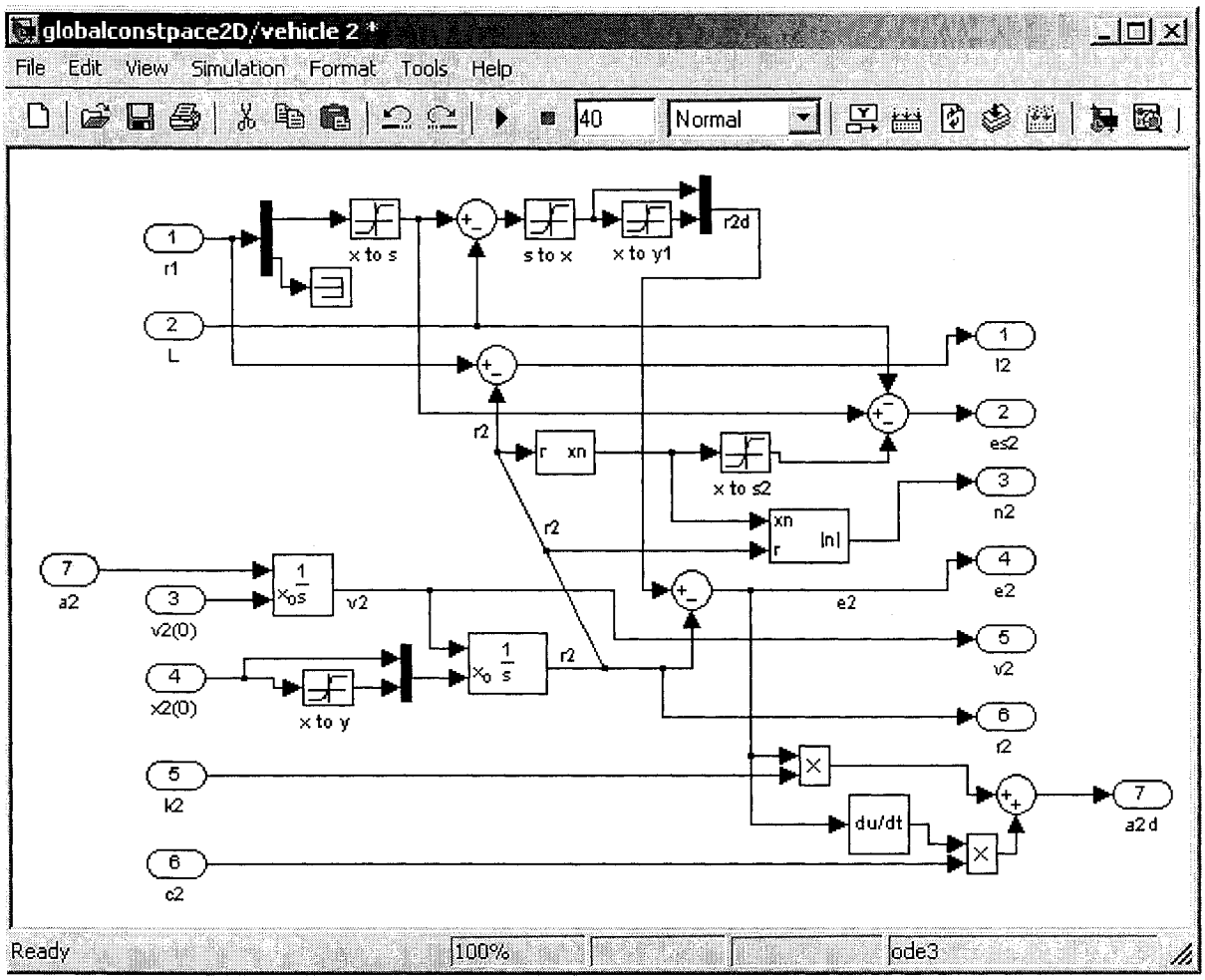

Vehicle 2 subsystem

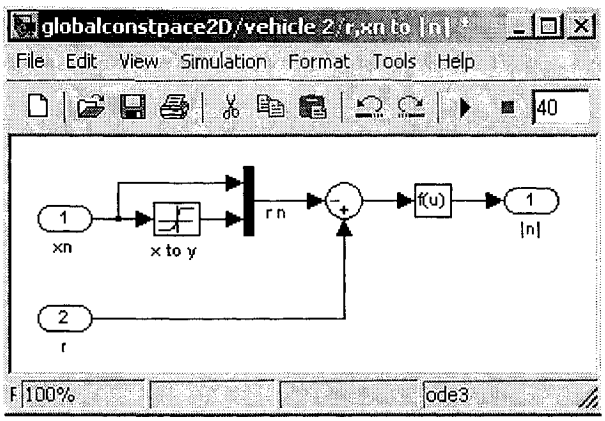

r, xn to |en| subsystem inside the vehicle subsystems, the f(u) block calculates the magnitude of the normal vector *|en|*.

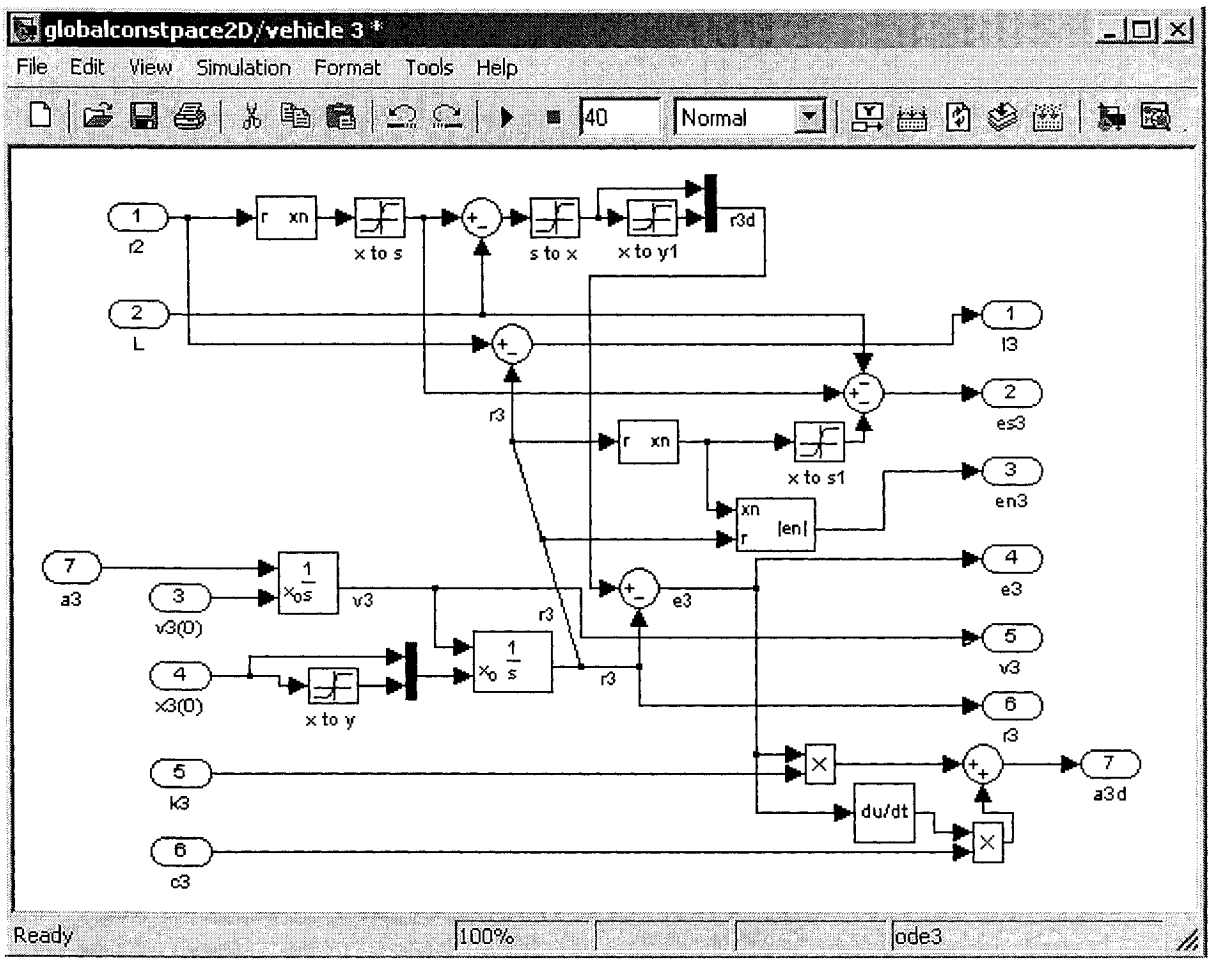

Vehicle 3 subsystem, same as vehicles 4 and 5

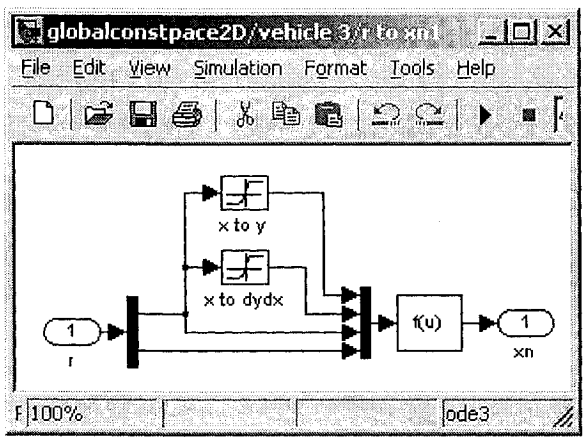

t to xn subsystem inside the *Vehicle* subsystems,

$f(u) = (u(3) + u(2)*(u(4) - u(1) + u(3)*u(2))) / (1 + u(2)^2)$, same as equation 5.11.4.

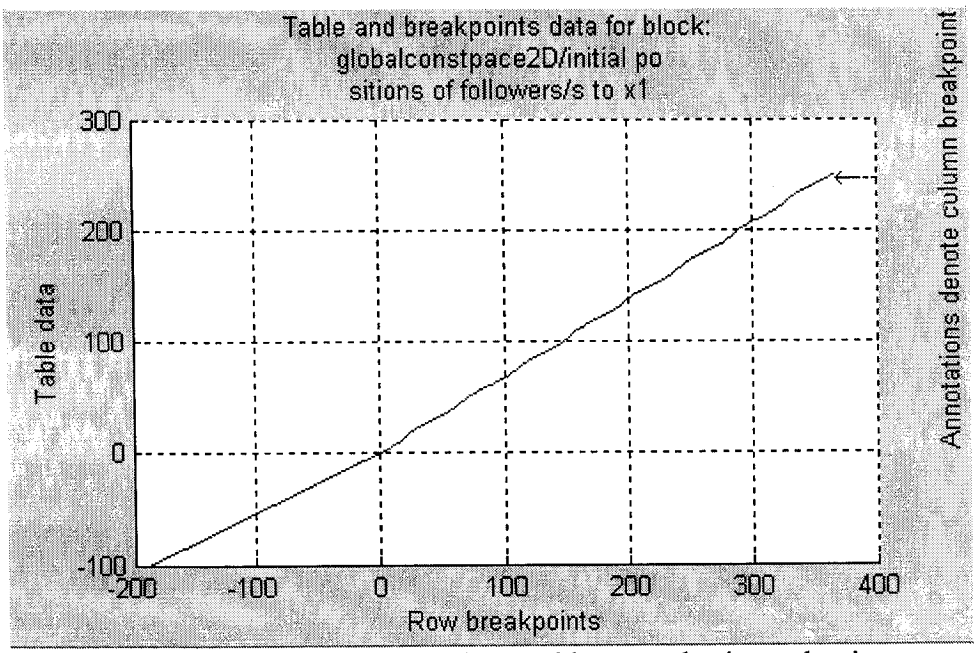

Graph of data used for all *s to x* look-up tables, *s* on horizontal axis

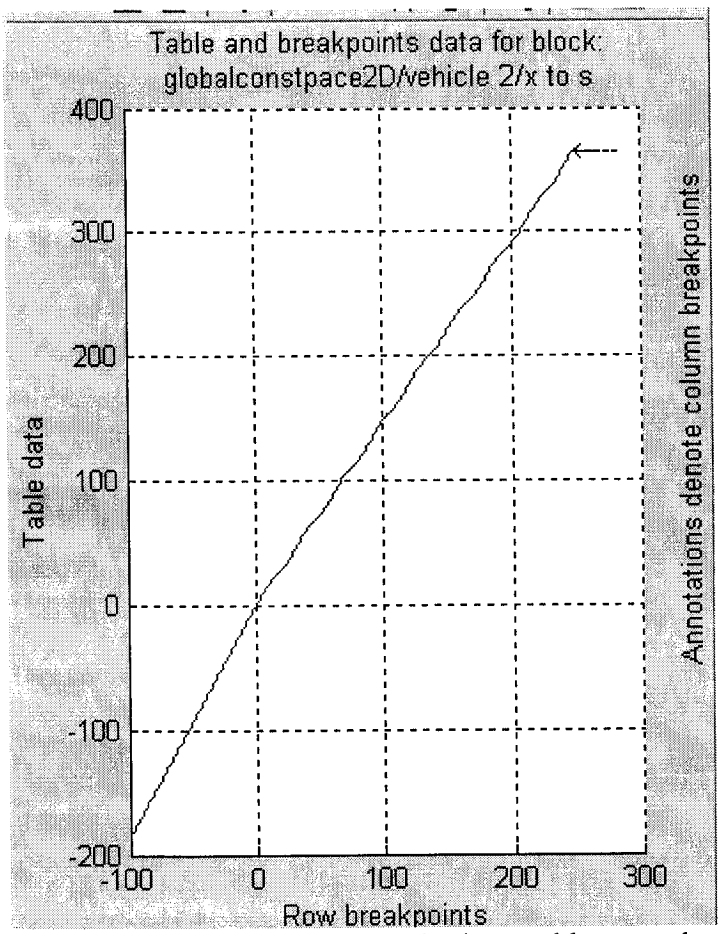

Graph of data used for all *x* to *s* look-up tables, *x* on horizontal axis

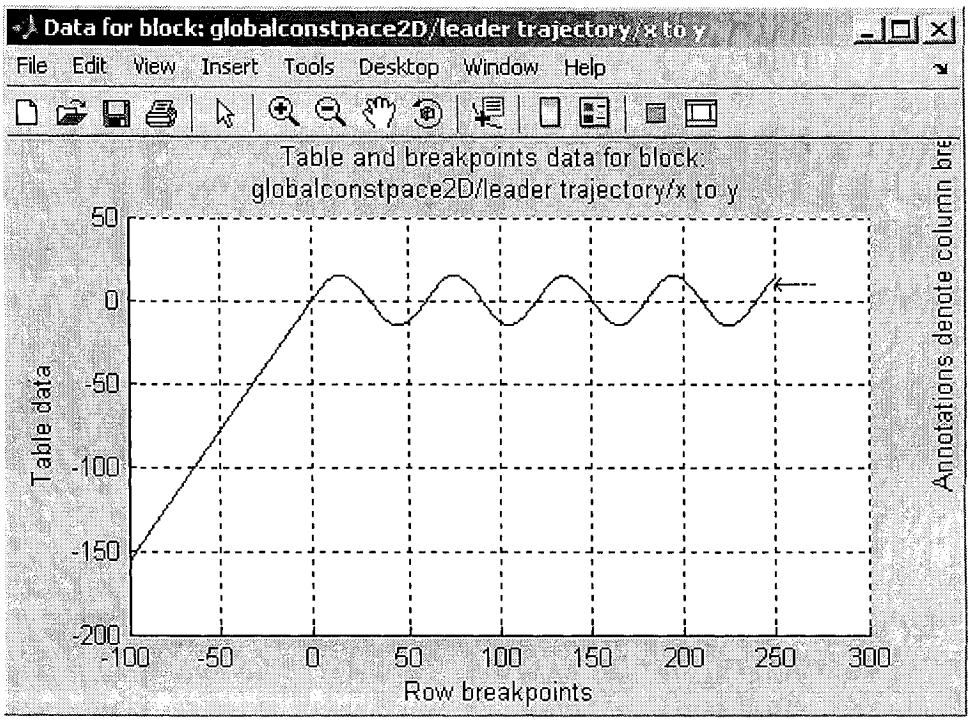

Graph of data used for all x to y look-up tables, x on horizontal axis

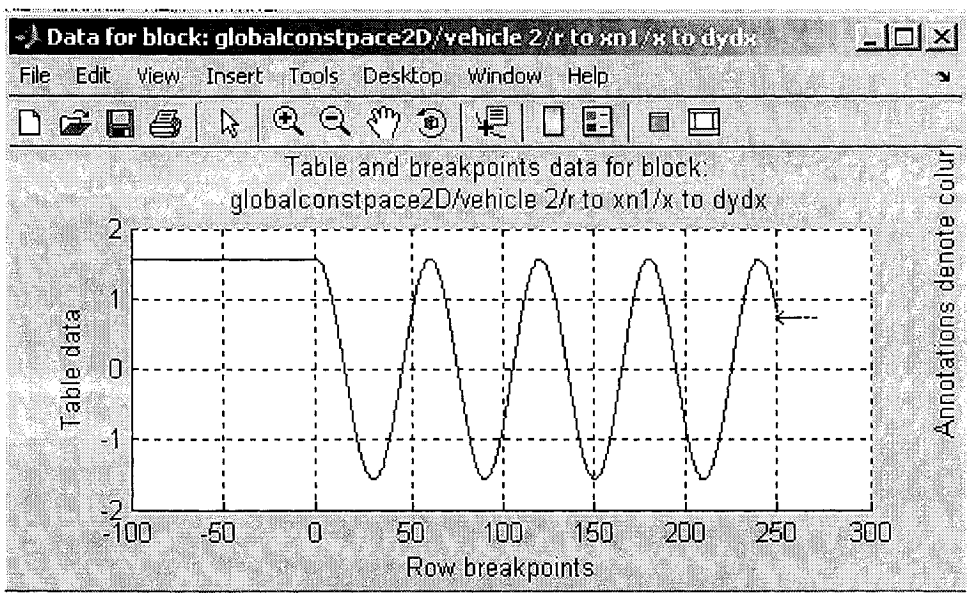

Graph of data used for all x to *dydx* look-up tables, x on horizontal axis